TIME-SPACE CHARACTERIZATION OF PRECIPITATION IN THE GANGES-BRAHMAPUTRA-MEGHNA RIVER BASIN FOR PROJECTING RIVERBANK EROSION IN THE BANGLADESH OUTLET

by

Muna Khatiwada

December, 2021

Director of Thesis: Scott Curtis, Ph.D.

Major Department: Geography, Planning, and Environment

ABSTRACT

The Ganges-Brahmaputra-Meghna (GBM) river basin is the world's third-largest river basin covering Nepal and Bhutan and certain parts of China, India, and Bangladesh. Literature show that changes in precipitation have a significant impact on climate, agriculture, and the environment in the GBM and many natural disasters such as drought, flood, landslides, and riverbank erosion are also a function of precipitation in the GBM river basin. Two satellite-based precipitation products, Precipitation Estimation from Remotely Sensed Information using Artificial Neural Networks-Climate Data Record (PERSIANN-CDR) and Multi-Source Weighted-Ensemble Precipitation (MSWEP), were used to study the relationship between seasonal precipitation as well as to analyze and compare precipitation trends over the GBM as a whole and for Pfafstetter level-05 sub-basins separately for the period 1983–2019. Positive correlations between precipitation within nearby hydrological sub-basins of the GBM were found during pre-

monsoon and monsoon seasons. However, only two sub-basins of the GBM show a significant correlation between pre-monsoon and monsoon precipitation among 32 hydrological basins based on PERSIANN-CDR. The correlation between ENSO and seasonal precipitation was also studied. A higher negative correlation between ENSO and precipitation in the monsoon season was found than in the pre-monsoon season. A non-parametric Modified Mann-Kendall test was applied to determine significant trends in monsoon (June–September) and pre-monsoon (March–May) precipitation. The results show an inconsistency between the two precipitation products. However, both products strongly indicate that precipitation has recently declined in the pre-monsoon and monsoon seasons in the eastern and southern regions of the GBM river basin, agreeing with several previous studies. The results did not support precipitation as a predictive driver in causing riverbank erosion in coastal Bangladesh. The findings of the present study provide useful information for managing water crises, agricultural production, and preparing for different natural hazards in the GBM river basin.

TIME-SPACE CHARACTERIZATION OF PRECIPITATION IN THE GANGES-BRAHMAPUTRA-MEGHNA RIVER BASIN FOR PROJECTING RIVERBANK EROSION IN THE BANGLADESH OUTLET

A Thesis

Presented To the Faculty of the Department of Geography, Planning, and Environment

East Carolina University

In Partial Fulfillment of the Requirements for the Degree

M.S. Geography

by

Muna Khatiwada

December, 2021

TIME-SPACE CHARACTERIZATION OF PRECIPITATION IN THE GANGES-BRAHMAPUTRA-MEGHNA RIVER BASIN FOR PROJECTING RIVERBANK EROSION IN THE BANGLADESH OUTLET

by

Muna Khatiwada

APPROVED BY:

DIRECTOR OF THESIS: _____

(Scott Curtis, Ph.D.)

COMMITTEE MEMBER: _____

(Thomas M. Rickenbach, Ph.D.)

COMMITTEE MEMBER: _____

(Hannah Sirianni, Ph.D.)

COMMITTEE MEMBER: _____

(Thomas W. Crawford, Ph.D.)

CHAIR OF THE DEPARTMENT

OF GEOGRAPHY, PLANNING,

AND ENVIRONMENT: _____

(Jeff Popke, Ph.D.)

DEAN OF THE

GRADUATE SCHOOL: _____

(Paul J. Gemperline, Ph.D.)

ACKNOWLEDGEMENTS

I extend my sincere thanks to East Carolina University, Department of Geography, Planning, and Environment for providing a platform to build my career and teaching me tremendously throughout this two-year journey. It was a mixture of joy, hard work, full of excitement, and a bundle of learnings.

First and foremost, I would like to express profound gratitude to my advisor Dr. Scott Curtis for believing in me and providing me an opportunity to work with him. I am always thankful for his continuous support, intellectual guidance, valuable suggestions, and moral encouragement throughout this journey. I am grateful for his motivation, patience, and accessibility any time I needed. I could not have imagined having a better advisor and mentor for my study. I would also like to express my gratitude to my research committee members: Dr. Tom Rickenbach, Dr. Thomas W Crawford, and Dr. Hannah Cooper. I am highly grateful for their guidance, support, and valuable comments throughout the research.

I would also like to express my sincere gratitude to Dr. Rosana Ferreira, a faculty member of the Geography department. She always supports and encourages me to achieve my goal. I am forever grateful for her effort as a graduate coordinator to make my journey easier and productive. My sincere thanks also goes to all faculty members of the department who helped me directly and indirectly through out this journey.

This study was funded by National Science Foundation (NSF), award number 1660447. I would like to thank the NSF-funded project “Coastal Erosion Vulnerabilities, Monsoon Dynamics, and Human Adaptive Response” and want to thank Nepal’s Department of Hydrology and Meteorology for providing rain gauge station data.

I would like to thank all my fellow classmates for all the beautiful memory we created in a very short time, though we could not create more memories together due to the pandemic. I would like to extend my gratitude to my husband Tulasi Subedi for his unconditional support and motivation throughout my journey. I am grateful to him for always creating the environment to complete my work on time. Lastly, I would like to thank my siblings, my parents, relatives, and friends for always encouraging me and showering their love even from thousands of miles apart of me.

TABLE OF CONTENTS

LIST OF TABLES

LIST OF FIGURES

CHAPTER 1: INTRODUCTION

1.1 Background

Precipitation is one of the most important climatic variables (Hamal et al., 2020; Sayemuzzaman & Jha, 2014) and has a direct connection to the economy, natural ecosystems, and human well-being (Stefanidis & Stathis, 2018). Precipitation recharges potable water supplies, increases hydropower generation and improves irrigation systems (Duncan & Biggs, 2012). In sum, precipitation and its distribution influence the development of society and the evolution of ecosystems (Ruiz-Alvarez et al., 2020). Therefore, it is essential to measure precipitation at a global scale for the understanding of the climate, weather, hydrology, and ecology (Wentz et al., 2007). People living in the Ganges-Brahmaputra-Meghna (GBM) river basin depend highly on the river system for agricultural, industrial, and domestic purposes (Mirza et al., 1998). Changes in precipitation have a huge impact on agriculture, economy and appropriate water resources planning for countries in the GBM (GC et al., 2021). For instance, 80% of the population in Bangladesh (Shahid, 2011) and Nepal (Karki & Gurung, 2012) depend on rain-fed agriculture, and agriculture contributes about 20% of the gross domestic product in India (Zaveri et al., 2016), indicating precipitation directly impacts the livelihood of countries within the GBM river basin (Duncan & Biggs, 2012). Unpredictable rainfall and extreme events affect land productivity, agriculture, food security, water availability, and livelihood (Shahid, 2011). Moreover, changes in precipitation cause many natural hazards, such as landslides, drought, flood, and riverbank erosion in the GBM (Stefanidis & Stathis, 2018; Hussain et al., 2018; Bisht et al., 2018). Therefore, it is essential to understand precipitation variations based on spatial and temporal patterns for a better understanding of regional water balances, risks of natural hazards, sustainable rural and forest

development, and effective management of water resources (Shahid, 2011; Sayemuzzaman & Jha, 2014; Stefanidis & Stathis, 2018; Bisht et al., 2018).

1.2 Problem Statement

Ganges-Brahmaputra-Meghna (GBM) river basin is the world's third-largest river basin covering approximately 1.72 million km^2 of five different nations. It is elongated from the foothills of the Himalayan Mountains to the Bay of Bengal and has a unique physiographic feature (Islam et al., 2010). Studying precipitation variability is essential in the GBM due to its high impact on agriculture, human settlements, and environments. Moreover, an abundant amount of water during the monsoon season leads to flooding and riverbank erosion in the GBM basin. To better understand whether monsoon rainfall could be a predictor for riverbank erosion, this study first examines the relationship between pre-monsoon (March-April-May) and monsoon (June-July-August-September) precipitation patterns of the GBM sub-basins. Secondly, this study investigates variability in seasonal precipitation during El Niño /Southern Oscillation (ENSO) with respect to hydrological basins and water routing distance to determine whether ENSO can be a predictor for riverbank erosion in the GBM river basin. Third, this study investigates trend detection on monsoon and pre-monsoon precipitation over the entire GBM river basin and within 34 pre-defined hydrological sub-basins of the GBM separately to better understand trends in erosion. There is a lack of research in precipitation trend analysis in hydrological sub-basins of the GBM, even though these spatial units are critical for water management. In addition to studying seasonal precipitation, the relationship of riverbank erosion with local extreme daily precipitation is investigated. Several previous studies have estimated the riverbank erosion in the GBM river basin, but none of the prior research has attempted to establish the relationship between precipitation and riverbank erosion, and the current research intends to fill this gap. Overall, this

research aims to examine the relationship between seasonal precipitation based on hydrological sub-basins for a more regionally refined analysis of precipitation variability, precipitation relationships with ENSO, and local daily extreme precipitation in causing riverbank erosion in the coastal Bangladesh. The research results will be useful to academics, governmental officials, national planners, and concerned authorities to plan a resilient society that minimizes risk from riverbank erosion.

1.3 Research Questions

The principal objective of the study is to analyze pre-monsoon and monsoon precipitation variability in the GBM river basin and its relation in causing riverbank erosion in coastal Bangladesh. This study will focus on the following research questions to realize the objective.

1. What is the relationship between pre-monsoon and monsoon precipitation in the GBM river basin based on hydrological sub-basins vs. water routing distance?
2. Do climate teleconnections, e.g., ENSO, have any relationship with seasonal precipitation in the GBM river basin?
3. What are the pre-monsoon and monsoon precipitation trends in the GBM river basin from 1983 to 2019?
4. What is the relative importance of localized extreme daily precipitation versus basin-scale seasonal precipitation for riverbank erosion in the study area?

CHAPTER 2: LITERATURE REVIEW

This chapter reviews literature and discusses monsoon precipitation, pre-monsoon precipitation, extreme daily precipitation, seasonal precipitation trends, satellite-based precipitation products, validation of satellite products, ENSO, water routing distance, and riverbank erosion research around the world.

2.1 Monsoon Precipitation

The term monsoon first originated from an Arabian word mausim, meaning season. Ramage (1971) defined monsoon as a seasonal variation in wind and precipitation. Alamgir (2009) described monsoon as a seasonal shift of winds created by the land's annual temperature variation in contrast with the connected ocean surface. Similarly, according to other researchers Kumar & Naidu (2020), monsoon rainfall occurs due to equatorial maritime air masses, and the general circulation associated with monsoon precipitation is of continental scale.

Generally, monsoon is denoted as a rainy phase of a seasonally changing pattern. While the spatial organization of precipitation, especially in remote areas, is uncertain due to the lack of data, certain temporal patterns of precipitation, such as those associated with the monsoon, are well established. The season that runs from June through September is called monsoon season in South Asia. The monsoon rainfall is highly erratic, and its prediction is essential in the South Asian context (Romatschke & Houze, 2011). Highly unpredictable monsoon causes severe hardship to millions of people living in the GBM basin, especially those living in the low land of Bangladesh and India. However, some spatial and temporal patterns may be predictable, which would aid decision-makers and stakeholders in managing water resources and natural hazards (Mosaffa et al., 2020). Most countries in South Asia, including Bangladesh, Nepal, India, and Bhutan, receive

70 to 80% of annual rainfall during the monsoon season (Mirza, 2011). Due to this reason, there is always a risk of moderate to severe floods affecting agricultural land, infrastructures, properties, human settlements, and environments in the GBM river basin during the monsoon months.

In contrast, the amount of drinking water availability, irrigation, and hydropower energy is also determined by the monsoon precipitation in South Asia (Duncan & Biggs, 2012). Precipitation during the monsoon season forms complex spatiotemporal patterns due to complex topography and atmospheric circulation (Malik et al., 2010). Therefore, it is necessary to analyze monsoon precipitation for better preparation and adaptation.

The flow of Ganges and Brahmaputra increases from 10000 m^3/s to 80000 m^3/s-140000 m^3/s until early September, accelerating different natural hazards such as landslides, floods, and riverbank erosion within the countries of GBM. The downstream countries predominantly suffer from riverbank erosion and flooding, and the upper reaches suffer from landslides. For example, the mean annual rainfall of Bangladesh varies from 1400mm in the western part to 5000mm in the northeast region (M. Rahman, 2013). The internal rainfall, high flows of three major rivers, and low-lying floodplains lead to wide inundation every year in Bangladesh (Ministry of Water Resources of the People's Republic of Bangladesh, 2000). Nepal and Bhutan experience more landslides during the monsoon season (Gerrard & Gardner, 2000) and (Dikshit et al., 2019). Landslides take human lives and damage infrastructures and road networks in Bhutan (Dikshit et al., 2019) and Nepal (DAHAL, 2012; Petley et al., 2007).

2.2 Pre-monsoon Precipitation

The pre-monsoon rainfall season occurs due to tropical maritime air masses, and the general circulation associated with pre-monsoon season is of subcontinental scale (Kumar &

Naidu, 2020). Due to this reason, pre-monsoon season is appropriate to refer to the southerlies or southwesterlies over the Indian peninsula during April and early May. Pre-monsoon starts from March to May in South Asia, where April and May contribute a higher amount of rainfall (Shahid, 2011). Only 15-20 % of annual rainfall occurs during the pre-monsoon season (March-April-May) in the GBM river basin (Bajracharya et al., 2015). In addition, pre-monsoon precipitation has a large spatial and temporal variation (Kumar & Naidu, 2020) in the GBM river basin. According to (Kumar & Naidu, 2020), the important rain-bearing systems during this season are mesoscale convective systems, thunderstorms, and tropical cyclones. The cloud grows vertically during the pre-monsoon season maximizing during the late afternoon and early evening hours. Storms are triggered by high temperature, low level moisture, and conditional instability. Moreover, pre-monsoon rainfall is patchy in nature (https://meteorologicalconsultant.wordpress.com/2017/04/09/difference-between-monsoon-and-pre-monsoon-rain). Recent research conducted by (Sharma et al., 2021) found that pre-monsoon precipitation is increasing a small amount in the GBM river basin using precipitation data from 1901 to 2016. Previous research particularly focusing on the countries of the GBM river basin, also shows that pre-monsoon precipitation is increasing over time. For instance, the amount of precipitation during the pre-monsoon is gradually increasing in Bangladesh over the time period of 1958–2007 (Shahid, 2011) and India (Kumar & Naidu, 2020) during 1970–2015. Alamgir (2009) also found that the pre-monsoon maximum rain rate is larger than the summer and winter monsoon (December–February) in Bangladesh using four years (2000–2003) of precipitation data. Rahman & Lateh (2017) also reported that rainfall during pre-monsoon and post-monsoon (October–November) is unpredictable in Bangladesh. He found that the pre-monsoon maximum rain rate is larger than the summer monsoon and winter monsoon at 114.19, 73.88, and 49.28

mm/h, respectively during the period of 1971 to 2010. The low land of Nepal has experienced significantly increasing pre-monsoon precipitation from 1981 to 2010 (Karki et al., 2017).

Pre-monsoon rainfall has importance in Bangladesh because 70% of total food grain is grown during this period (Shahid, 2011). However, the activity of pre-monsoon precipitation is low compared to the monsoon and winter seasons in India. Pre-monsoon precipitation is useful for mango, jute, rice, and tea cultivation in West Bengal, India, but it provides little rain to dry areas. There is less literature on pre-monsoon rainfall than summer monsoon and winter monsoon rainfall (Kumar & Naidu, 2020).

2.3 Extreme Daily Precipitation

An extreme event is a rare meteorological event at a particular place or time of the year, such as heatwaves, cold waves, heavy rainfall, drought, and floods. When the daily precipitation exceeds a climatological threshold of its seasonal or annual precipitation, it can be considered extreme daily precipitation (Liebmann et al., 2001). According to the authors, heavy precipitation events are disruptive in nature, damaging crops and infrastructures, displacing urban populations and contributing to flooding and riverbank erosion. Likely, Ruiz-Alvarez et al. (2020) emphasize that normal rainfall is beneficial to rain-fed agriculture, ecosystems, and daily life, but frequent extreme events have adverse effects on accelerating floods, riverbank erosion, landslides, and high runoff (Ruiz-Alvarez et al., 2020). Precipitation extremes change in a warming climate (Shiu et al., 2012), and according to their findings, about 100% increase for the annual top 10% heavy precipitation and about 20% decrease for the light and moderate precipitation for one degree warming in global temperature. Other studies support that increasing extreme precipitation might be due to global warming (Marelle et al., 2018; Roy & Balling, 2004). One researcher (Liebmann et al., 2001) mentions that there is an expectation that the frequent occurrence of extreme events

in some places may have a relationship to the state of ENSO. However, detail studied is needed to make any conclusion for a particular region. From the past two decades, extreme events have received the attention and interest of many researchers as evidence mounts for increasing extreme precipitation events around the globe (Roy & Balling, 2004; Ajjur & Riffi, 2020). Several studies also found that extreme precipitation days are increasing, and the seasonality of extreme precipitation is shifting. For instance, South Asia is suffering from the consequences of extreme daily precipitation in late October (https://blogs.agu.org/landslideblog/2021/10/20/south-asian-monsoon-1/). Marelle et al. (2018) studied the changing seasonality of extreme daily precipitation using global and regional climate models from the Coupled Model Intercomparison Project phase 5 and the Coordinated Regional Downscaling Experiment, in 1871–1900, 1976–2005, and 2071–2100 for an extreme future emission scenario. The findings show that that extreme precipitation seasonality will be shifted by the end of 21st century.

2.4 Seasonal Precipitation Trends in the GBM river basin

Precipitation trend analysis can help to better interpret changes in hydrology and ecosystem services for countries within the GBM (Karpouzos et al., 2010). According to Gajbhiye et al. (2016), it is essential to study long-term precipitation trends in India because food supply and economic well-being are based on rain-fed agriculture. Ahmad et al. (2015) mention that a precise precipitation trend analysis can be useful to improve the future economy in Pakistan because of their rain-fed agriculture. Scholars have conducted various studies to estimate precipitation trend analysis over the years in river basins within the GBM (Mirza et al., 1998; Sharma et al., 2021; Khandu et al., 2017; Kothyari et al., 1997; Janes et al., 2019; Immerzeel, 2008). Mirza et al. (1998) studied the trends and persistence in precipitation in the GBM river basin and found that the Ganges river basin has a stable precipitation trend, but Meghna and Brahmaputra basins show

contrasting results for upstream and downstream. Sharma et al. (2021) analyzed precipitation trends using historical Climate Research Unit (CRU) monthly precipitation gridded data in the GBM river basin for four distinct seasons. The results show that the precipitation is decreasing in most places of the GBM river basin during the monsoon season (June–September), whereas the precipitation was slightly increasing in most of the regions during the pre-monsoon season from 1901 to 2016. The study reported no such change for winter, and only a negligible precipitation trend was seen in the post-monsoon season. A study by Khandu et al. (2017) showed that precipitation in the high rainfall regions of northeast India, Bhutan, Nepal, and Bangladesh decreased up to 39 mm per decade in the monsoon season from 1998 to 2013.

2.5 Satellite-based precipitation products

The three promising primary methods to measure precipitation around the world are rain gauges, radars, and satellites. Among them, rain gauges provide reliable ground-based direct rainfall data. However, intermittent data coverage over most of the continents is the main constraint. Radar-based products are not available in many countries due to the cost and beam blockage by terrain. These two products, radar and rain gauge, do not measure precipitation over oceans, whereas satellite-based products provide rainfall measurements from both land and sea with generally good accuracy (Nguyen et al., 2018). In fact, satellite-based products have been rapidly developing over the past few decades and are highly applicable for estimating precipitation at regional and global scales.

The Tropical Rainfall Measurement Mission (TRMM) was developed in 1997 as the first satellite-based mission to estimate precipitation (Kummerow et al., 2000) and marked the beginning of a new era (Nguyen et al., 2018). It ended after a successful 17 years of precipitation measurement and was followed by the Global Precipitation Measurement (GPM) mission (Hou et

al., 2014). During this time, multiple satellite-based products were developed and are being used around the globe. These products mainly use infrared and passive microwave imagery (Guo et al., 2015), and the algorithms are different for each product (Nguyen et al., 2018). They vary in measurement accuracy, sampling frequency, and merging methodology (Hou et al., 2014). The commonly used satellite-based precipitation products around the globe are TRMM Multisatellite Precipitation Analysis (Huffman et al., 2007), Climate Prediction Center morphing technique (CMORPH) (Joyce et al., 2004), Precipitation Estimation from Remotely Sensed Information Using Artificial Neural Networks (PERSIANN) (Sorooshian et al., 2000), and Integrated Multisatellite Retrievals for Global Precipitation Measurements (IMERG) (Huffman et al., 2019). These products are highly useful for developing countries where long-term gauge-based data are not available. The current study uses PERSIANN-Climate Data Record (CDR) because it has successfully been used in GBM river basin by several researchesr, for instance, Shah & Mishra (2016), Mondal et al. (2018), Hussain et al. (2018), Curtis et al. (2017), and Multi-Source Weighted Precipitation (MSWEP) products due to its higher 0.1 degree spatial resolution for precipitation estimation and analysis. TRMM is not used because of its shorter data record.

2.6 Validation of Satellite-based Precipitation Products

Satellite-based precipitation products are highly applicable in regions where rain gauge station data are sparsely distributed, and unable to provide continuous data for long-term studies (Atiah et al., 2020; dos Reis et al., 2017). It is necessary to validate satellite estimates because the accuracy of these rainfall products over different spatial and temporal scales is unknown. Researchers around the world have worked at validating satellite-based precipitation products against traditional rain gauge stations (Ashouri et al., 2016; Atiah et al., 2020; dos Reis et al., 2017, 2017; Katiraie-Boroujerdy et al., 2017; Mazzoleni et al., 2018;Thiemig et al., 2012). Validation

mainly focuses on checking the reliability of hydrometeorological measures, such as seasonal precipitation, dry season, extreme daily precipitation, etc. (Thiemig et al., 2012).

For the GBM, rain gauge station data are limited due to the steep topography, climatic conditions, and lack of funding. Moreover, limited numbers of rain gauges make spatial averaging more difficult. In contrast, satellite-based rainfall products estimate precipitation with high spatial and temporal resolution, covering the whole globe, including oceans, high mountains, and remote areas. Using satellite data helps resolve the issue of data scarcity and discontinuity, especially in developing countries. This study aims to evaluate the performance of two satellite-based rainfall products (PERSIANN-CDR and MSWEP) against Nepal's 223 rain gauge station data from 1983 to 2009. Nepal was chosen due to the availability of data (the author is Nepali) and the importance of validation in high-elevation variable terrain. Although, evaluating the performance of satellite-based precipitation products over complex topography of the GBM river basin are still very limited (Bajracharya et al., 2015).

Some example of validation studies comparing PERSIANN-CDR and MSWEP with ground-based observations and radar data are as follows. PERSIANN-CDR compared favorably, during Hurricane Katrina 2005, with gauge-adjusted stage IV radar data, and PERSIANN-CDR reproduced a major flood event over Sydney, Australia, in 1986 with similar results as a gridded daily gauge product (Ashouri et al., 2015). In a comparison between the probability density function of PERSIANN-CDR and CPC gauge data and TMPA v7 over the contiguous United States, PERSIANN-CDR only underestimated the frequency distribution (Ashouri et al., 2015). PERSIANN-CDR was used to study the extreme daily precipitation in the eastern China monsoon region. It produced a similar result with the ground-based East Asia product in estimating extreme daily precipitation (Miao et al., 2015). (Ashouri et al., 2016) also studied the efficacy of the

PERSIANN-CDR product in simulating streamflow in three river basins in Oklahoma, Arkansas, and Missouri, United States. PERSIANN-CDR proved capable in hydrological rainfall-runoff modeling applications over three decades. PERSAINN-CDR also performed better in Indian subcontinental basins for real-time streamflow simulation (Shah & Mishra, 2016). Thus, there is evidence that PERSIANN-CDR can be used as a long and reliable data set for climate and hydrological studies (Ashouri et al., 2015). Similarly, researchers have conducted some validation tests for the MSWEP precipitation product around the world. However, more work is needed. (Bai & Liu, 2018) recently validated precipitation on the Tibetan plateau comparing five different satellite products CHIRPS, CMORPH, PERSIANN-CDR, TMPA 3B42 including MSWEP during the period 1998-2012. The five products were validated against precipitation data from 21 rain gauge station using the point to pixel method. Among the five products, MSWEP showed the best consistency with the gauge observations. Another validation study was conducted by (Nair & Indu, 2017) for MSWEP over India. They concluded that MSWEP only performed well for the estimation of daily precipitation and was unsuitable for the daily extremes. On the contrary, MSWEP performed well in the Lancang-Mekong river basin, suggesting MSWEP could be used for scientific research for this river basin (Tang et al., 2021). (Awange et al., 2019) evaluated MSWEP over Australia and Africa from 1981-2016. Their study shows that MSWEP performed well over most of Australia except in those areas where heavy monsoon rainfall occurs. The study did not find any outstanding improvement compared to other products in Africa. However, they suggested that MSWEP has a potential application to water storage flux, discharge and climate impacts over the two continents. Lakew (2020) compared the five precipitation products of gauge adjusted Climate Prediction Center Morphing Technique (CMORPH), Tropical Rainfall Measuring Mission (TRMM) Multi-Satellite Precipitation Analysis 3B42 version 7 (TMPA),

ERA-Interim (ERAI), Global Precipitation Climatology Centre (GPCC), and MSWEP for the Upper Blue Nile basin using gauged rainfall and streamflow data. His results indicate that MSWEP precipitation shows consistently better performance when compared to other precipitation products for the Upper Blue Nile basin.

2.7 El Niño /Southern Oscillation (ENSO)

An important climate phenomenon in the Pacific Ocean that has been shown to influence the monsoon is the El Niño/Southern Oscillation (ENSO). ENSO denotes the interannual variability of the global climate system that irregularly occurs around 2 to 8 years of interval and is characterized by warmer (El Niño) and colder (La Niña) than usual ocean temperature in the equatorial eastern Pacific (Nyenzi & Lefale, 2006).

Walker (1924) first introduced possible linkages between the Southern Oscillation and Indian summer monsoon rainfall (ISMR). Afterward, many studies have been conducted to examine the relationship between ENSO and ISMR (Kirtman & Shukla, 2000;Ashok et al., 2004; Wu & Kirtman, 2004; Gadgil et al., 2004; Ashok & Saji, 2007; Ihara et al., 2008; Xavier et al., 2007; Curtis et al., 2018). These studies continually reveal the association between ENSO and monsoon variability. For example, several monsoon drought and flood years are associated with ENSO (Turner & Annamalai, 2012). Bhatla et al. (2015) studied the 142-year long historical rainfall data record and found that the severe droughts in the Indo Gangetic Plains are associated with El Niño events. Moreover, ENSO induces decreased South Asian monsoon rainfall by regulating the length of the rainfall season (Goswami & Xavier, 2005). Again, Bhatla et al. (2015) found that summer monsoon rainfall is enhanced in the El Niño years and subdued in the La Niña years. Chowdhury (2003) studied the relationship between ENSO and precipitation in the GBM basin from 1962 to 2000 and found an association. This study showed significant rainfall deficits

in strong El Niño years, whereas rainfall remained moderate to high during the moderate El Niño and La Liña years. According to Chowdhury (2003) if the Walker circulation is weak, the Hadley circulation is strong and upper tropospheric winds in the Western Pacific are westerly and as a consequences, the tropical disturbances are transported northward or north eastward depriving Bangladesh from precipitation and causing rainfall deficit or drought. On the contrary, when the southern oscillation index (SOI) is negative in moderate El Niño years, the Hadley circulation is not as strong as during major El Niño years and, therefore, it allows the tropical disturbances to cross into the Bay of Bengal and Bangladesh causing heavy rainfall and flooding (Chowdhury, 2003). Furthermore, this study revealed that the Ganges is a drier basin, and the rainfall variability in normal years is higher than in the wetter basins like Brahmaputra and Meghna. This finding is also supported by the earlier study of (Ropelewski & Halpert, 1987), who examined the world's 19 regions, including India, for a relationship between precipitation and ENSO. This finding indicates that the Ganges has a strong negative association with El Nino (Figure 1).

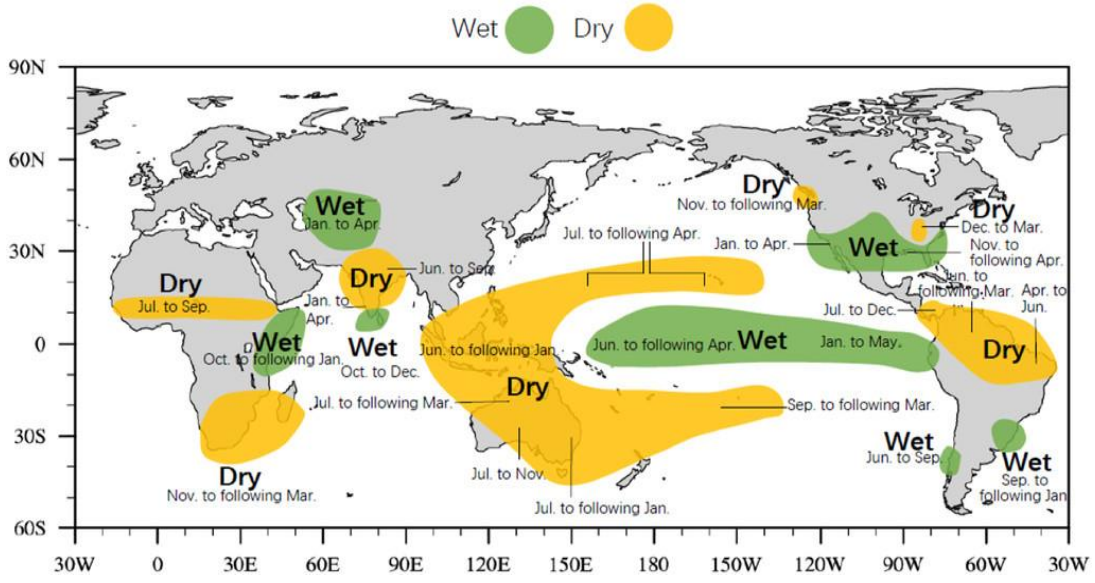

Figure 1: Global precipitation anomalies due to El Nino (Source: https://iri.columbia.edu/our-expertise/climate/enso/)

Another researcher, Whitaker et al. (2001), used streamflow data of the Ganges river from 1934 to 1993 to study the relation with ENSO. The results show the existence of a strong linear association, and the rate of change of ENSO is statistically related to the Ganges flow. Moreover, in the GBM river basin, Khandu et al. (2017) found that ENSO influenced about 10-20 % of the total annual rainfall over Bhutan, Nepal, Bangladesh, and north-eastern India from 1998 to 2013. Shrestha (2000) also revealed a significant relationship between monsoon precipitation and the Southern Oscillation Index (SOI) in Nepal. According to his result, precipitation was less in Nepal when the SOI was low.

2.8 Riverbank erosion in Bangladesh

Riverbank erosion is a regular phenomenon in a river system. When a river is in the natural flow state, and no external disturbances (human caused changes such as grazing, logging, construction of dams and flood control levees, channelization, urban development etc.) are present, the amount of material eroding from the riverbank and deposited as new sediments into the point bars become balanced. Ideally, the river cannot flow without any external disturbances all the time. When external factors play roles in the river system, they disturb the flow and turn the river into a non-equilibrium state. This process widens the channel and accelerates riverbank erosion. At this point, the deposited amount of sediment cannot balance the bank erosion, and rather it widens the bank (Madej et al., 1994).

Riverbank erosion is one of the major and unpredictable hazards of the world (Abidin et al., 2017). The major river systems with high riverbank erosion rates include the Ganges-Brahmaputra-Meghna (GBM) and Mekong rivers of Asia, Mississippi-Missouri river system of North America, Amazon river of South America, and Nile river of Africa (Das et al., 2014). The loss of land triggered by riverbank erosion is often a permanent phenomenon. Such a loss of

productive land creates a long-term effect on the economy, livelihood, and the environment. Moreover, it is hard to recover these lands once eroded (Das et al., 2014).

Bangladesh, a low-lying delta of the Ganges, Brahmaputra, and Meghna river basin, is highly susceptible to riverbank erosion (Islam & Rashid, 2011). Riverbank erosion is a perennial process (Chowdhury & Ward, 2004), where 92 percent of the total annual runoff generated from the GBM basin flows through Bangladesh. Moreover, Bangladesh consists of more than 700 rivers and their tributaries and 2400 kilometers of coastlines, making it highly susceptible to floods and riverbank erosion in different locations, towns, and growth centers (Islam & Rashid, 2011). Annually the GBM basin carries nearly one billion tons of sediments and one trillion cubic meters of water, which erode a thousand hectares of the flood plain in Bangladesh (Islam & Rashid, 2011). According to (ADB, 2013), GBM eroded approximately 2000 km^2 of land in Bangladesh over the past 40 years. Further, the Brahmaputra river eroded 3.82 square kilometers from 1996 to 2005 and accreted 6.1 square kilometers from 1995 to 2015 (Hassan et al., 2017). Rahman (2013) also reported evidence of riverbank erosion and land accretion in Bangladesh. Figure 2 shows an example of net riverbank erosion and land accretion in coastal Bangladesh from 1984 to 2007. As a result, erosion poses a threat to the people, agricultural land, infrastructures, and religious monuments (Rahman, 2013). Riverbank erosion compels thousands of Bangladeshis to migrate to safer places from their original land every year. According to the Ministry of Water Resources of the People's Republic of Bangladesh (2000), 729,000 people were displaced from their original land due to riverbank and char-land erosion from 1981 to 1993 in Bangladesh, which also erodes the family, kinship, and social ties. It is estimated that about one million people will directly or indirectly be affected by riverbank erosion each year (Islam & Rashid, 2011). It increases unemployment rates, poverty, and landlessness (Rahman, 2013).

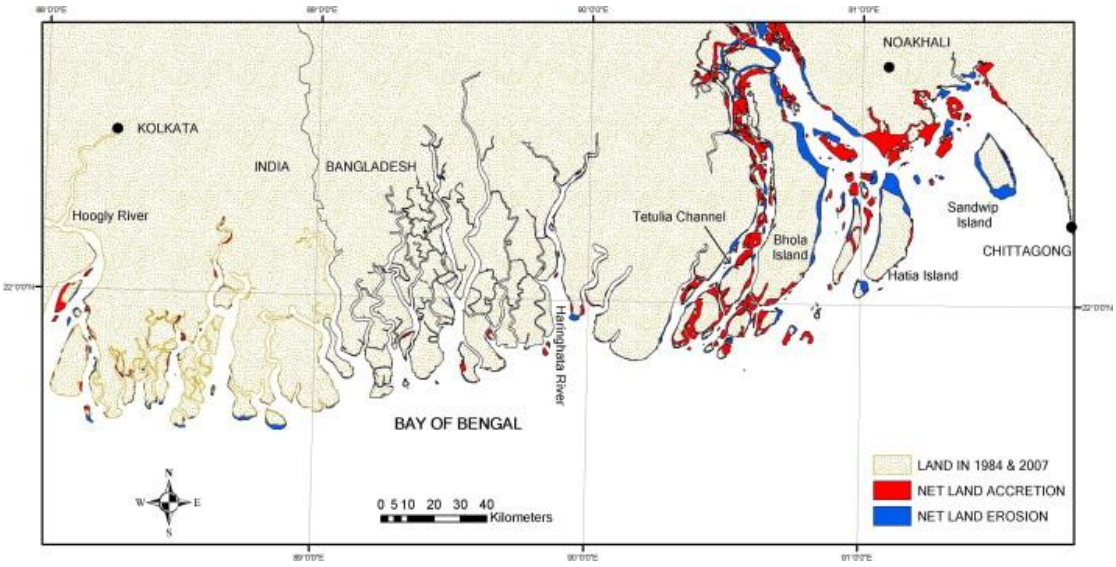

Figure 2: Coastal Bangladesh's land accretion and erosion from 1984 to 2007 (Source: Brammer, 2014).

The reasons behind the increasing riverbank erosion are alluvial deposits, regular shifting of the river channel, and continuous changing of shape and depth (Islam & Rashid, 2011; Nath et al., 2013). For example, the annual channel shifting of the three major rivers Ganges, Brahmaputra, and Meghna, ranges between 60 m to 1600 m (Rahman, 2013). Another reason that triggers riverbank erosion in the Ganges is riverbed siltation that decreases the river's depth and increases the pressure on both walls of the river during heavy discharge (Thakur et al., 2012). When the threshold of carrying a sediment load is exceeded, the river changes the structures from meandering to braided, which are highly prone to riverbank erosion (Leopold & Wolman, 1970). Brahmaputra river has a braided nature and a high erosion rate (Richardson & Thorne, 2001; Sarma & Acharjee, 2018), and every year significant land that is occupied by inhabitants erodes (Akhtar et al., 2011).

CHAPTER 3: MATERIALS AND METHOD

3.1 Study Area

The Ganges-Brahmaputra-Meghna (GBM) River Basin is the world's third-largest river basin after Amazon and Congo river basins (Chowdhury & Ward, 2004). It covers approximately 1.75 million km^2 (Mirza et al., 1998) and is home to 630 million people (FAO, 2011). GBM is a transboundary river basin (FAO, 2011) comprised of India (64%), China (18%), Nepal (9%), Bangladesh (7%), and Bhutan (3%) (Sharma et al., 2021 & FAO, 2011). Nepal and Bhutan are located entirely within the Ganges and Brahmaputra river basins, respectively. Whereas India and Bangladesh share areas with all three rivers basins and China is part of only the Ganges and Brahmaputra basins (FAO, 2011) (Figure 3).

The GBM elevation ranges from −24 to 8642 m above sea level, as shown in Figure 4, prepared using hydrological data and maps based on the SHuttle Elevation Derivatives at multiples Scales (HydroSHEDS) data layer in ArcGIS. The GBM river basin is elongated from the higher mountainous region to the Bay of Bengal and has unique climatic and physiographic features that leads to four seasons: pre-monsoon, monsoon, post-monsoon, and winter (FAO, 2011). This study only focuses on pre-monsoon and monsoon seasonal precipitation analysis in the GBM river basin. Among the four seasons, more than 80% of the 1500 mm of GBM annual rainfall (FAO, 2011) accumulates in the monsoon season between June to September and the remaining 20% to 30% in the dry season. Less precipitation occurs in the Ganges compared to the Brahmaputra and Meghna river basins (Mirza et al., 1998). The Ganges river enters Bangladesh through the western side, and the Brahmaputra enters from the northern side. The three rivers meet in Bangladesh's Chandpur district and flow into the Bay of Bengal as the Meghna river (Islam et al., 2010), comprising the world's third-largest freshwater system (Mirza, 2011). This river system forms the

largest delta in the world (GOB-Bangladesh Planning Commission, 2018). A delta forms when larger rivers continuously deposit sediments at the land-sea interface over hundreds and thousands of years. The deposited sediments are highly productive and nutrient-rich (Ibáñez et al., 2019). Apart from the negative impacts like floods, riverbank erosion, climate change, sea-level rise, and drought, the GBM delta supports the lives of millions of people by creating opportunities in agriculture, fishing, and sea transportation. The land is highly fertile because of the deposited sediments and fine soils from upstream (GOB-Bangladesh Planning Commission, 2018).

Figure 3: Study area map of the GBM river basin

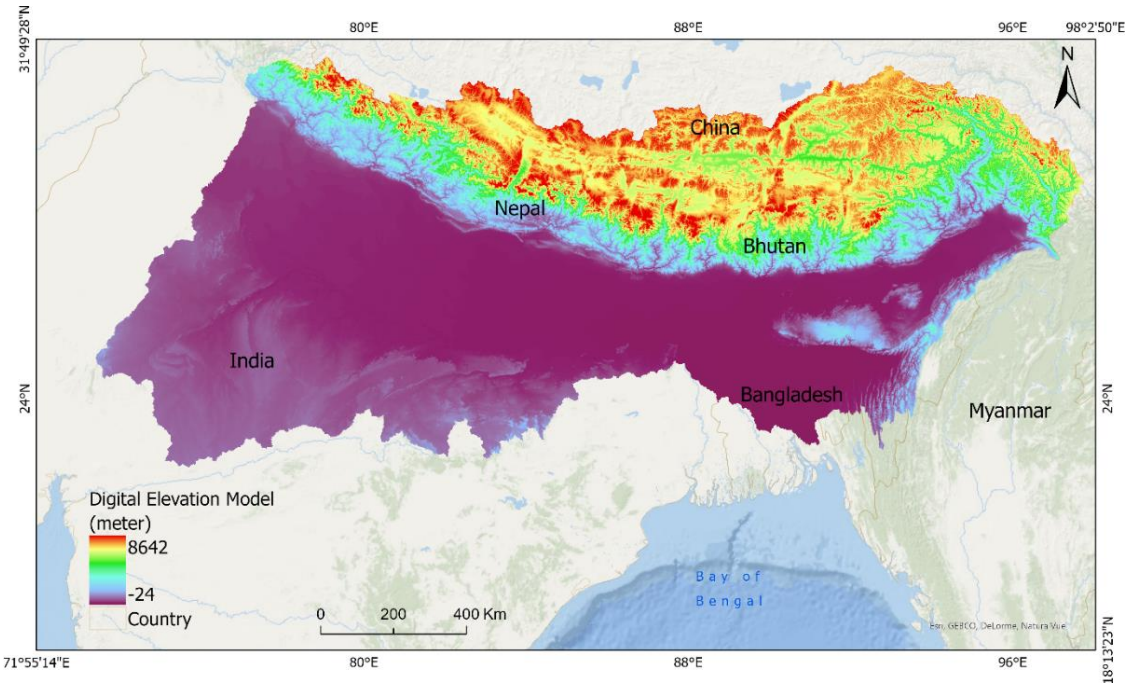

Figure 4: Digital elevation model of the GBM river basin.

3. 2 Data

3.2.1 Precipitation Estimation from Remotely Sensed Information Using Artificial Neural Networks- Climate Data Record (PERSIANN-CDR)

Over the last two decades, various studies have been conducted by the PERSIANN family, namely PERSIANN, PERSIANN- CLOUD CLASSIFICATION SYSTEM (PERSIANN-CCS), and PERSIANN-CDR (Nguyen et al., 2018). The PERSIANN algorithm uses combined infrared imagery and passive microwave information from multiple Geosynchronous Equatorial Orbit (GEO) and Low Earth Orbit (LEO) satellites as an input to the Artificial Neural Network model. The PERSIANN-CDR used a modified PERSIANN algorithm to estimate the precipitation from 1983 to the present (Ashouri et al., 2015). The PERSIANN-CDR precipitation product (Ashouri et al., 2015) was developed at the Center for Hydrometeorology and Remote Sensing (CHRS) at

the University of California, Irvine in collaboration with National Aeronautics and Space Administration (NASA), National Oceanic and Atmospheric Administration (NOAA), and the United Nations Educational, Scientific and Cultural Organization (UNESCO) program for the Global Network on Water and Development Information for Arid Lands (Table 1). This PERSIANN-CDR algorithm eliminates passive microwave imagery and only uses the high temporal and spatial resolution infrared imagery from various international GEO satellites. This product uses the National Centers for Environmental Prediction (NCEP) stage IV hourly precipitation to train the Artificial Neural Network model. It is adjusted using the Global Precipitation Climatology Project (GPCP) version 2.2 monthly precipitation product to reduce the bias in the PERSIANN-CDR product. The bias-corrected final product uses a modified PERSIANN algorithm that adjusts gridded satellite infrared data (GridSat-B1) by the Global Precipitation Climatology Project (GPCP) monthly products to estimate global daily precipitation with 0.25 × 0.25-degree spatial resolution (Ashouri et al., 2015). It covers latitudes between 60° S and 60° N and provides rainfall data every 3 h from 1983 to the present. The gauge adjusted PERSIANN 3-hourly rainfall with 0.25° resolution ensures the precipitation data consistency and quality. Figure 5 explains the simplified algorithm process of PERSIANN-CDR (Ashouri et al., 2015). These characteristics make the PERSIANN-CDR a reliable and useful satellite-based product for global climate studies and extreme weather events (Ashouri et al., 2015). It has been used continuously for different studies throughout the world by researchers in climate change, hydrology, water resources management, and natural hazards (Nguyen et al., 2018). Some other researchers around the globe have also shown the usefulness of the PERSIANN-CDR data by studying daily, monthly, and extreme precipitation patterns (Katiraie-Boroujerdy et al., 2017; Arvor et al., 2017; Miao et al., 2015; Ashouri et al., 2016; Ashouri et al., 2015). Shah & Mishra

(2016), Mondal et al. (2018), and Hussain et al. (2018) have further demonstrated the usefulness of PERSIANN-CDR in South Asia. Finally, this study extends Curtis et al. (2017), who studied monsoon precipitation patterns from 1983 to 2015 using the PERSIANN-CDR product in the GBM basin. Thus, PERSAINN-CDR has a track record of success in estimating rainfall in South Asia. It addresses the need for relevant, high-resolution, and long-term precipitation data for hydrological and climate studies (Ashouri et al., 2015). The required PERSIANN-CDR precipitation data from 1983 to 2019 was retrieved from the Center for Hydrometeorology and Remote Sensing (CHRS) data portal website at https://chrsdata.eng.uci.edu. The number of grid boxes covered by GBM river basin was 2309 (see Table 1 and Figure 6).

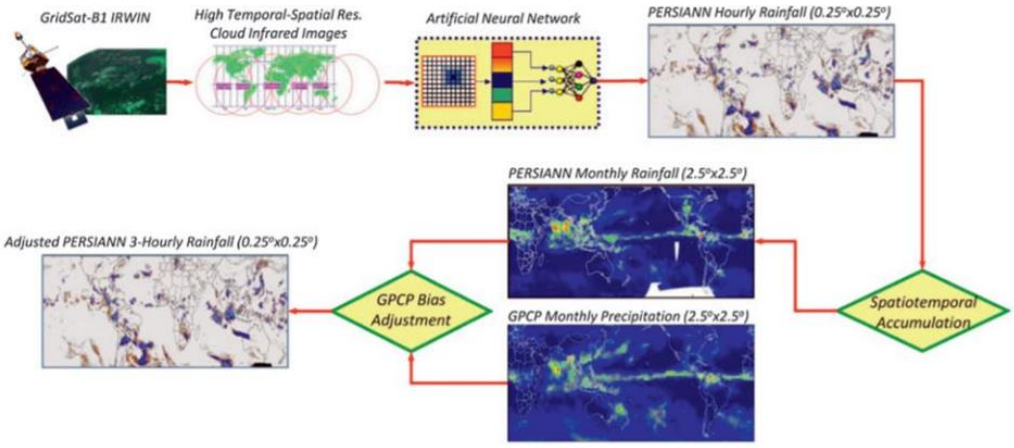

Figure 5: A schematic diagram of the PERSIANN-CDR algorithm (Source: Ashouri et al., 2015)

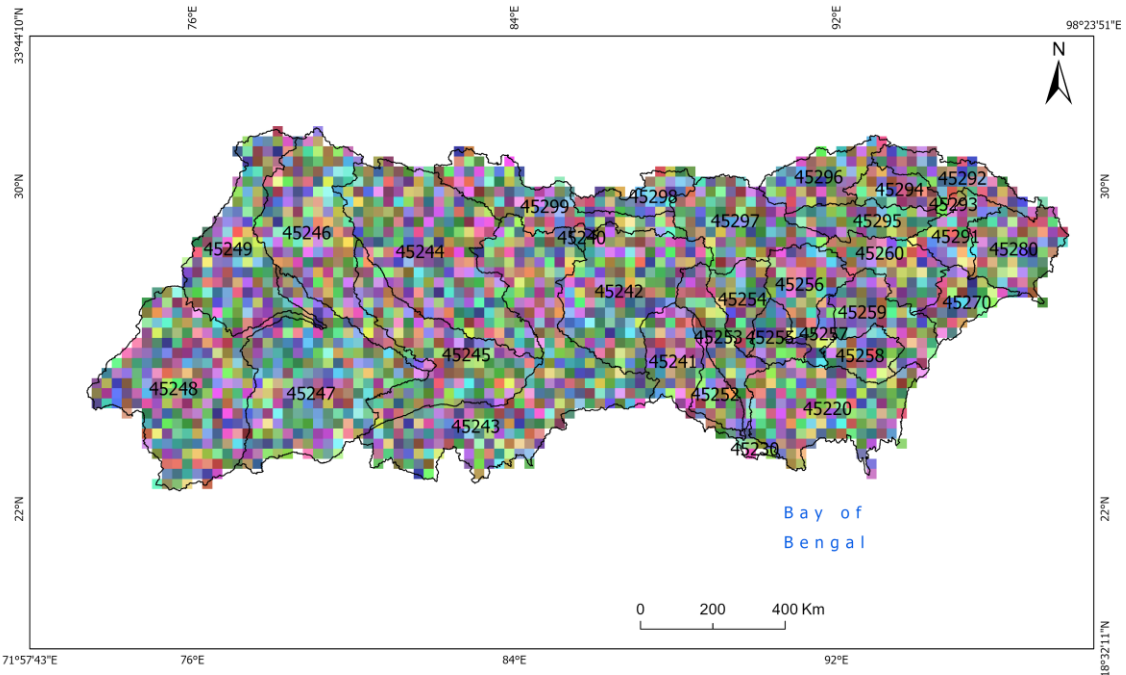

Figure 6: A map showing the grid boxes covered by PERSIANN-CDR. Colors are randomized to show the grid resolution

3.2.2 Multi-Source Weighted Ensemble Precipitation (MSWEP)

MSWEP (Version 2) is a newly developed global precipitation product with 0.1-degree spatial resolution (Beck et al., 2019) that provides rainfall data at 3 hour temporal resolution from 1979 to the present (Table 1). Figure 7 explains the detailed steps implemented to produce MSWEP. It uses gauges (WorldClim, Global Historical Climatology Network-Daily (GHCN-D), Global Summary of the Day (GSOD), and others), satellites (CMORPH, GridSat, Global Satellite Mapping of Precipitation (GSMaP), and TRMM Multi-satellite Precipitation Analysis (TMPA) 3B42RT), and reanalysis-based products (European Centre for Medium-Range Weather Forecasts (ECMWF) interim reanalysis (ERA-Interim), Japanese 55-year Reanalysis (JRA-55), and National Centers for Environmental Prediction-Climate Forecast System Reanalysis (NCEP-CFSR)) to estimate precipitation over the entire globe (Beck et al., 2017). Compared to other precipitation products, MSWEP is more accurate in estimating precipitation over mountainous regions (Beck et

al., 2019). It also uses a precipitation gauge correction approach at a daily time scale to improve time mismatching (Beck et al., 2019). All these quality enhancements maximize the reliability of this product (Awange et al., 2019). However, there is a lack of scientific research using MSWEP. The required precipitation data was retrieved from the GloH2O website at http://www.gloh2o.org/mswep. The number of grid boxes covered by GBM river basin was 14,401 (see Table 1 and Figure 8)

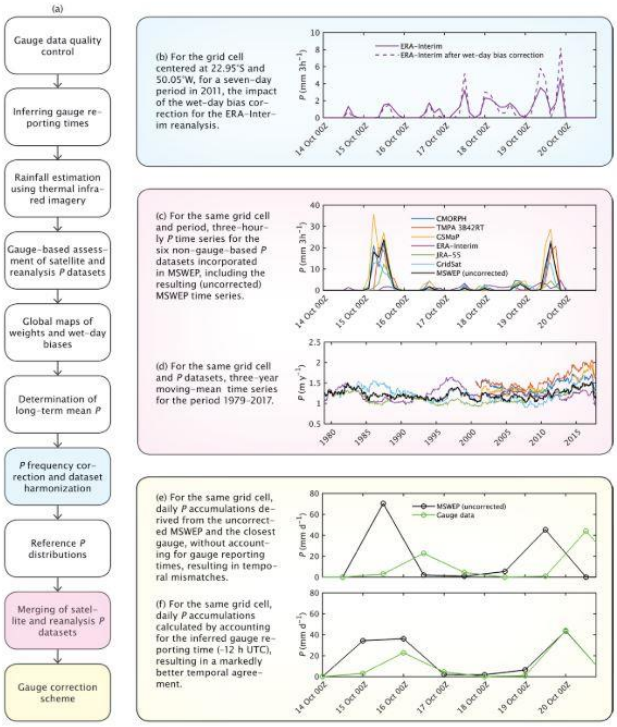

Figure 7:Flowchart showing the main process implemented to produce MSWEP V2 (Source: Beck et al., 2019).

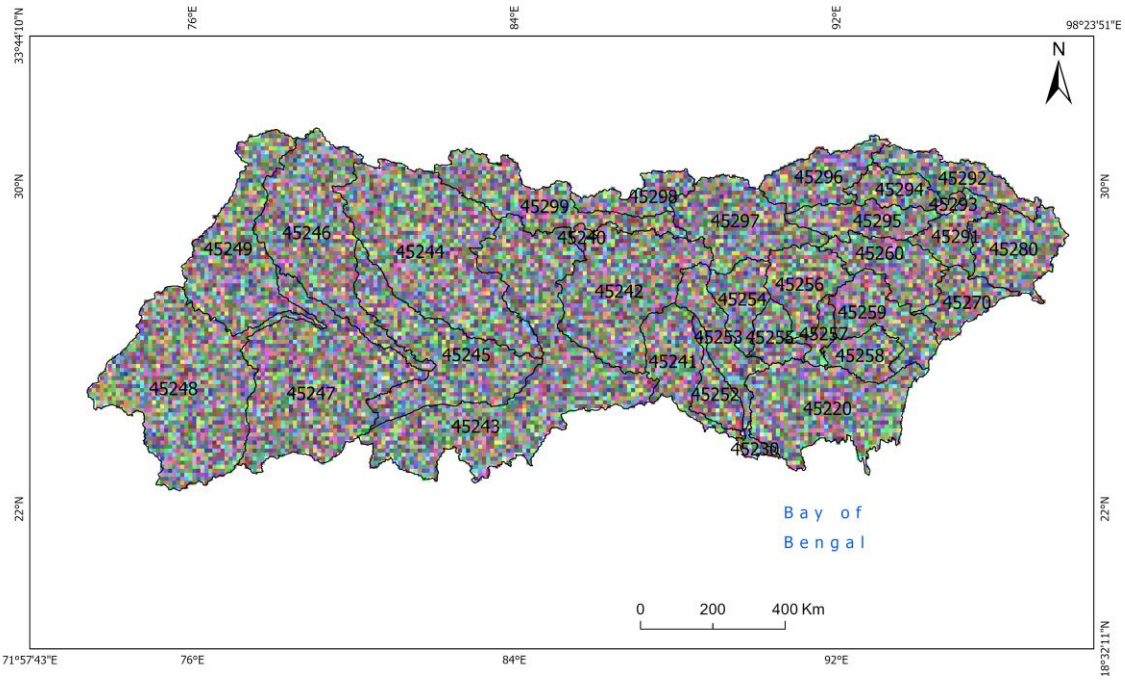

Figure 8: A map showing the grid boxes covered by MSWEP in the GBM river basin. Colors are randomized to show the grid resolution.

Table 1: Summary of satellite-based precipitation product used in this study.

Satellite-Based Precipitation Product	Spatial Resolution	Temporal Resolution	Spatial Coverage	No. of Grid Boxes Covered by GBM	Data Availability	References
MSWEP	0.1°	3h	Fully global	14,401	1979–Present	Beck et al. (2019)
PERSIANN-CDR	0.25°	3h	60°S–60°N globally	2309	1983–Present	Ashouri et al. (2015)

3.2.3 Rain Gauge Station Data

Traditional rain gauge stations provide the most accurate rainfall data and are considered as an important complement for satellite-based observations. However, rain gauge data collection is challenging in many parts of the world due to the topography, economy, and a variety of administrative and technical reasons. GBM river basin has a similar problem with inadequate

gauge coverage for the whole basin. This study uses 223 daily rain gauge observations from Nepal located entirely within the Ganges river basin (Figure 3) for validation (see Figure 9). Rain gauge station data was purchased from the Department of Hydrology and Meteorology of Nepal (http://dhm.gov.np/meteorological-station). The rain gauge data covers the period from 1983-2009 for this analysis. The station data are randomly distributed (see Figure 9), but a large number of stations are installed at low elevation and very few are at higher elevation (Figure 9). The reason for choosing Nepal only, is the unavailability of rain gauge station data from other countries and the priority for validation over mountainous terrain. Generally, the validation of global satellite-based precipitation products are based on direct comparison with rain gauge networks and their predictive ability of streamflow rate in the hydrological modelling categories (Bitew & Gebremichael, 2011; Hirpa et al., 2010). This study follows the direct comparison of satellite products PERSIANN-CDR and MSWEP to the rain gauge station data. This study assesses the accuracy and intercomparison of these two high-resolution satellite-based precipitation products (PERSIANN-CDR and MSWEP) for Nepal (GBM) from 1983 to 2009.

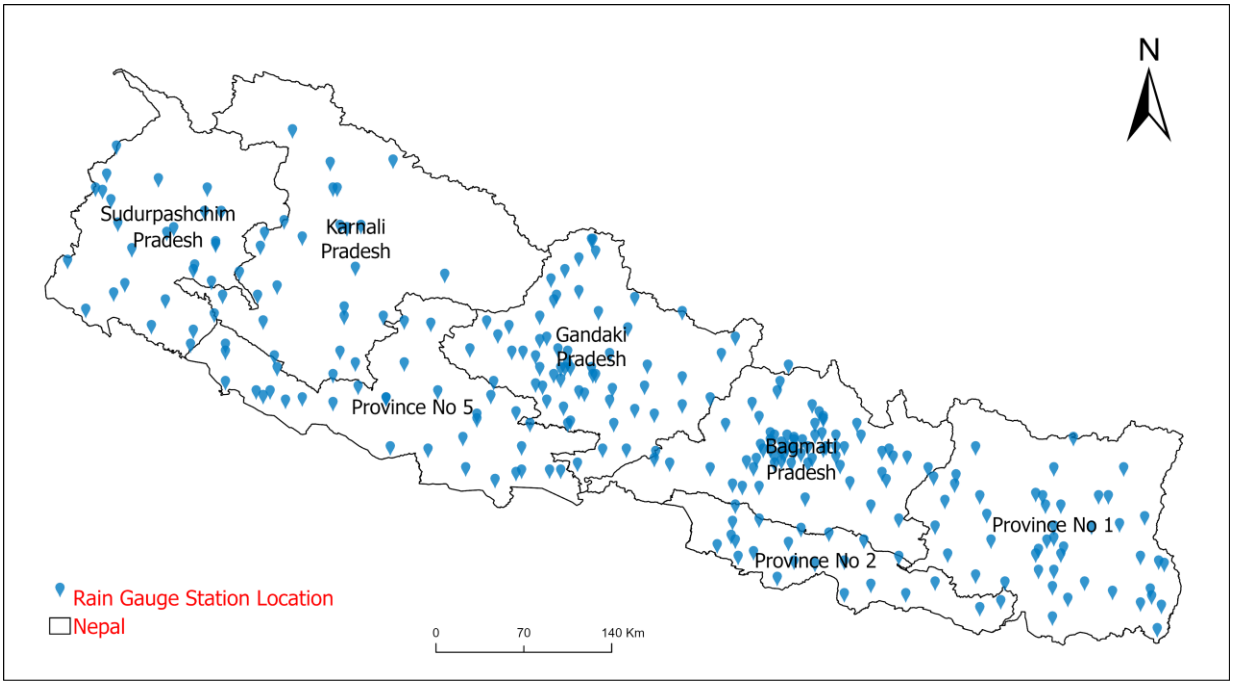

Figure 9: A Map of Nepal showing Locations of the 281 Rain Gauge Station.

3.3 Method

This section first discusses the continuous statistical indicator method to validate and compare two satellite products against the rain gauge station of Nepal. Secondly, the Pearson correlation coefficient method is described for the relationship between seasonal precipitation and ENSO based on hydrological sub-basins and water routing distance. Third, this section describes the modified Mann-Kendall test to study the precipitation trend from 1983 to 2019. Fourth, the shoreline transects and number of extreme daily precipitation are defined in determining the relationship between riverbank erosion and extreme precipitation in coastal Bangladesh.

3.3.1 Analysis Methods for the Validation of the MSWEP and PERSIANN-CDR over Nepal (GBM)

Before working on the main research questions, this study first evaluated the performance of two satellite-based rainfall products in providing reliable rainfall estimates for Nepal, one of the

countries of the GBM river basin. The results of the validation will be useful in selecting or rejecting these two products for Nepal. However, these findings limit any solid conclusion for the efficacy of these two products for whole GBM.

At first, data from 281 daily rain gauge station were collected for the validation of PERSIANN-CDR and MSWEP products. This study excluded those stations that had less than 26 years of precipitation data and excluded those years that were missing values more than 3 days of precipitation for both pre-monsoon and monsoon seasons. Therefore, this study only uses a yearly averaged sum of pre-monsoon and monsoon precipitation of 223 rain gauge stations from 1983 to 2009 for the validation. Both pre-monsoon (March-April-May) and monsoon (June-July-August-September) days were summed and averaged separately for validation using an R programming language. After that, MSWEP and PERSIANN-CDR precipitation data were averaged separately over the pre-monsoon and monsoon seasons for all grid boxes which lie within the latitude and longitude location of the Nepal station data. ArcGIS Pro 2.8.1 was used for averaging the satellite data.

There are multiple ways to compare and validate different satellite-based precipitation products with other rainfall measurements on global and regional scales such as using categorical and volumetric indices, and continuous statistical measures (Ayehu et al., 2018). This study applied continuous statistical indicator to compare the precipitation between the rain gauge and these two satellite-based precipitation products (Tan et al., 2015; Tan et al., 2017). This method was successfully implemented by (Tan et al., 2015; Tan et al., 2017) on validating the PERSIANN-CDR and other products with Malaysian rain gauge stations. The coefficient of determination (R^2), Root Mean Square Error (RMSE), and the Relative Bias (RB) are included in the continuous indices. The coefficient of determination is widely used to evaluate the correlation between two

data sets, Root Mean Square Error measures the differences between two data sets, and Relative Bias estimates the systematic bias of satellite precipitation. The value of the coefficient of determination ranges between 0 and 1. The zero value shows no relationship between the data sets, and 1 shows the perfect correlation. The value of zero is a perfect score for RMSE. Therefore, the higher values of the coefficient of determination combined with the lower root mean square errors (RMSE) and relative biases (RB) indicate rainfall accuracy (Tan et al., 2015; Tan et al., 2017).

The equations are as follows:

$$R^2 = \frac{\sum_{i=1}^{n}(O_i - O)(E_i - E)}{\sqrt{\sum_{i=1}^{n}(O_i - O)^2}\sqrt{\sum_{i=1}^{n}(E_i - E)^2}} \quad (1)$$

$$RMSE = \sqrt{\frac{\sum_{i=1}^{n}(E_i - O_i)^2}{n}} \quad (2)$$

$$RB = \frac{\sum_{i=1}^{n}(E_i - O_i)}{\sum_{i=1}^{n} O_i} \quad (3)$$

Where the O_i and E_i denote the observed and expected rainfall at the *ith* value of the time series and n is the number of values, respectively. This research would be the first to validate the PERSIANN-CDR and MSWEP in the GBM basin.

This study also tested the correlation between elevation of the rain and relative differences. The relative difference (RD) was first calculated as the absolute difference between rain gauge station data and satellite data. Then the final value was divided by rain gauge station data. The equation are as follows:

$$RD = \frac{Rain\ guage\ precipitation - Satellite\ precipitation}{Rain\ gauge\ precipitation}$$

3.3.2 Correlation Analysis

Correlation analysis is a statistical method to measure degree of association between two quantitatively measured variables. The major work of this study was to analyze correlation between two variables. This study used the common Pearson Correlation Coefficient (*r*) to assess the strength of the two quantitative variables. For the two variables X and Y, correlation coefficient r is computed by the following equation:

$$r = \frac{\sum(X_i - \bar{X})(Y_i - \bar{Y})}{\sqrt{\sum(X_i - \bar{X})^2 \ \sum(Y_i - \bar{Y})^2}}$$

The values of *r* always lie between -1 to 1. It is a unitless measure of correlation. This study tested correlation for significance at the 5 % level.

3.3.3. Analysis Methods for the Relationship Between Pre-monsoon and Monsoon Precipitation in the GBM River Basin

MSWEP and PERSIANN-CDR seasonal precipitation data were then averaged over the entire GBM river basin and within 34 pre-defined hydrological sub-basins of the GBM separately. The sub-basin boundaries correspond to the HydroBASIN GIS layer from the World Wildlife Fund (Lehner & Grill, 2013). Figure 10 shows the Pfafstetter level-05 sub-basins boundaries of the GBM obtained from the World Wildlife Fund (Gland, Switzerland). The Pfafstetter coding system was developed by Otto Pfafstetter in 1989 and is widely used for the description of watersheds or basins. It assigns ID numbers based on the topology of the land surface to describe watersheds as either basin, inter-basin, or internal basin. Pfafstetter level-05 corresponds to inter-basin due to the contribution of additional water to the main stem (Pfafstetter, 1989). Here, the coding number of each sub-basin increments from downstream to upstream. This study only considered 32 pre-

defined hydrological sub-basins among the total of 34 when using PERSIANN-CDR. We excluded the two smallest sub-basins that were not covered by the 0.25-degree grid resolution of PERSIANN-CDR.

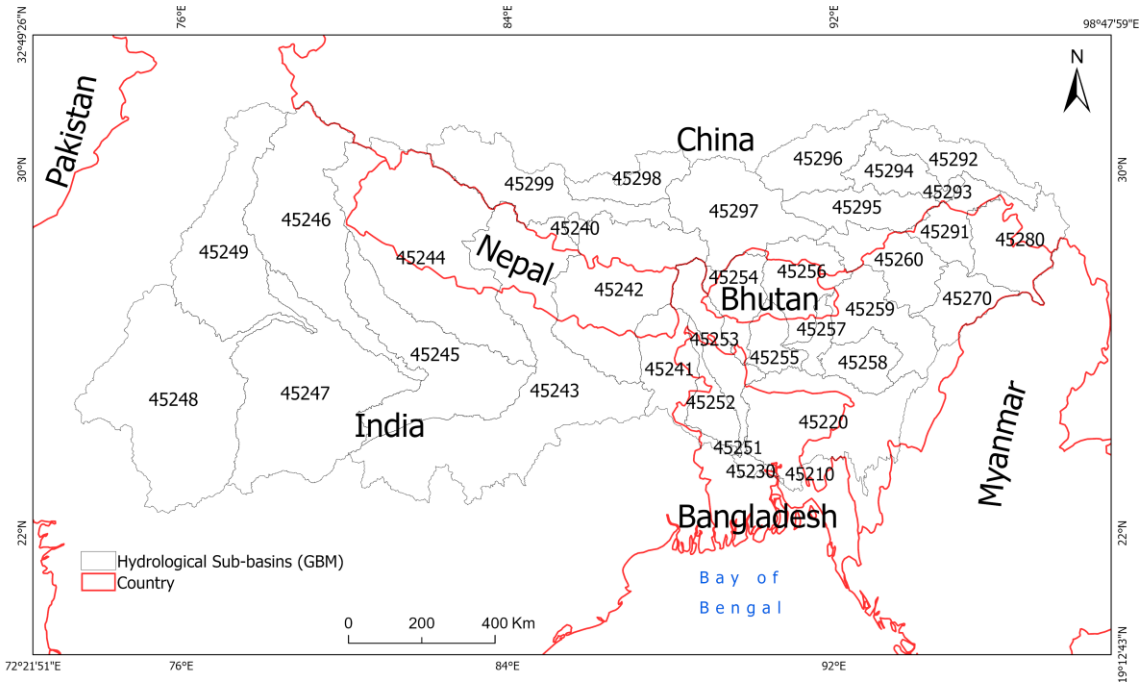

Figure 10: Hydrological sub-basins boundaries of the Pfafstetter level-05 of GBM. Numbers are the Pfafstetter identification codes. Country boundaries are the red lines.

3.3.4 Water Routing Distance

A Water routing distance also known as flow length is the distance from one defined point to the outlet of the watershed. It calculates both the upstream and downstream distance. The main objective of the water routing tool is to calculate the longest flow path within a given basin. (https://desktop.arcgis.com/en/arcmap/latest/tools/spatial-analyst-toolbox/flow-length.htm). It is a method to measure distance traveled by streamflow within the river basin. Figure 11 shows that the higher the distance of the water bodies to the main channel, the smaller the water level fluctuations. This figure clearly shows the importance of flow length distance of water bodies to

the main channel to accelerate any natural hazard such as riverbank erosion. The objective of using water routing distance based sub-basins is to provide an alternative in relating precipitation variability in the GBM with riverbank erosion in the outlet of Bangladesh.

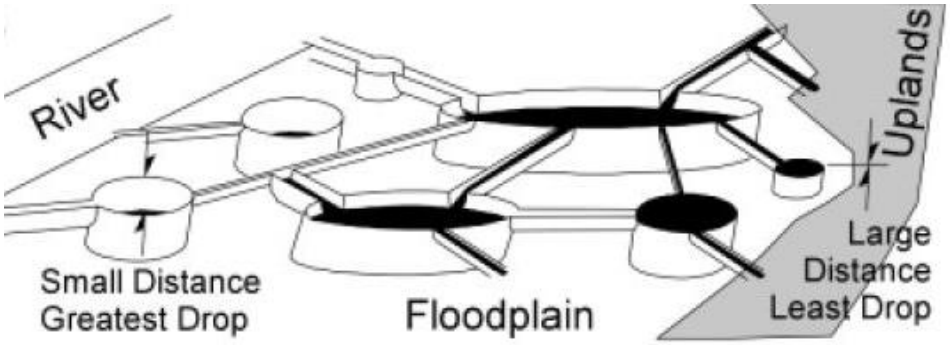

Figure 11: Flood plain geomorphology schematic (Source: Alsdorf, 2003*).*

Using drainage direction at 30 arc-second resolution extracted from HydroSHEDS, the water routing distance (Figure 12) to the outlet were studied in ArcGIS for every PERSIANN-CDR grid cell in the GBM. Seasonal precipitation averages were taken over cells with equal flow lengths (EFL) (Figure 13) from 1983 to 2019. From this information, ten distance classifications were defined (Figure 13) using the equal interval method in ArcGIS Pro. While there are relationships between the EFL-based classifications and the pre-defined hydro basins (compare Figure 10 and Figure 13), the EFL-based classifications can be divided spatially. For example, water would travel an equally long distance from the western GBM as the northern GBM (see 9 and 10 in Figure 13). Finally, this study adopted the same correlation statistics as the hydrological sub-basins in the R programming language. Figure 14 shows the average sizes of water routing distance and hydrological sub-basins.

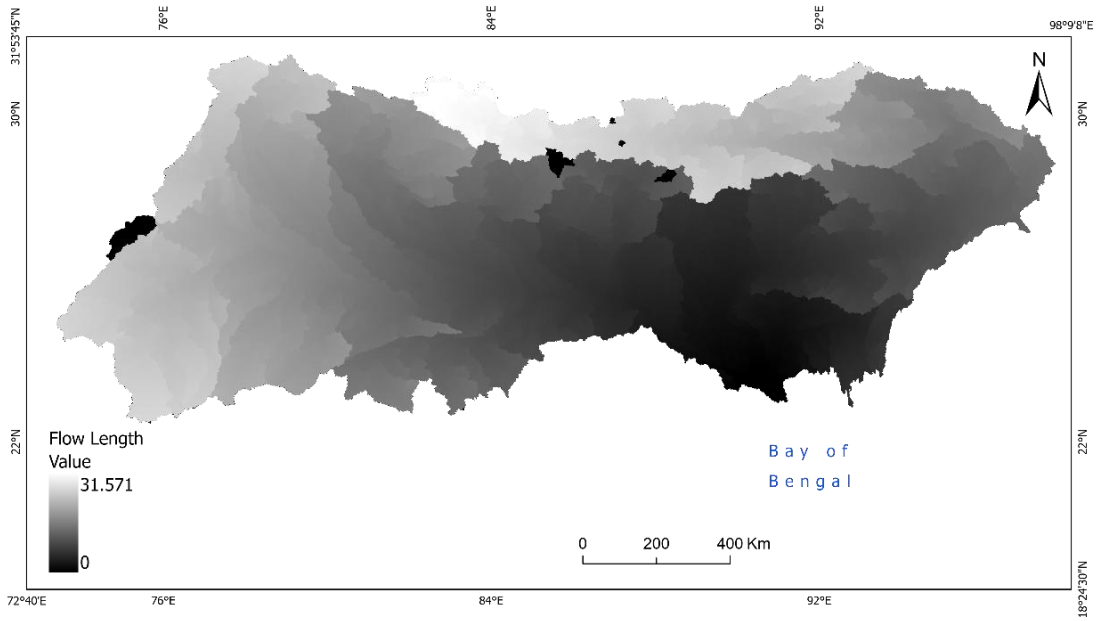

Figure 12: Initial water routing distance also known as flow length Map of GBM River Basin.

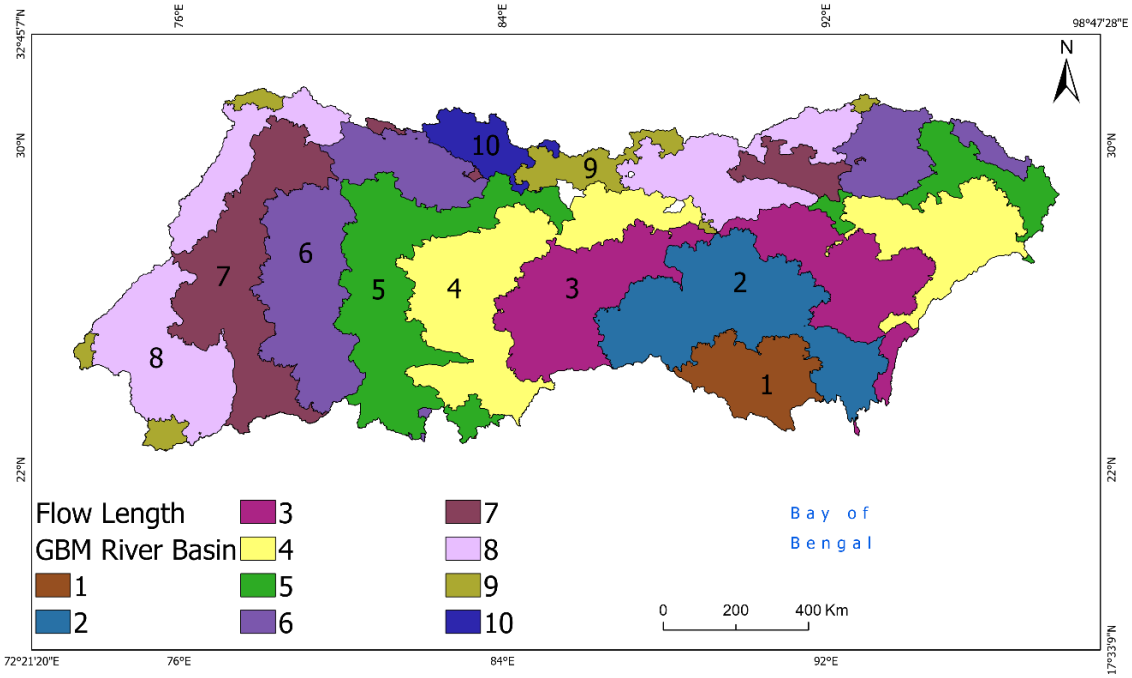

Figure 13: Classification of water routing distance (flow length) based on GBM river basin. Sub-basin 1 indicates the shortest distance to reach the outlet of the basin once the precipitation occurs compared to 10.

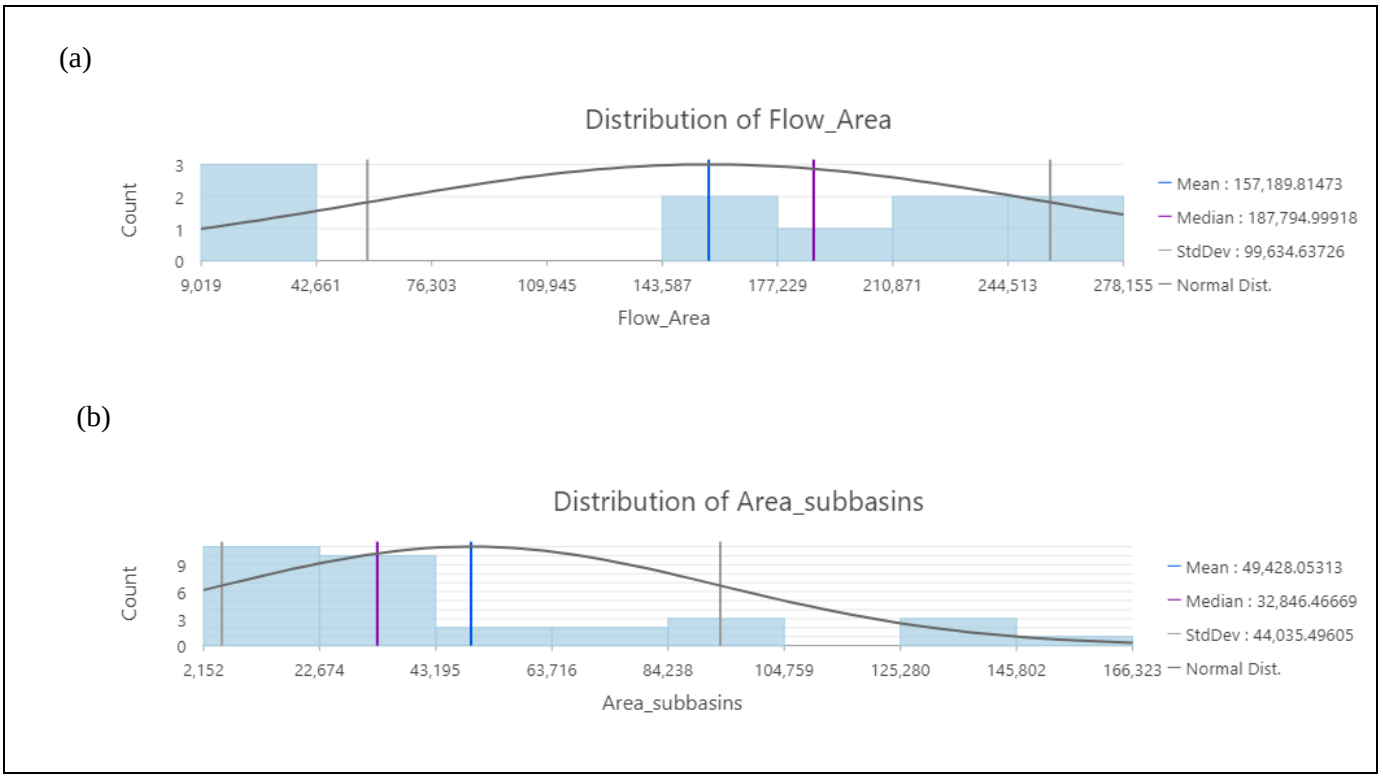

Figure 14: (a) shows the average sizes of water routing distance of the grid cells and (b) shows the average sizes of hydrological sub-basins of GBM river basin.

3.3.5 Analysis Methods for the Relationship Between Multivariate ENSO Index (MEI) and Seasonal Precipitation Based on Hydrological Sub-basins and Water Routing Distance in the GBM River Basin

This study investigated the interannual variability in seasonal precipitation related to ENSO in the GBM river basin based on 32 hydrological sub-basins and water routing distance. This study only uses PERSIANN-CDR satellite-based precipitation data for the analysis. MSWEP could have also been used, but we found a strong year-to-year correlation between the two products, so any differences are likely to be small (see Figures 32 and 33 and accompanying discussion). There are several ways to measure ENSO based on mean sea level pressure difference, sea surface temperature, outgoing longwave radiation, and wind across the tropical pacific (Jiménez-Esteve &

Domeisen, 2018). The widely used indicators are the Southern Oscillation Index and several sea surface temperature indices. A multivariate ENSO index (MEI) is generated to integrate more information on coupled ocean-atmosphere phenomena. It includes sea level pressure, sea surface temperature, zonal and meridional components of surface wind, surface air temperature, and cloudiness. In this study, MEI was chosen to study ENSO and data was retrieved from the NOAA Physical Science Laboratory (https://psl.noaa.gov/data/climateindices/list/). This study used correlation statistics in the R programming language for correlation between MEI and seasonal precipitation based on hydrological sub-basins and water routing distance in the GBM river basin. ArcGIS Pro 2.8.1 was used to create maps for this study.

3.3.6 Analysis Methods for Precipitation Trends in the GBM River Basin Using Seasonal Precipitation Based on PERSIANN-CDR and MSWEP

The Modified Mann-Kendall test was applied to quantify and compare the trend pattern of the long-term time series of PERSIANN-CDR and MSWEP seasonal precipitation. The 'modifiedmk' package was used in R to write the algorithm for the non-parametric modified Mann-Kendall trend test, and ArcGIS Pro 2.8.1 was used to create maps for this study. The methodology is described in Figure 15.

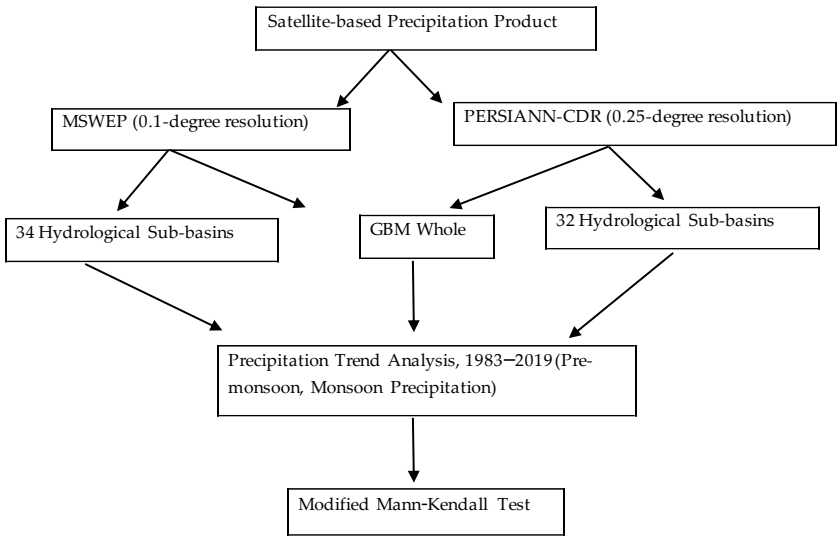

Figure 15: Flow chart of the methodology demonstrating the steps used in precipitation trend in this study.

3.3.6.1 Mann-Kendall Test

Various statistical methods such as parametric, non-parametric, and Bayesian methods have been used to detect trends. Many researchers have used the Mann-Kendall test to estimate precipitation trends in different parts of the world (Sayemuzzaman & Jha, 2014) (Mirza et al., 1998); Kothyari et al., 1997), (Ghalhari et al., 2016),(Júnior et al., 2020),(Hu et al., 2019). A Mann-Kendall trend test is a non-parametric test used (Mann, 1945) and (Kendall, 1975) to identify trends in time series data. It is frequently used to study spatial variation and temporal trends of hydro-climatic time series (Mondal et al., 2012). The null hypothesis of the Mann-Kendall trend test assumes that there is no trend in the data. The statistical method is briefly discussed below.

The Mann-Kendall statistic Mann (1945), Kendall (1975) is given as:

$$S = \sum_{i=1}^{n-1} \sum_{j=i+1}^{n} sgn(x_j - x_i) \quad (1)$$

where,

n = number of data points,

x_i = data value in time series I,

$i = 1, 2, \ldots, n - 1$,

x_j = data value in time series j (where $j > i$),

$j = i + 1, i + 2, \ldots, n$,

$sgn\ (x_i - x_j)$ is the sign function.

The variance is computed as:

$$Sgn(x_j - x_i) = \begin{cases} +1, if(x_j - x_i) > 0 \\ 0, if(x_j - x_i) = 0 \\ -1, if(x_j - x_i) < 0 \end{cases} \quad (2)$$

$$Var(S) = \frac{n(n-1)(2n+5) - \sum_{i=1}^{m} t_i(t_i - 1)(2t_i + 5)}{18} \quad (3)$$

where,

n = number of data points,

m = number of tied groups,

t_i = number of ties of extent i (a tied group is a set of sample data having the same value).

The standard normal test statistics Z is computed using Equation (4):

$$Z = \begin{cases} \frac{S-1}{\sqrt{v_{ar(S)}}}, if\ S > 0 \\ 0, if\ S = 0 \\ \frac{S+1}{\sqrt{var(S)}}, if\ S < 0 \end{cases} \quad (4)$$

Positive values of *Z* indicate increasing trends, while negative *Z*-values indicate decreasing trends. Testing trends is based on the specific α significance level of 0.05. The null hypothesis is rejected if the |*Z*| value is greater than 1.96, which corresponds to the 95% significance level based on a look-up table.

3.3.6.2 Modified Mann-Kendall Test

The Mann-Kendall test failed to address autocorrelation in the time series data. Therefore, the Modified Mann-Kendall (MMK) test is used to resolve this concern. The modification of the test improves the accuracy rate of the significance levels and decreases the chance of a nonexistent trend (Hamed & Rao, 1998). This study used the Modified Mann-Kendall test based on the variance correction approach introduced by (Hamed & Rao, 1998).

The modified variance (*S*) is given by:

$$Var(S) = \frac{n(n-1)(2n+5)}{18}\frac{n}{n_S^*}$$

Where,

$$\frac{n}{n_S^*} = 1 + \frac{2}{n(n-1)(n-2)} \times \sum_{i=1}^{n-1}(n-i)(n-i-1)(n-i-2)\rho_S(i)$$

n = actual number of observations,

$\rho_S(i)$ = autocorrelation function of the ranks of the observations,

$\frac{n}{n_S^*}$ = represents a correction due to the autocorrelation in the data.

3.3.7 Analysis Methods for the Relationship Between Riverbank Erosion in Coastal Bangladesh with Local Extreme Daily Precipitation and Monsoon Precipitation of the GBM River Basin

This portion of study only used the MSWEP satellite-based precipitation product for the analysis of local extreme daily precipitation and its relation to riverbank erosion. We used only MSWEP due to its higher spatial resolution given the size of the study area (Figure 16). The local study area (Figure 16) was covered by 9 gird boxes of MSWEP and divided into north, central and south regions for the analysis. Each region was covered by three grid boxes. At first, MSWEP NetCDF formatted data was retrieved using the R programming language. Extreme precipitation was defined as the 95th percentile of daily rainfall for all monsoon days from 1988 to 2017. Once the extreme daily precipitation was identified per grid box, then the total number of extreme precipitation days was counted for each region, north, central, and south, separately.

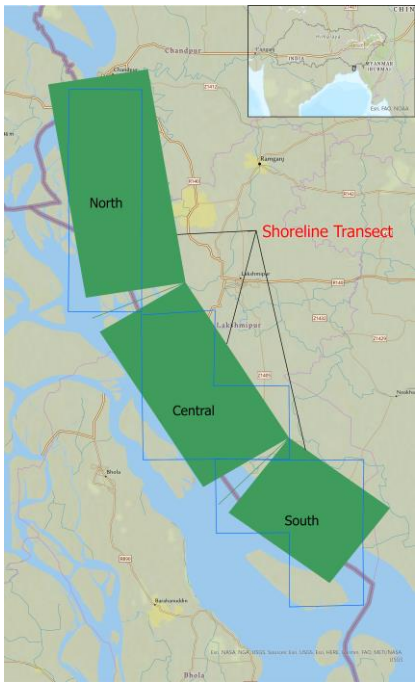

Figure 16: A map shows the shoreline study area located in the east bank of the lower Meghna estuary (Coastal Bangladesh). The North, Central, and South green boxes indicate the three regions, and each boxes of the green color indicates the shoreline transect for each region.

As this research is a part of the broader project "Coastal Erosion Vulnerabilities, Monsoon Dynamics, and Human Adaptive Response," all the required riverbank erosion data was provided by other investigators (Crawford et al., 2020). At first, Landsat imagery with 30 m pixel resolution with free cloud coverage was used to produce and describe a thirty-years of shoreline change for an 80-km stretch of the Lower Meghna estuary using Digital Shoreline Analysis (DSAS) software (Crawford et al., 2020). Riverbank erosion was quantified by the study of shoreline change analysis. Figure 17 shows an example of the shoreline transect preparation in the study area (Crawford et al., 2020). This study uses End Point Rate (EPR) for the annual change of shoreline in meters per year. Only changes greater than 30 m are considered due to the resolution of the pixels.

Changes for each transect over the north, central, and south regions were summed separately (see green boxes in Figure 16), with erosion as negative values and accretion as positive values. In summary, this study analyzed the relationship between total monsoon precipitation in the GBM along with localized extreme daily precipitation frequency in the north, central, and south regions, with riverbank erosion for the north, central and south regions respectively. Correlation statistics were produced in the R programming language.

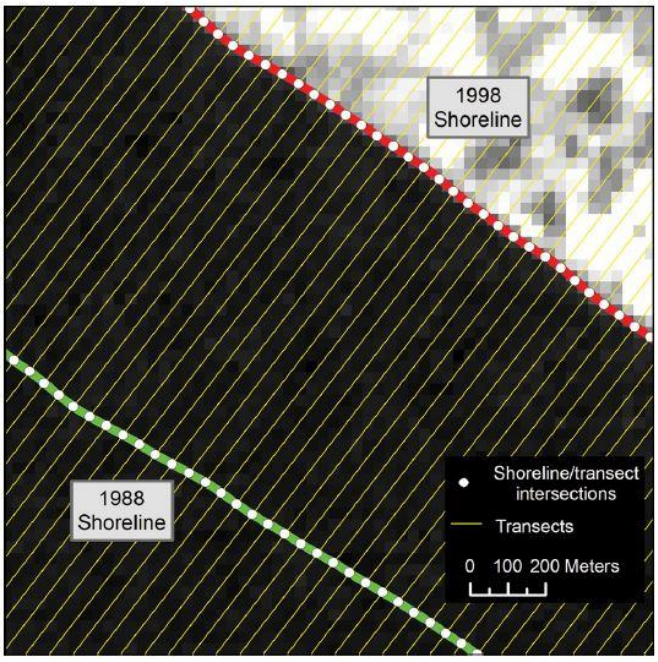

Figure 17: An example of preparation of shoreline transect in the study area using DSAS software (Source: Crawford et al., 2020*).*

CHAPTER 4: RESULT

4.1 Results of the Validation of the MSWEP and PERSIANN-CDR over Nepal (GBM)

The result of the statistical assessment of the 26-year (1983-2009) comparisons between PERSIANN-CDR and MSWEP seasonal precipitation versus 223 rain gauge station observation for Nepal is listed in Table 2 and a scatter plot is provided in Figures 18 and 19. The statistics shows that MSWEP has higher coefficient of determination for both pre-monsoon and monsoon precipitation than PERSIANN-CDR. The value of the coefficient of determination for MSWEP pre-monsoon is 0.53, while PERSIANN-CDR has only 0.38. The RMSE value for MSWEP is 58.59 mm and 34.55 mm for PERSIANN-CDR. Likewise, the value of coefficient of determination for MSWEP monsoon is 0.3, while PERSIANN-CDR has a very low 0.07.

Table 2: Statistical analysis for pre-monsoon and monsoon precipitation (1983-2009) between Precipitation Products (MSWEP and PERSIANN-CDR) and rain gauges.

Time	MSWEP		PERSIANN-CDR
Pre-monsoon	R^2	0.53	0.38
	RMSE (mm)	58.59	34.55
	RB%	5%	-15%
Monsoon	R^2	0.3	0.07

	RMSE (mm)	308.62	261.69
	RB%	-9%	-30%

In addition, the result of relative bias shows that MSWEP overestimated by 5% for pre-monsoon precipitation; on the contrary, PERSIANN-CDR underestimated by -15%. However, monsoon precipitation was underestimated by -9% and -30% by both MSWEP and PERSIANN-CDR products, respectively. The RMSE error for monsoon precipitation based on MSWEP and PERSIANN-CDR is 308.62 mm and 261.69 mm, respectively.

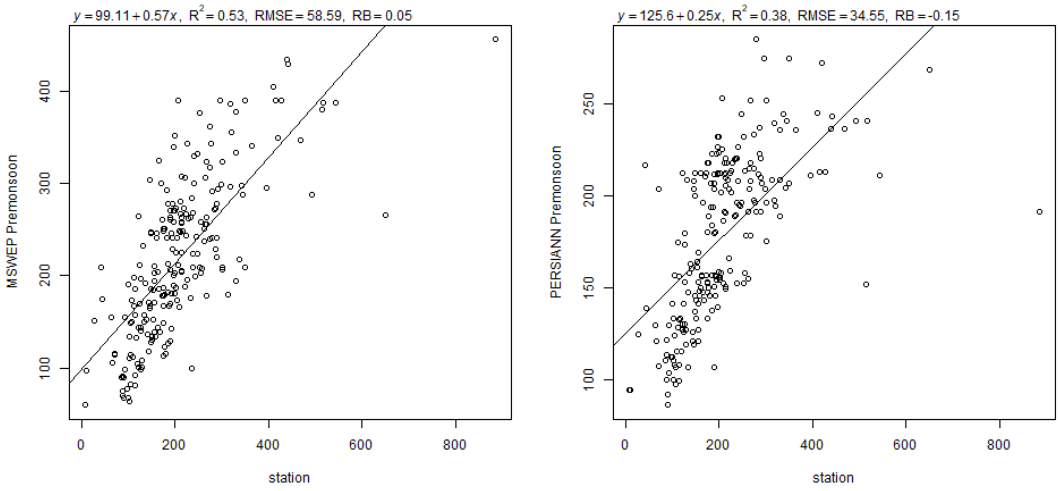

Figure 18: The scatter plot result of validation test for pre-monsoon precipitation based on MSWEP and PERSIANN-CDR.

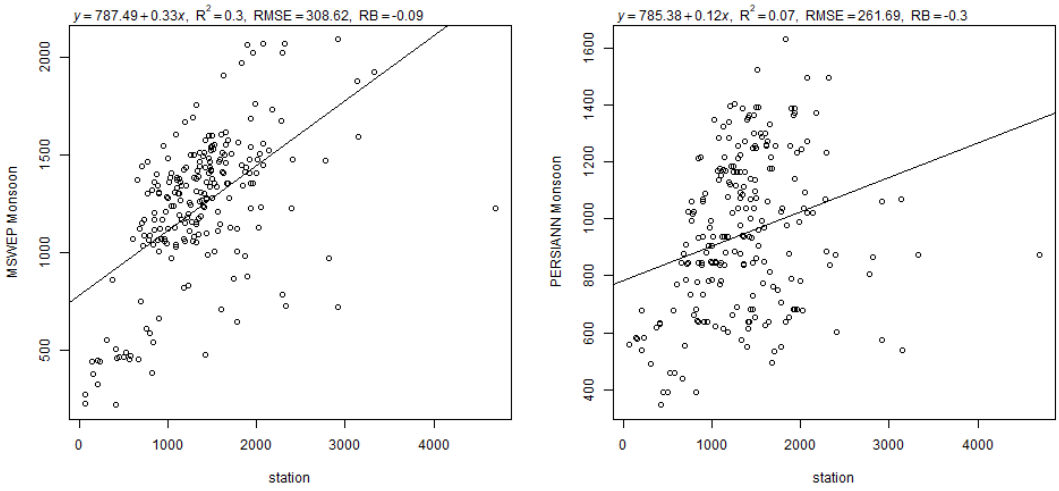

Figure 19: The scatter plot result of validation test for monsoon precipitation based on MSWEP and PERSIANN-CDR.

Similarly, this study also conducted the correlation test between relative differences vs elevation of the rain gauge stations. Figure 20 shows a significant correlation between relative differences of pre-monsoon and monsoon precipitation with elevation, at 0.05 significance level. However, the results are biased with a few stations above 3000m having the largest relative differences.

It is important to bear in mind the limitations of PERSIANN-CDR and MSWEP when evaluating the results in the remainder of the thesis. PERSIANN-CDR is used for evaluating the relationships between pre-monsoon and monsoon rainfall, ENSO and water routing distance. PERSIANN-CDR and MSWEP are both used in the trend analysis and in relating GBM precipitation to riverbank erosion to provide additional comparison. Finally, due to the superior spatial resolution, MSWEP alone is used for the localized riverbank erosion analysis.

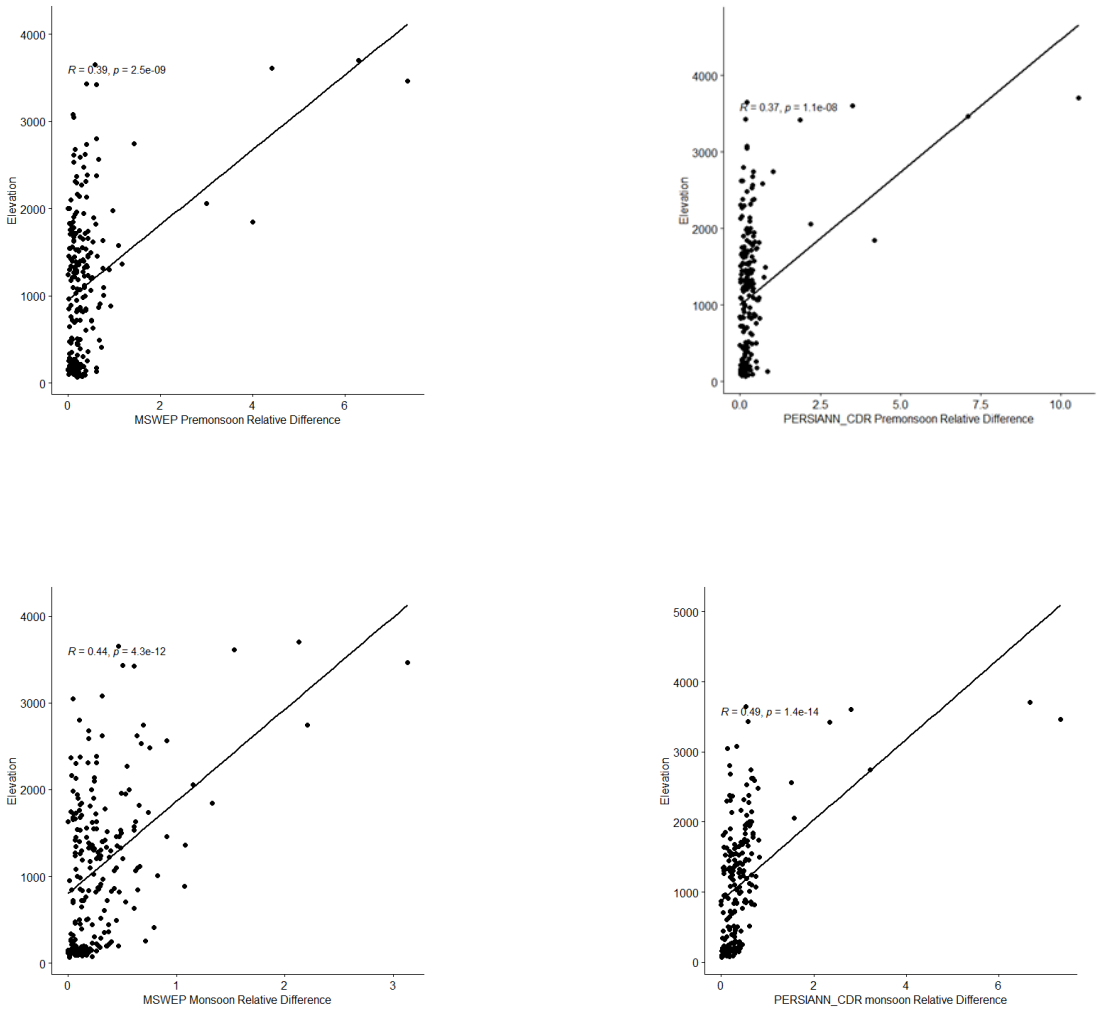

Figure 20: The plot shows the correlation result between relative difference and elevation for pre-monsoon and monsoon precipitation based on MSWEP and PERSIANN-CDR.

4.2 Results of Relationship Between Pre-monsoon and Monsoon Precipitation in the GBM River Basin based on Hydrological Sub-basins

Figures 21 and 22 show the correlation among the 32 hydrological sub-basins for pre-monsoon and monsoon precipitation respectively. Each row or column of the figure shows the correlation of one sub-basin with all sub-basins. The blue color indicates a positive correlation, and the red color indicates a negative correlation. Brighter colors with a bigger circles indicate

stronger correlations between sub-basins. It should be noted that there are many more positive correlations in the monsoon case compared to the pre-monsoon case. The only sub-basin that has a preponderance of large negative correlations with other sub-basins in the monsoon season is 45248 in the far western GBM (see Figure 22). Figure 23 (a) and (b) are examples of the correlation between sub-basin 45243 in the central GBM and all other sub-basins for pre-monsoon and monsoon, respectively, which is the same as the sixth row and column of Figures 21 and 22. Each map's brighter blue and green color indicates a strong positive correlation. The maps clearly show the typical spatial dependency of precipitation in the GBM during pre-monsoon and monsoon seasons.

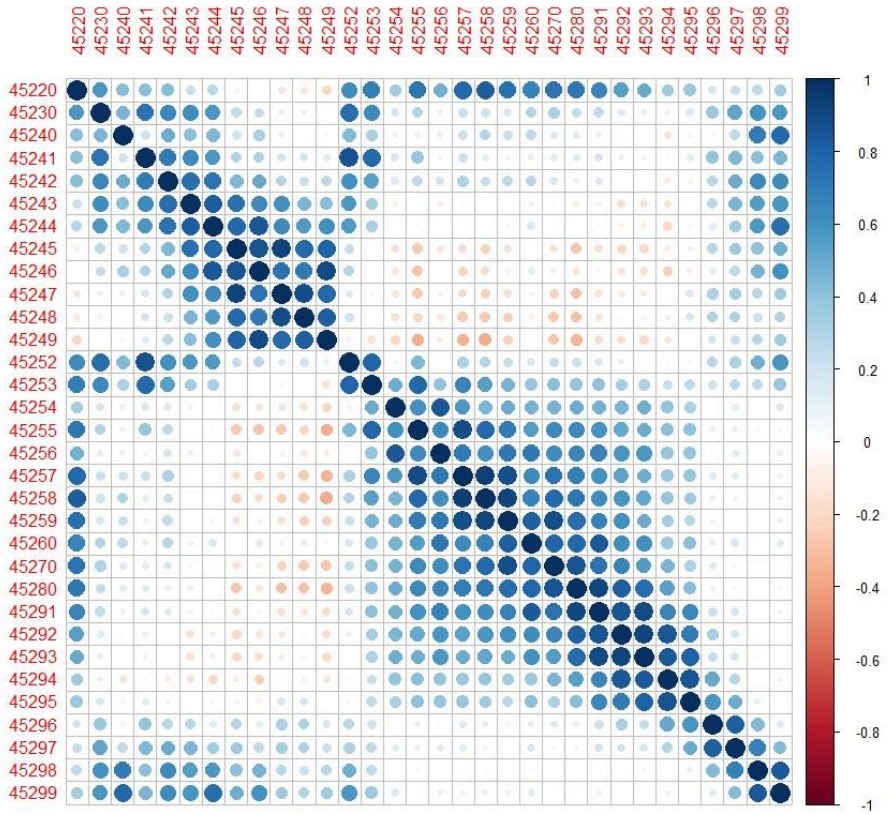

Figure 21: The pre-monsoon precipitation correlation between 32 hydrological sub-basins of GBM. Each row and column show one result for a single sub-basin with the other.

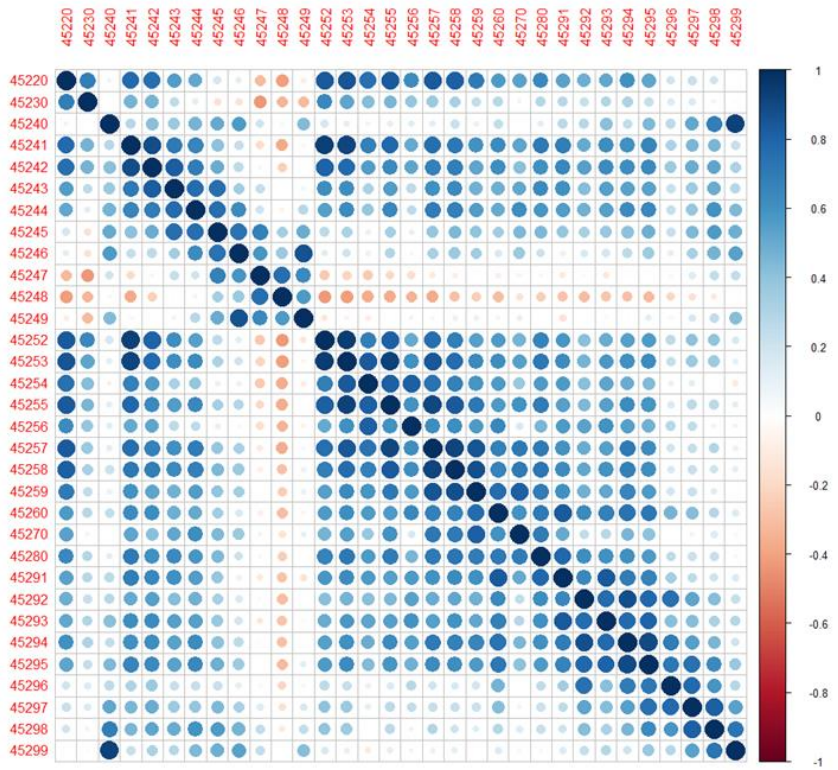

Figure 22: Monsoon precipitation correlation between 32 hydrological sub-basins. Each row and column show one result for a single sub-basin with the other.

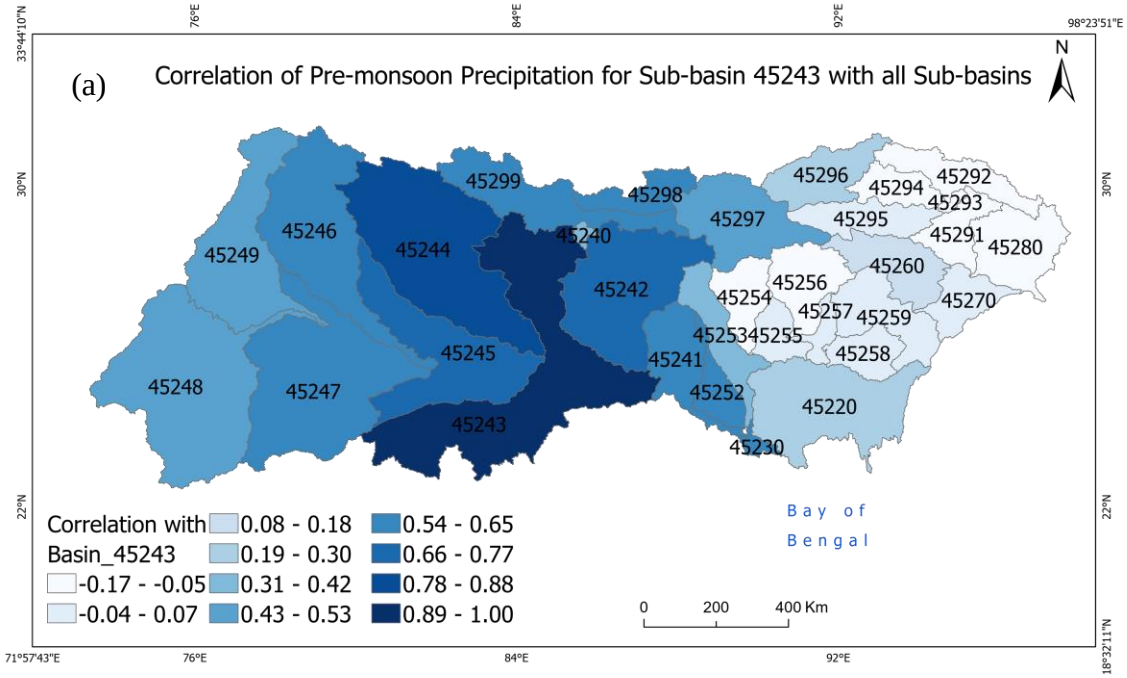

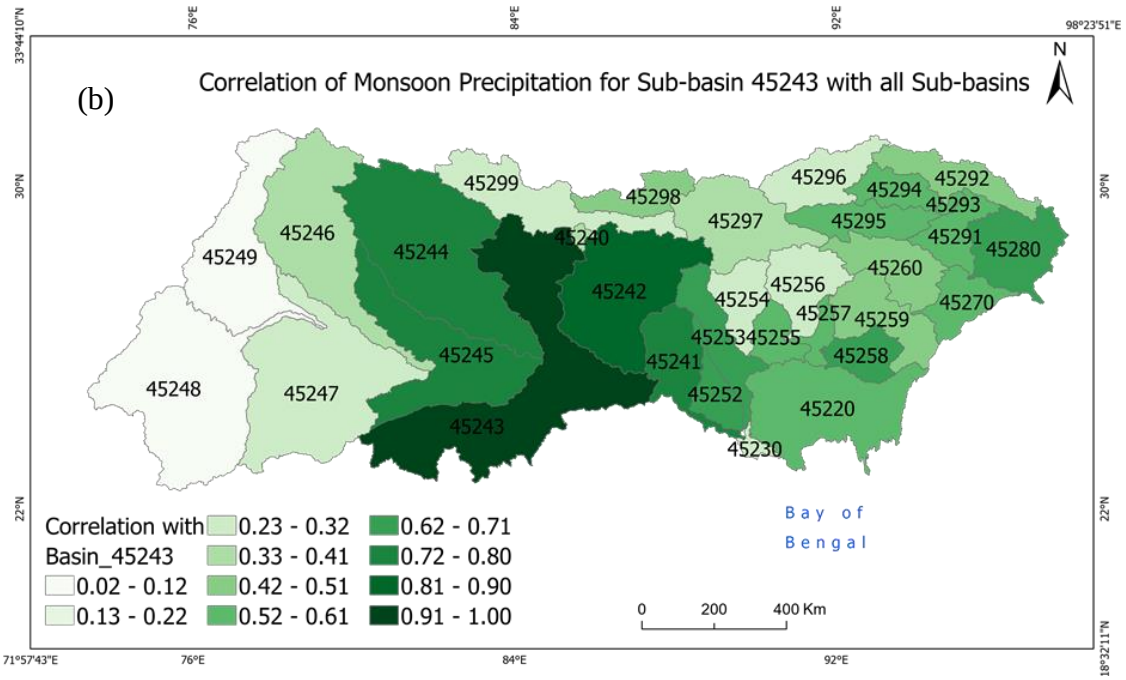

Figure 23: (a) Example of pre-monsoon precipitation correlation for sub-basin 45243 with all sub-basins. (b) Example of monsoon precipitation correlation for sub-basin 45243 with all sub-basins.

The correlation between pre-monsoon and monsoon precipitation is varied (Figure 24). Among the 32 hydrological sub-basins, only two sub-basins of the GBM show a significant correlation between pre-monsoon and monsoon precipitation, as shown in Figure 24. Sub-basin 45245 has a significant negative correlation, and 45280 has a significant positive correlation. The overall pattern is for negative correlations in the western and northern GBM and positive correlations in the eastern and southern GBM.

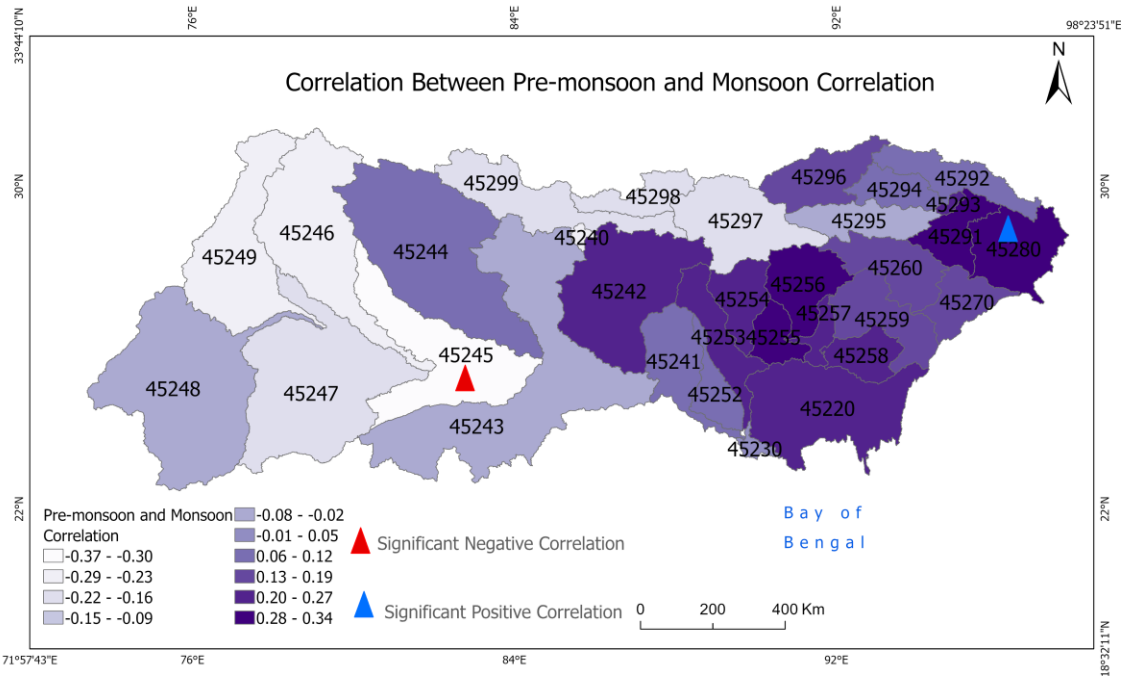

Figure 24: Correlation between pre-monsoon and monsoon precipitation showing only two sub-basins are significant.

4.3 Results of Relationship between Pre-monsoon and Monsoon Precipitation in the GBM River Basin based on water routing distance

Figures 25 and 26 show the correlation among the 10 sub-basins based on water routing distance for pre-monsoon and monsoon precipitation respectively. Each row or column of the figure shows the correlation of one sub-basin with all sub-basins. The blue color indicates a positive correlation, and the red color indicates a negative correlation. Brighter colors with a bigger circles indicate stronger correlations between sub-basins. It should be noted that there are many more positive correlations in the pre-monsoon case compared to the monsoon case. Sub-basin 10 with the longest distance to the outlet has a large number of positive correlations for pre-monsoon as compared to monsoon.

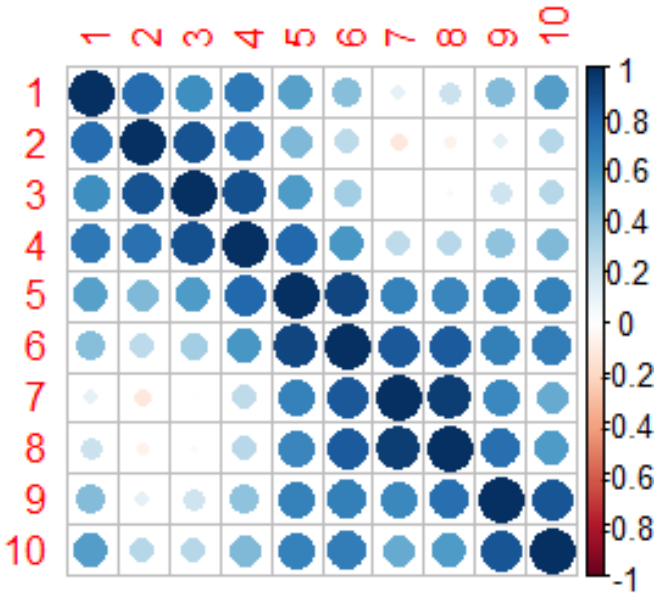

Figure 25: Correlation of pre-monsoon precipitation based on water routing distance flow length between 10 sub-basins

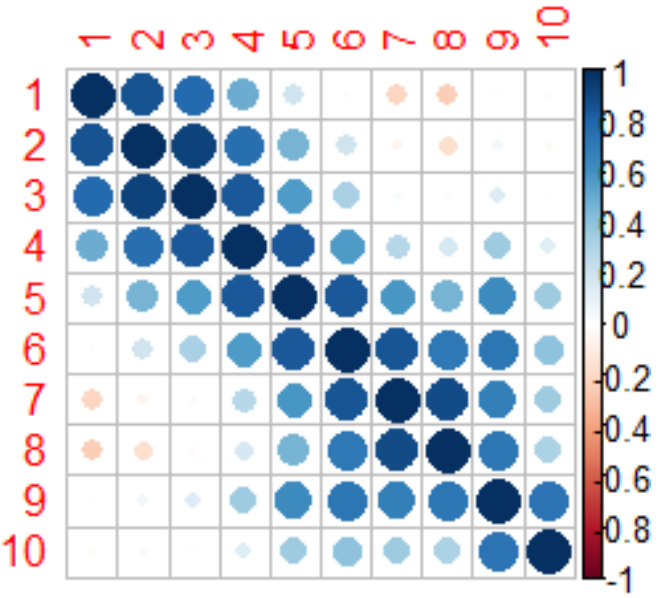

Figure 26: Correlation of monsoon precipitation based on water routing distance between 10 sub-basins

The correlation between pre-monsoon and monsoon precipitation shows that sub-basins near costal Bangladesh have a positive correlation (Figure 27). Although this map has a similar

pattern of positive and negative correlations to what was presented using sub-basins in Figure 24, no single water routing region shows a significant correlation between pre-monsoon and monsoon precipitation.

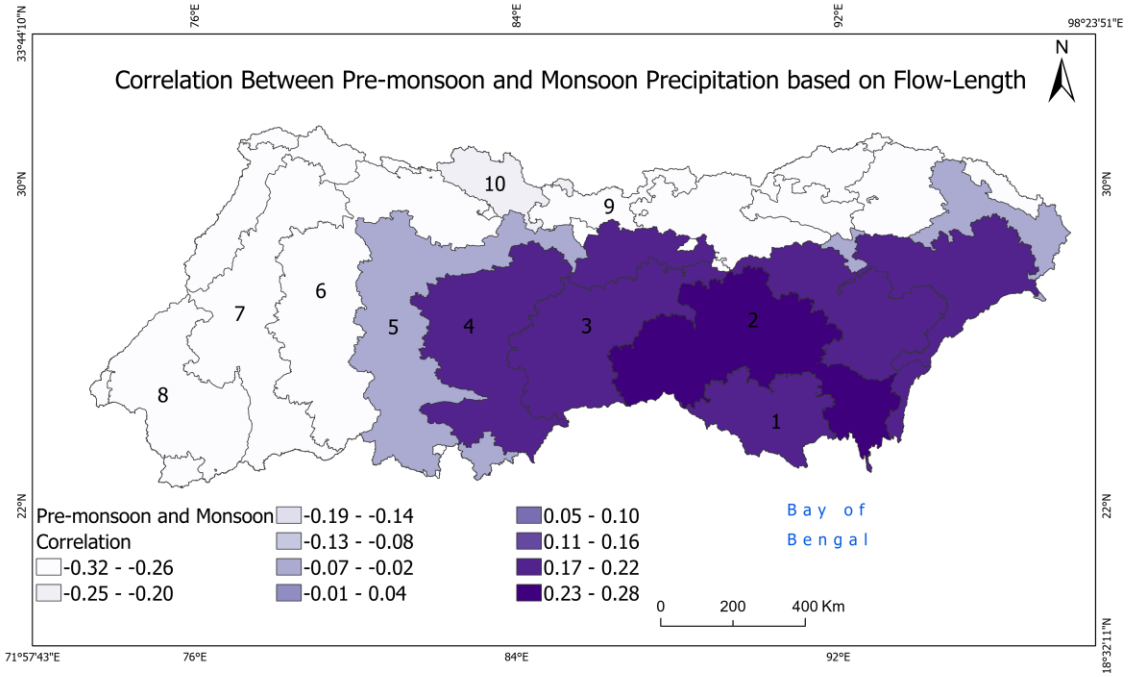

Figure 27: Map showing no significant correlation between pre-monsoon and monsoon precipitation based on water routing distance (flow length).

4.4 Results of Relationship Between MEI (ENSO) and Seasonal Precipitation Based on 32 Hydrological Sub-basins of GBM

Only three sub-basins, 45246, 45240, and 45260 show significant positive correlations between MEI and pre-monsoon precipitation based on 32 hydrological sub-basins (see Figure 28a). On the contrary, seven sub-basins, 45249, 45246, 45245, 45299, 45240, 45298, and 45297 show significant negative correlations between MEI and monsoon precipitation (Figure 28b, indicating the far northern and western regions of the GBM experience a dry monsoon during El Nino events (Figure 28b).

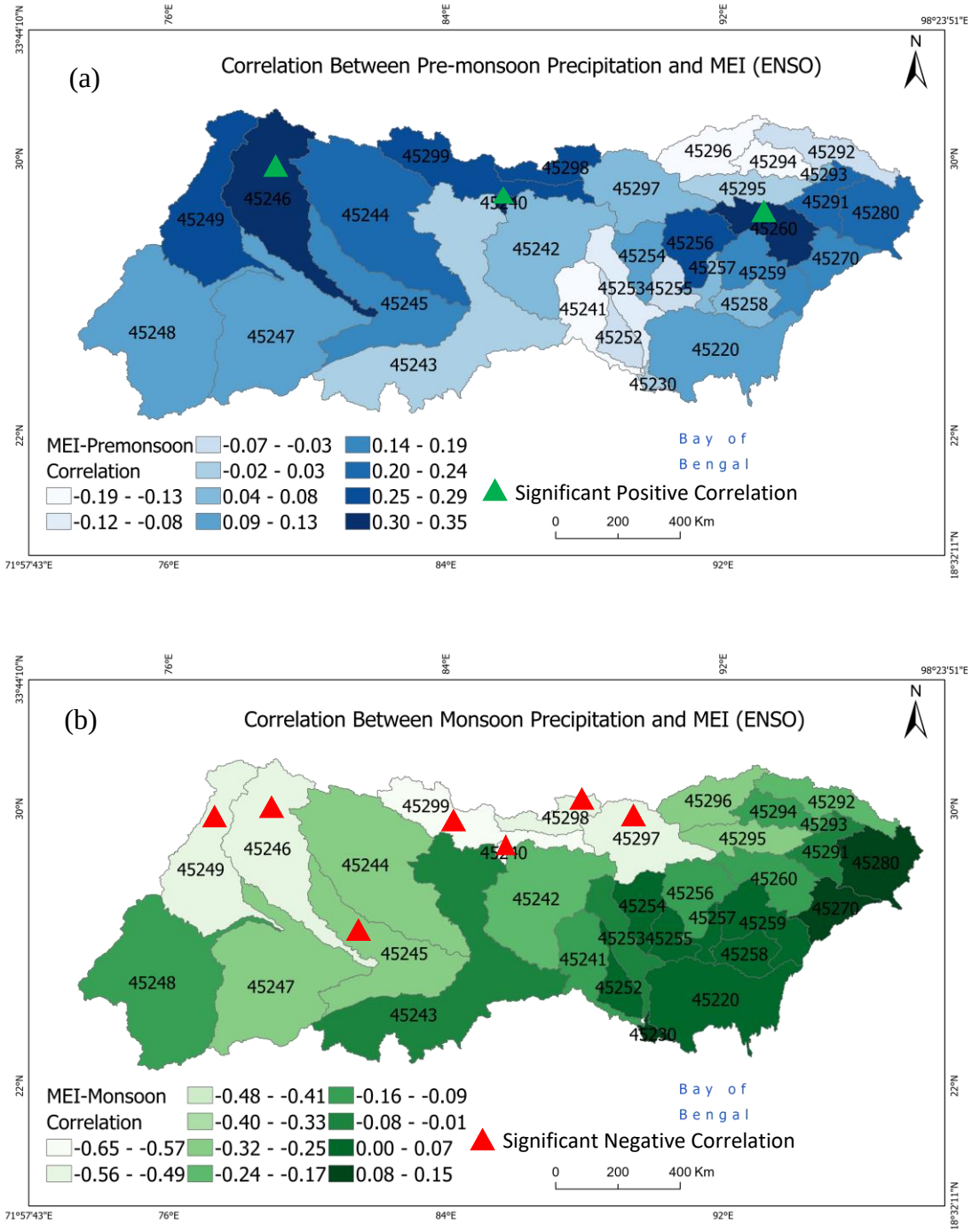

Figure 28: Figure 28 (a) shows the correlation between Pre-monsoon Precipitation and MEI ENSO, including significant test results, (b) shows the correlation between Monsoon Precipitation and MEI ENSO, including significant test results.

4.5 Results of Relationship Between MEI(ENSO) and Seasonal Precipitation Based on Water Routing Distance of GBM River Basin

There are no significant correlations between MEI and pre-monsoon precipitation based on water routing distance (flow length) (Figure 29). However, monsoon precipitation based on water routing distance and MEI shows significant negative correlation in 6, 7, 8, 9, and 10 sub-basins of GBM (see Figure 30), which correspond to the further distances and somewhat agrees with Figure 28b. However, more of the GBM experiences drying with El Nino when considering water routing than when considering sub-basin divisions.

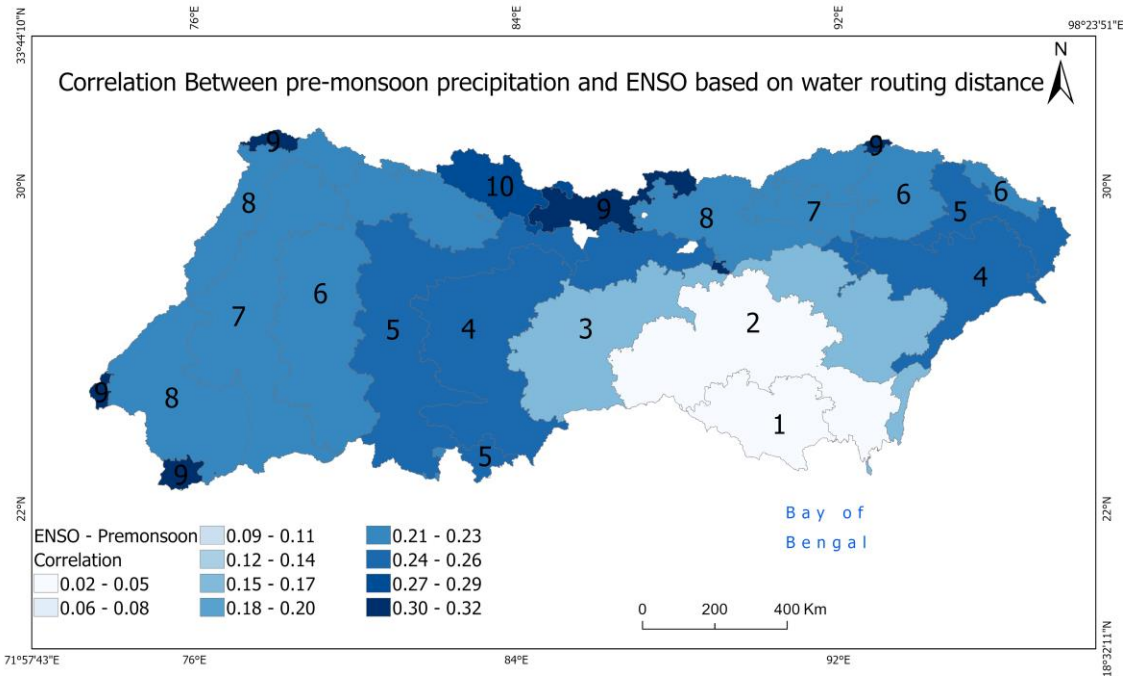

Figure 29: The figure shows the correlation between Pre-monsoon Precipitation and MEI (ENSO) based on water routing distance

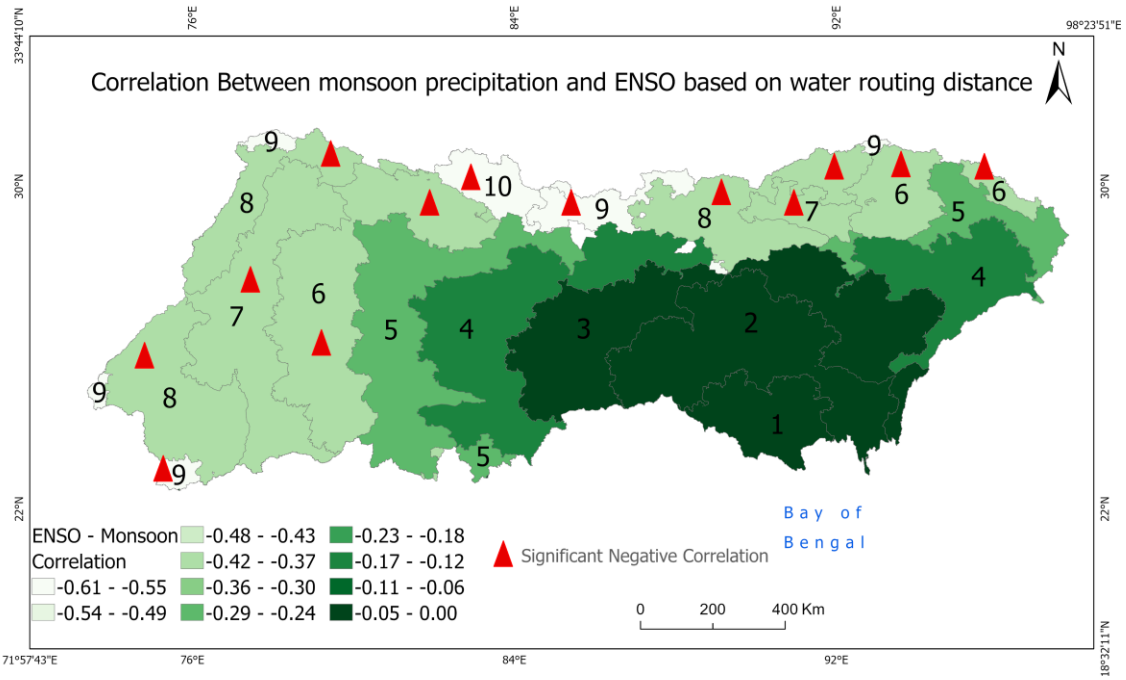

Figure 30: The figure shows the correlation between monsoon Precipitation and MEI (ENSO) based on water routing distance including significant test result

4.6 Results of Seasonal Precipitation Trend Analysis in the GBM River Basin

Precipitation trend analysis was performed on the whole GBM river basin and pre-defined hydrological sub-basins of the GBM river basin. Both MSWEP and PERSIANN-CDR precipitation products are used for the trend analysis and comparison. This study used pre-monsoon and monsoon precipitation based on 32 and 34 hydrological sub-basins for PERSIANN-CDR and MSWEP, respectively.

4.6.1 Precipitation Trend of Ganges-Brahmaputra-Meghna River Basin

The precipitation trend test results for both MSWEP and PERSIANN-CDR are shown in Figure 31, and all the Z-values and *p*-values for the Modified Mann-Kendall trend test are shown in Table 3. This study found that MSWEP pre-monsoon precipitation has a significant positive

trend at the 95% significance level, whereas no significant trend was detected for the PERSIANN-CDR precipitation.

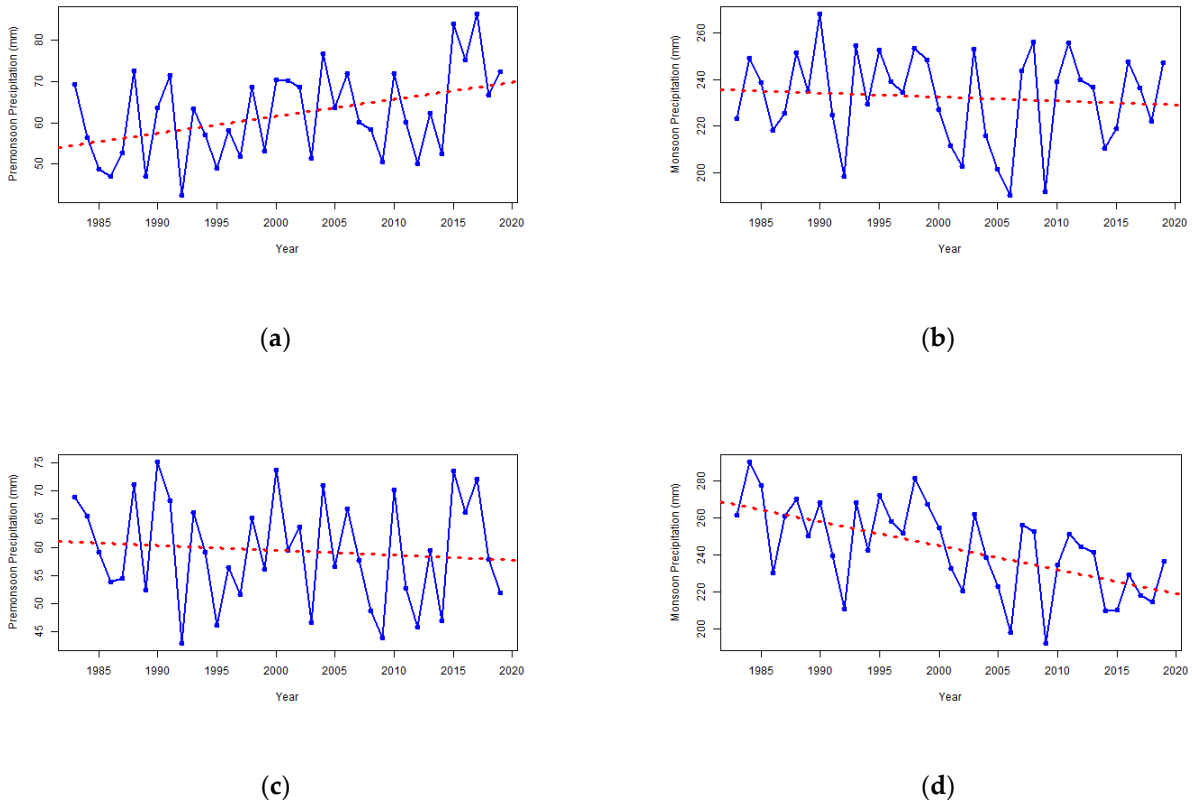

Figure 31: a) MSWEP pre-monsoon precipitation trend; (b) MSWEP monsoon precipitation trend; (c) PERSIANN-CDR pre-monsoon precipitation trend; (d) PERSIANN-CDR monsoon precipitation trend. The red dotted line indicates the linear regression.

Table 3: p- and Z-value of pre-monsoon and monsoon precipitation trends using Modified Mann-Kendall for the GBM river basin during 1983–2019.

Satellite-Based	**Pre-Monsoon**		**Monsoon**	
Precipitation Product	**Z-value**	***p*-Value**	**Z-Value**	***p*-Value**
MSWEP	2.236	0.025	−0.554	0.579
PERSIANN-CDR	−0.536	0.592	−33.071	< 0.000

The Z-value of the MSWEP pre-monsoon precipitation trend was 2.236, and that of PERSIANN-CDR was −0.5362. On the contrary, a strong significant negative precipitation trend was detected in the PERSIANN-CDR monsoon precipitation with the Z-value of −33.07, while no significant precipitation trend was seen in the MSWEP. The Z-value using MSWEP was −0.554. However, the correlations between the time series are highly positive and significant for the pre-monsoon (R = 0.79) and monsoon (R = 0.78) seasons (Figure 32 and 33), indicating that the satellite products have similar year-to-year variability.

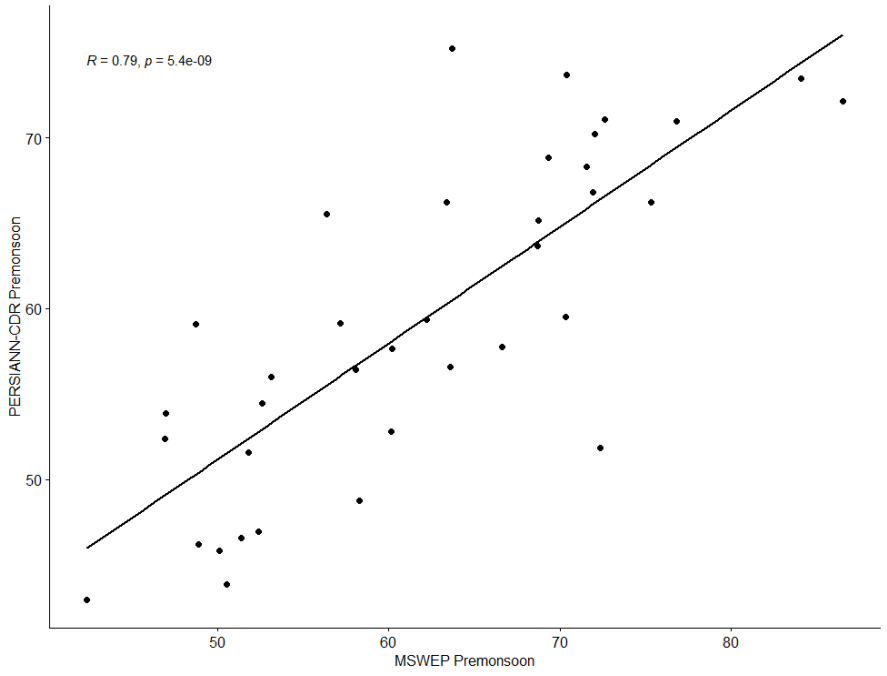

Figure 32: The figure shows the scatter plot result between MSWEP Pre-monsoon VS PERSIANN-CDR Pre-monsoon

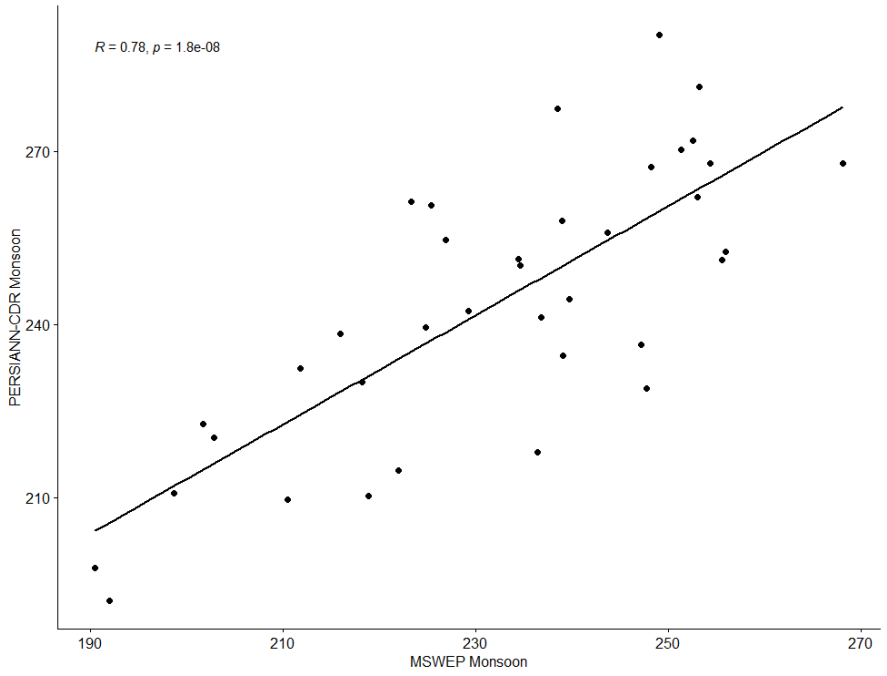

Figure 33: The figure shows the scatter plot result between MSWEP monsoon VS PERSIANN-CDR monsoon

4.6.2 Precipitation Trends of Pre-Defined Hydrological Sub-Basins of the GBM River Basin

The MSWEP pre-monsoon precipitation had a significant positive trend in 13 sub-basins. In contrast, only four sub-basins had a significant positive trend in PERSIANN-CDR precipitation. Significant positive precipitation trends were mostly found in the central, far north, and western region of the basin, as shown in Figure 34. Among the 34 hydrological sub-basins, only six sub-basins in MSWEP showed negative Z-values, but none were significant. Meanwhile, for PERSIANN-CDR, 22 hydrological sub-basins showed negative Z-values, and only sub-basin 45280, situated in the eastern region, showed a significant negative precipitation trend.

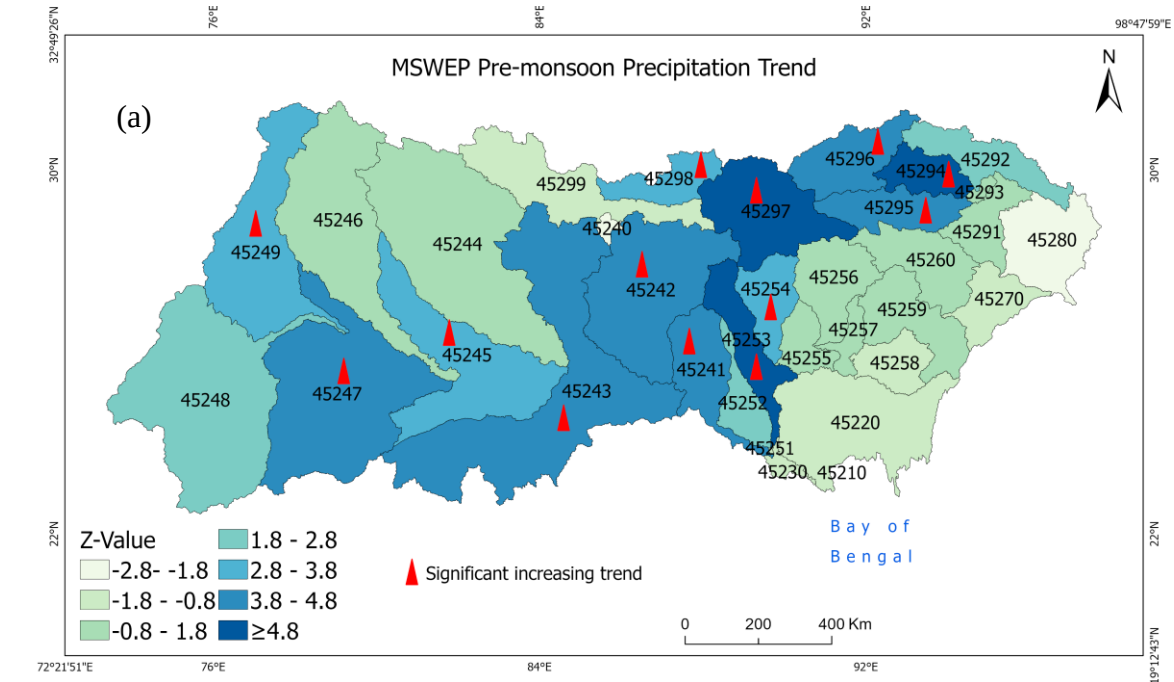

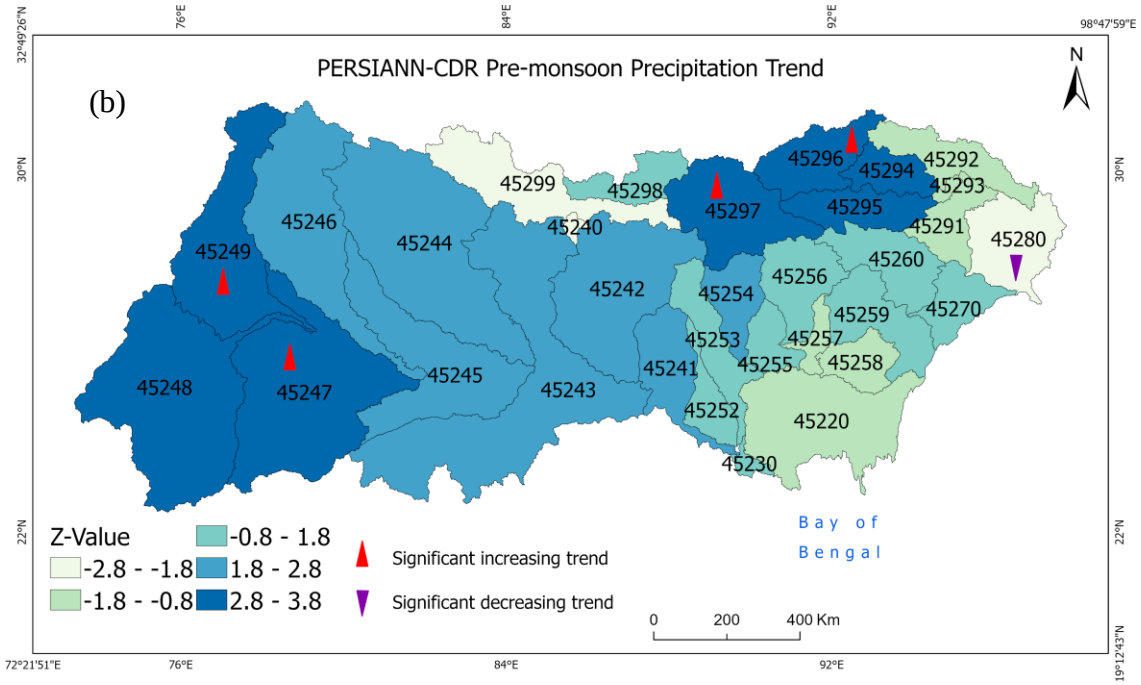

Figure 34: Pre-monsoon precipitation trend for (a) MSWEP and (b) PERSIANN-CDR. A red color upright triangle indicates a significant increasing trend ($p < 0.05$), and a purple color downright triangle indicates a significant decreasing trend.

Regarding the monsoon season, eight sub-basins had a significant negative trend for monsoon precipitation in MSWEP (Figure 35a), whereas 19 sub-basins had a significant negative precipitation trend in the PERSIANN-CDR (Figure 35b). The eight MSWEP sub-basins with significant negative precipitation trends were found near Bangladesh and in the eastern region. Similarly, in PERSIANN-CDR, significant negative precipitation trends were mostly found near the southern, central, and eastern parts of the GBM (Figure 35b). On the contrary, significant positive precipitation trends were detected in the three sub-basins situated in the upper Himalayas (45299, 45298, and 45240) in MSWEP, whereas, in PERSIANN-CDR, those three sub-basins showed negative Z-values. Only three sub-basins, 45296 (upper Himalayas), 45247, and 45248, situated in the western region, had positive Z-values in PERSIANN-CDR, though they were not significant.

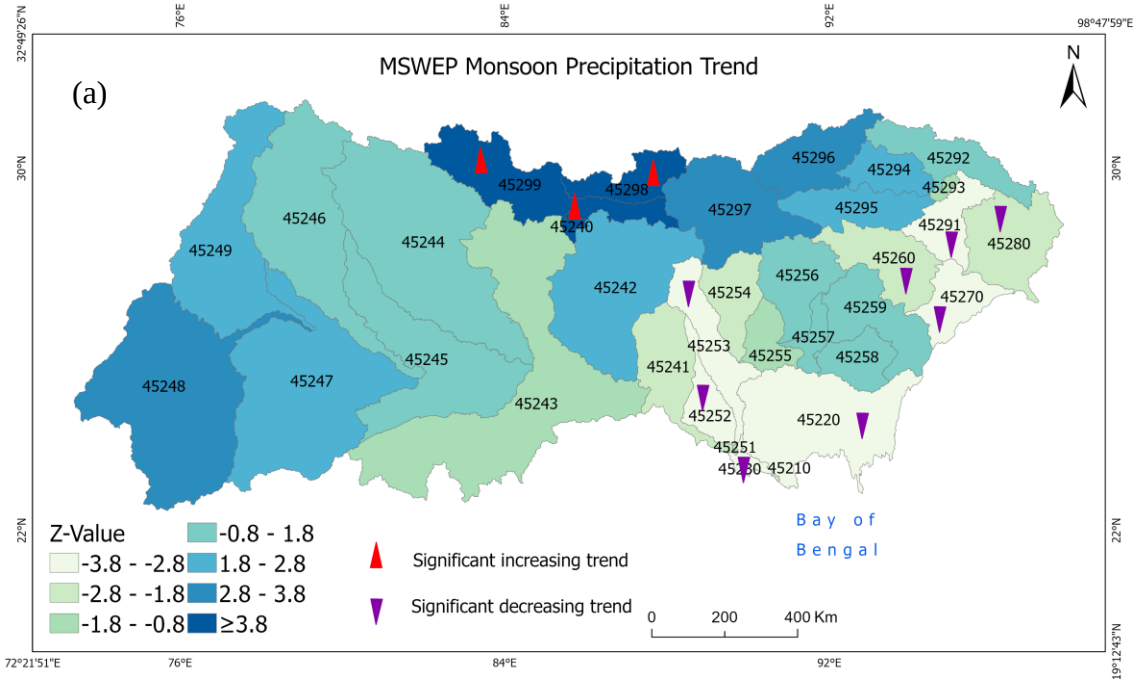

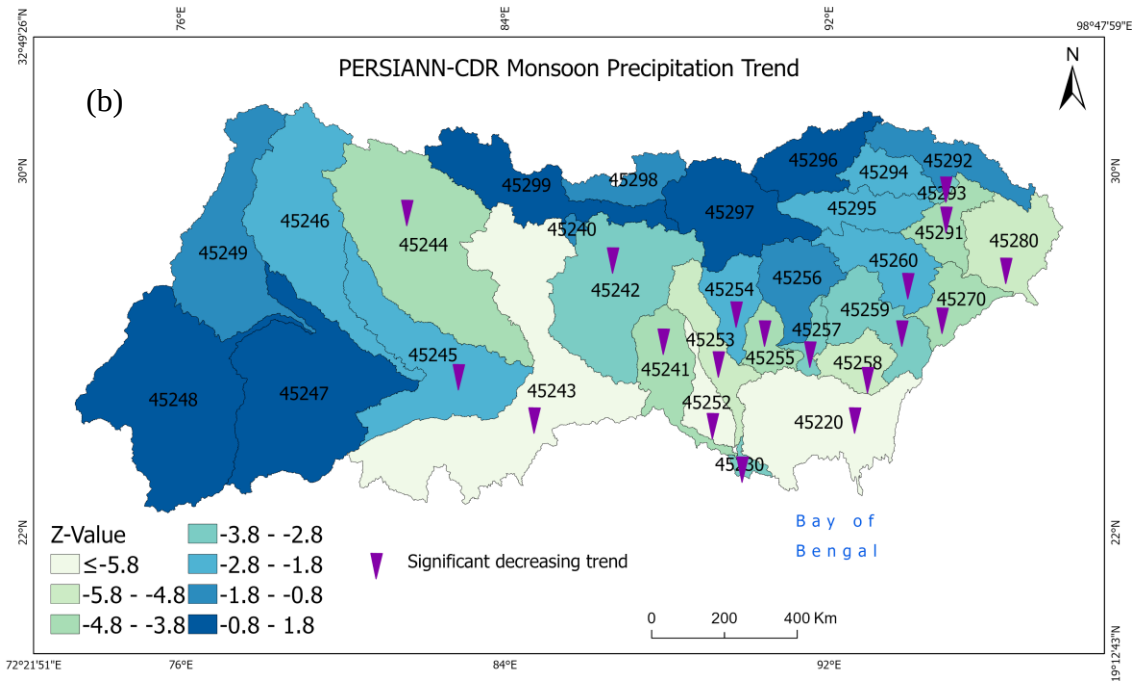

Figure 35: Monsoon precipitation trend for (a) MSWEP and (b) PERSIANN-CDR. A red color upright triangle indicates a significant increasing trend ($p < 0.05$), and a purple color downright triangle indicates a significant decreasing trend.

4.7 Results of the Relationship Between Riverbank Erosion and Precipitation

The analysis of MSWEP showed no significant relationship between local extreme daily precipitation and annual riverbank change (positive = accretion and negative = erosion) in the study area of coastal Bangladesh. In addition, no significant relationship was found between riverbank change and monsoon precipitation for the entire GBM based on either PERSIANN-CDR and MSWEP. However, when examining the relationship between riverbank change and monsoon precipitation based on GBM hydrological sub-basins significant correlations were achieved. Six sub-basins 45220, 45244, 45253, 45255, 45257, and 45258 showed significant positive correlations between PERSIANN-CDR monsoon precipitation and riverbank change in the central region (Figure 37), indicating anomalously high rainfall is related to anomalous accretion. In

addition, MSWEP based monsoon precipitation also showed a significant positive correlation for two sub-basins, 45252 and 45255, whereas sub-basin 45298 showed a significant negative correlation with the central region (Figure 38). Only one basin, 45255, overlaps and should be investigated further (see Figure 36). There was no significant relationship between monsoon precipitation and riverbank change in the north and south regions in the study area.

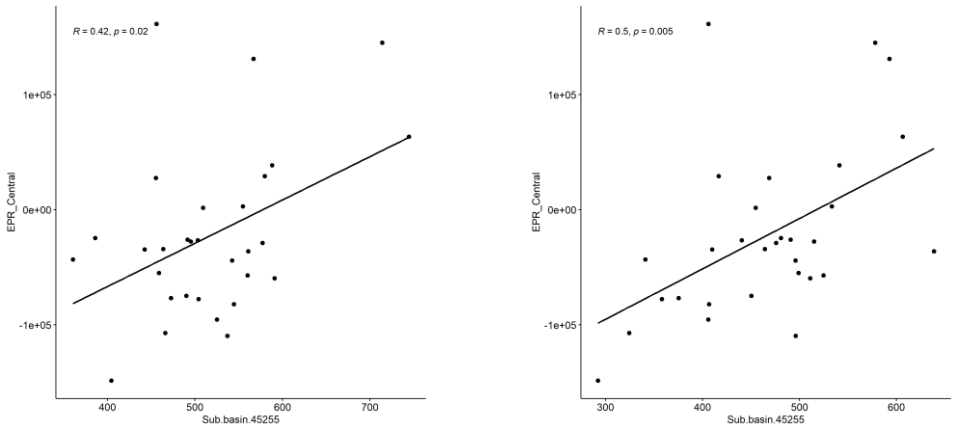

Figure 36: Scatter plots showing the correlation between sub-basin 45255 and riverbank erosion in the central region based on MSWEP (left) and PERSIANN-CDR (right) respectively

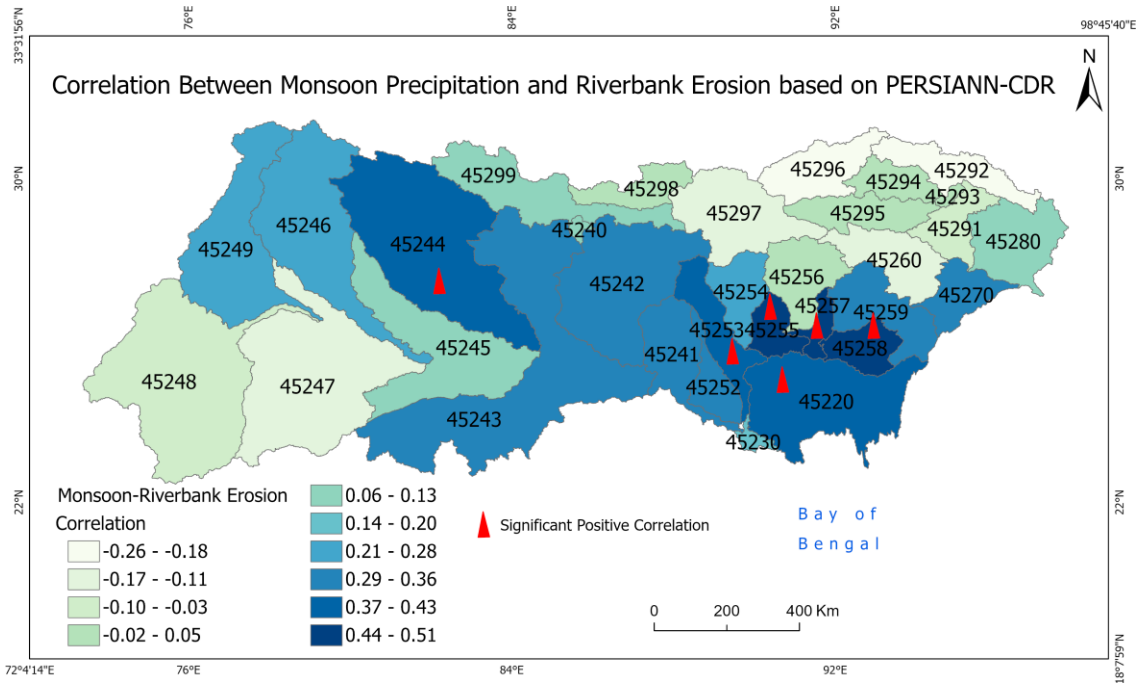

Figure 37: Map showing the significant correlation between monsoon precipitation and riverbank change based on PERSIANN-CDR

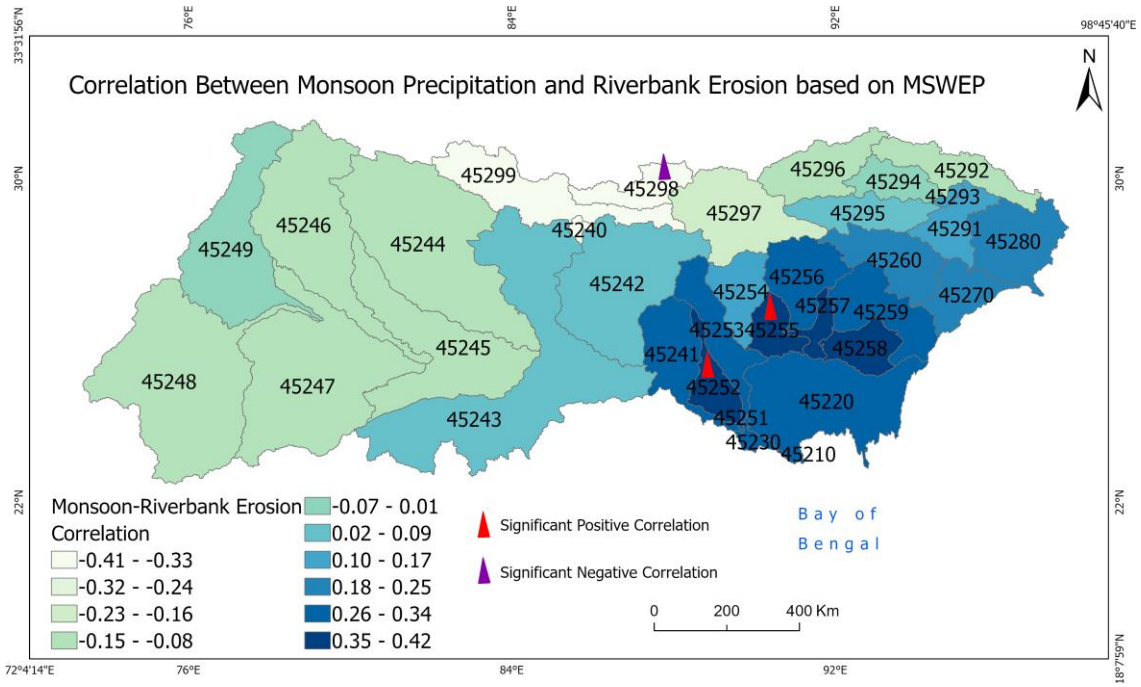

Figure 38: Map showing the significant correlation between monsoon precipitation and riverbank change based on MSWEP

CHAPTER 5: DISCUSSION

5.1 Validation of the MSWEP and PERSIANN-CDR over Nepal (GBM)

Two satellite-based precipitation products were correlated with a dense rain gauge network in Nepal for the pre-monsoon and monsoon seasons from 1983 to 2009. The results showed that MSWEP performed better than PERSIANN for both seasons. The coefficient of determination value for MSWEP pre-monsoon was 0.53 and RMSE error 58.59mm. Whereas the relative bias percentage indicated that MSWEP only overestimated by 5%. The reason for the differences seen over Nepal could be the difference in spatial scale of the products. The spatial resolution of MSWEP is 0.1 degree, whereas PERSIANN-CDR has a 0.25 degree grid spacing. MSWEP was able to resolve more station locations than PERSINN-CDR which gives it advantage when using the direct comparison methodology. Furthermore, MSWEP merges gauge, satellite, and reanalysis data to obtain the highest quality precipitation data locally (Beck et al., 2019). However, MSWEP's performance was not as satisfactory in the monsoon season.

The underperformance of PERSIANN-CDR has been noted in the literature. One of the possible reason of underestimation of PERSIANN-CDR is due to warm orographic rainfall that cannot be detected by microwave and infrared sensor (Bajracharya et al., 2015). According to Gao et al. (2018) PERSIANN-CDR cannot accurately measure the spatial distribution of precipitation events compared to other products. They compared two reanalysis data sets and two satellite-based datasets in the Xiang river basin in China at two spatial and temporal scales. PERSIANN-CDR underestimated monthly precipitation and performed poorly compared to the other data sets (Gao et al., 2018). In addition, (Vu et al., 2018) used three satellite-based precipitation products namely, Tropical Rainfall Measuring Mission (TRMM 3B42 V7), Precipitation Estimation from Remotely

Sensed Information using Artificial Neural Networks (PERSIANN), and PERSIANN-Climate Data Record (PERSIANN-CDR), to simulate the streamflow of the Han River Basin. PERSIANN-CDR performed low compared to other products.

The reason both products had lower correlations with gauges in the monsoon versus the pre-monsoon season could be related to the mode of precipitation delivery. The rainfall in the monsoon season is convectively driven making it more sporadic and intense as compared to the pre-monsoon season, which is controlled by advancing air masses (Kumar & Naidu, 2020). There was a strong correlation between station elevation and relative bias for both products in both seasons. The relative bias was especially large for a few high elevation stations. Thus, topography is seen as a limitation in the usefulness of satellite estimates, and according to (Decker et al., 2012) errors are expected to be higher in complex topography. I am unable to assess the validity of PERSIANN-CDR and MSWEP in other parts of the GBM and so additional validation studies are required to fully address the first research question.

5.2 Relationship Between Pre-monsoon and Monsoon Precipitation in the GBM River Basin based on Hydrological Sub-basins, Water Routing Distance, and ENSO

The first and second research questions were: *What is the relationship between pre-monsoon and monsoon precipitation in the GBM river basin based on hydrological sub-basins vs. water routing distance?* and *Do climate teleconnections, e.g., ENSO, have any relationship with seasonal precipitation in the GBM river basin?* To answer these questions PERSIANN-CDR was averaged over 32 hydrological sub-basins and 10 water routing distance divisions. All of the regions were then correlated with each other within seasons, across seasons and with an ENSO index. It was found that the pre-monsoon season has less spatial dependency in precipitation as organized by sub-basin boundaries compared to the monsoon season, mainly because of the large

number of positive correlations between sub-basins during the monsoon compared to pre-monsoon season (see Figure 21 and 22). The only sub-basin that has a preponderance of large negative correlations with other sub-basins in the monsoon season was 45248 in the far western GBM. The result suggests that pre-monsoon precipitation over the GBM river basin is highly variable in space as compared to the monsoon precipitation.

It was hypothesized that the pre-monsoon precipitation may have some influence on monsoon precipitation locally in the GBM river basin. A researcher (Narayanan et al., 2013) also postulated that the pre-monsoon season may impact the intensity of monsoon precipitation in India. However, no such relation was found between pre-monsoon and monsoon precipitation in the hydrological sub-basins of the GBM river basin. In fact, sub-basin 45245, located in India, has a significant negative correlation, whereas sub-basin 45280 in the far eastern GBM has a significant positive correlation. The reason for this lack of persistence from one season to the next might be because pre-monsoon rainfall occurs due to maritime air masses (Kumar & Naidu, 2020); on the contrary, monsoon rainfall occurs due to the seasonal shift of winds created by the land's annual temperature variation in contrast with the connected ocean surface (Alamgir, 2009). Similarly, Kiguchi et al. (2016) also conducted research on the relationship between the intermittent pre-monsoon rainfall and monsoon onset over the Indochina peninsula and found no such relationship. Likewise, this study did not find any such relationship between pre-monsoon and monsoon precipitation based on the water routing distance classification.

To determine if there were any teleconnections, a study was conducted to reveal the relationship between seasonal precipitation and ENSO (MEI) within the watersheds of the GBM river basin. It showed that only three sub-basins have positive significant correlation between pre-monsoon precipitation and ENSO, even though there were many sub-basins that showed positive

correlation (see Figure 28a). The significantly positive sub-basins were sparsely distributed and located a distance from the coastal region of the GBM river basin. Positive correlations indicate wet conditions during the El Nino phase (Chowdhury, 2003) and the wide coverage suggests that ENSO has some role to play in increasing pre-monsoon precipitation in the GBM river basin.

The study revealed that monsoon precipitation has a strong significant negative correlation with ENSO in the outer regions of the basin, namely sub-basins, 45249, 45246, 45245, 45299, 45240, 45298, and 45297 (see Figure 28b). With regards to the monsoon season (Chowdhury, 2003) also found that Southern Oscillation Index (SOI) has strong relation with the rainfall in the upstream portions of the GBM basin whereas no relationship was found in the context of Bangladesh climate. The negative relation indicates dry conditions in the GBM river basin during El Nino (Chowdhury, 2003), including the western Ganges, consistent with previous studies like Whitaker et al. (2001). In addition, the findings of the study also showed consistency with (Ropelewski & Halpert, 1987), Ganges has a strong negative association with ENSO. Interestingly, no significant relationship was found between ENSO and pre-monsoon precipitation based on water routing distance. However, there was more spatial consistency in the correlations, as all water routing regions showed positive correlation with ENSO, whereas this was not the case for the sub-basin analysis. For the monsoon season, the water routing regions had strong negative correlations with ENSO, where the area of significance exceeded that of the sub-basins. This is an interesting finding and indicates that the distance from the outlet of the GBM river complex may be an important consideration when determining ENSO relationships in this mega river basin. Specifically, the periphery of the GBM river basin has a strong dry response to El Nino during the monsoon season as compared to the central to southern GBM.

5.3 Seasonal Precipitation Trend Analysis

The third research question was: *Do precipitation trends in the GBM river basin show consistency in satellite-based products?* The pre-monsoon and monsoon precipitation trends were studied for the GBM and pre-defined hydrological sub-basins of the GBM for 1983–2019 using the non-parametric Modified Mann-Kendall test. This study compared two different satellite-based precipitation products, MSWEP and PERSIANN-CDR. While the two data sets were significantly correlated over the pre-monsoon and monsoon seasons, the precipitation trend analysis found differences in the GBM river basin. Different resolutions of the precipitation products likely play a significant role in the contrasting results between PERSIANN-CDR and MSWEP (see Table 1). MSWEP may detect rainfall that PERSIANN-CDR does not. Moreover, the precipitation estimation process is different in these two products. PERSIANN-CDR is developed from infrared and passive microwave observations, whereas MSWEP estimates precipitation using gauge, satellite, and reanalysis-based products. Small biases in rainfall estimates can lead to large differences in the GBM because of the vagaries of the Indian monsoon and the orographic effects of the Himalayan mountains (Khandu et al., 2017). The significant increasing pre-monsoon precipitation trend identified by MSWEP and significant decreasing monsoon precipitation trend identified by PERSIANN-CDR are similar to (Sharma et al., 2021), reflecting that seasonal precipitation has changed in the GBM river basin. However, precipitation trends vary with the length of record, and the results are not suitable to extrapolate into the future (Blöschl et al., 2019; Luca et al., 2020). The sixth assessment report of the Intergovernmental Panel on Climate Change (IPCC, 2021) and other investigators (Kothyari et al., 1997; Immerzeel, 2008; Janes et al., 2019) have reported that monsoon precipitation decreased in South Asia, especially during the 1960s to 1980s, likely due to local cooling from human-caused aerosol emissions. However, future

projections from CMIP 6 model runs (IPCC, 2021) predict an increase in monsoon precipitation due to anthropogenic emissions of greenhouse gases (Sharma et al., 2021). The MSWEP precipitation trends are more consistent with this picture.

Very few sub-basins have similar trend results between the two satellite products for pre-monsoon and monsoon precipitation. Only four sub-basins show a significant increasing pre-monsoon precipitation trend for both MSWEP and PERSIANN-CDR. Thus, there is greater confidence that rainfall has increased in the central, far north, and western region of the GBM river basin (45246, 45249, 45295, and 45297). Sharma et al. (2021) also found that pre-monsoon precipitation trend increased gradually in that same region of the GBM. Ahmed et al. (2017) found a similar result in India consistent with the significant increasing pre-monsoon precipitation trend found in sub-basins 45247 and 45249. Similarly, the sub-basins 45242, 45243, and 45244, which cover Nepal, had a significant increasing trend in pre-monsoon precipitation based on MSWEP. Karki et al. (2017) also found pre-monsoon precipitation trend significantly increased from 1970–2012 in the lowlands and central hill area of Nepal using daily precipitation data from the Department of Hydrology and Meteorology (DHM), Nepal, and applying a Mann-Kendall test. Bhutan is covered mostly by two sub-basins: 45254 and 45256, and 45254 shows significant increasing pre-monsoon precipitation trend based on MSWEP.

One sub-basin (45280) in the far eastern region shows a significant decreasing pre-monsoon precipitation trend based on PERSIANN-CDR, and eight sub-basins show significant decreasing monsoon precipitation trends based on both products. The overall trends strongly indicate that precipitation has declined in the pre-monsoon and monsoon seasons in the eastern and southern regions of the GBM river basin. These regions include the Brahmaputra and Meghna river basins. According to Khandu et al. (2017), Brahmaputra and Meghna basins' precipitation

declined up to 39 mm per decade in the monsoon season from 1998 to 2013. Sharma et al. (2021) also suggest similar decreasing precipitation trend in pre-monsoon and monsoon seasons in this area. On the contrary, Ahmed et al. (2017) found that Bangladesh monsoon precipitation increased by 3.04 mm/year and did not find any decreasing monsoon precipitation trend across Bangladesh from 1948 to 2012 using both parametric and non-parametric approaches. However, it should be noted that unlike Sharma et al. (2021) and Ahmed et al. (2017), our study area only covers the northern area of Bangladesh (Figure 3) and does not extend to the coast. (Baidya et al., 2008) found increasing daily extremes in precipitation and heavy precipitation events from 1961–2006 in Nepal. Similarly, MSWEP-based monsoon precipitation also has a significant increasing monsoon precipitation trend in the upper GBM, primarily in Tibet-China. The 0.1-degree grid resolution of MSWEP may help it to resolve precipitation processes in this highly mountainous region better than PERSIANN-CDR. Finally, it is interesting to note that the MSWEP trend in the Tibetan Plateau is consistent with the IPCC's projected trend in monsoon precipitation, where by 2100, rainfall is expected to increase by 38–45% with a 2 °C increase in temperature.

5.4 Relationship Between Riverbank Erosion and Precipitation

The final research question was: *What is the relative importance of localized extreme daily precipitation versus basin-scale seasonal precipitation for riverbank erosion in the study area?* Riverbank erosion is the perennial issue for the NSF project that funded my work and has a huge impact on Bangladesh's livelihood, environment, and the economy. It plays an important role to socio-environmental changes in Bangladesh (Islam & Rashid, 2011). This study was focused on studying the relationship between riverbank erosion and precipitation based on local extreme daily precipitation and monsoon precipitation of the GBM river basin. The local study area was divided into three region; North, Central, and South to obtain more stable results and to be consistent with

the regions used by Crawford et al. (2020). However, the study showed no significant relationship between the frequency of local extreme daily precipitation events and riverbank change in coastal Bangladesh. Only a few sub-basins of the GBM showed significant positive correlations between monsoon precipitation and riverbank change, and all in the central region of our study area. This is an interesting finding as the central region was dominated by accretion from 1988-2008 before being dominated by erosion from 2008-2018 (Crawford et al. 2020). One possible explanation for the relationships may be the long-term trends in GBM rainfall. The areas that experienced a decline in monsoon rainfall based on MSWEP and especially PERSIANN-CDR were also areas that showed the positive correlations with riverbank change. It is hypothesized that the lack of rain and flooding over time would reduce sediment transport to the study area reducing the accretion.

It should be noted that this study was solely focused on precipitation as the main driver for riverbank erosion in the GBM basin. However, other factors may have a role, including soil type, vegetation and other anthropogenic factors. According to (Rahman et al., 2015), the factors that affect riverbank erosion are: changes of river course, decrease or increase in shear strength, characteristics of erosion prone bank and bed materials, pressure imbalance at the bank face, rapid drawdown, poor vegetation cover, obstacle in the streams, wind wave and boat wakes. To improve the local analysis, future studies should also consider these factors and attempt to collect finer scale precipitation data in Bangladesh. Regarding the large-scale analysis, this study was only concerned with 80 km of shoreline area from Chandpur to Lakshmipur where transects were calculated. Future studies should consider a longer stretch of coastline and include both sides of the riverbank when computing riverbank erosion statistics. Integrating larger areas of land change would likely have a stronger relationship with upstream accumulated precipitation amounts.

CHAPTER 6: CONCLUSION

This study has important findings that elucidate the time-space characterization of precipitation in the Ganges-Brahmaputra-Meghna (GBM) river basin based on PERSIANN-CDR and MSWEP satellite products. Validation of these two satellite-based products against rain gauge station data over Nepal was conducted to elucidate the reliability of any results generated. Further validation is required before making any firm conclusion, however, MSWEP performed better than PERSIANN-CDR overall and especially for pre-monsoon precipitation over Nepal. The main objective of the study was to examine the relationships between seasonal precipitation, precipitation trends, and extreme precipitation as predictive drivers in causing riverbank erosion in the coastal Bangladesh.

The findings showed no significant relationship between pre-monsoon and monsoon precipitation in the GBM river basin based on hydrological sub-basins and water routing distance. On the contrary, one of the most important contributions was refining the relationship between ENSO and pre-monsoon and monsoon precipitation in the GBM river basin. In particular, El Nino leads to dry conditions in the periphery of the GBM, or the areas of the GBM where water the water routing distance is large. Further, this study conducted a precipitation trend analysis from 1983 to 2019 using MSWEP and PERSIANN-CDR. The modified Mann-Kendall test was used to detect precipitation trends for the GBM basin as whole and pre-defined hydrological sub-basins within the GBM. The precipitation trend test result obtained from two satellite-based products was compared and results were conflicting. Pre-monsoon precipitation trend significantly increased according to MSWEP while monsoon precipitation trend significantly decreased according to PERSIANN-CDR for the period of record. However, the study found that pre-monsoon precipitation based on PERSIANN-CDR, and monsoon precipitation based on MSWEP, have no

significant negative or positive trend for the GBM whole. A closer examination of sub-basins within the GBM showed regionality of these precipitation trends. The last and final objective of the study was to compare the relationship between riverbank erosion and local extreme precipitation and monsoon precipitation over the GBM river basin. Only a few hydrological sub-basins showed significant relationships that would suggest accretion rates increase with monsoon precipitation. The findings of the present study provide useful information for managing water crises, agricultural production, and preparing for different natural hazards in the GBM river basin.

6.1 Limitations and Future Work

Despite the contributions of the thesis, there are certain limitations. The first is related to the use of satellite-based precipitation products. We did not use those products which have shorter records of precipitation data, such as TRMM, even though they have comparatively higher accuracy. Second, the validation study was done only for Nepal. It would be better if we could separate the area into low land, mid hills, and higher mountains to compare the efficacy of these two satellite products against rain gauge because of the unequal distribution of the rain gauge station locations. Also, this study was limited to point to grid comparison. An interpolation of the gauge data accounting for elevation may have led to a better comparison. A curious finding was the conflicting trends in rainfall between PERSIANN-CDR and MSWEP, and additional investigations are required.

The analysis of extreme precipitation and riverbank change was limited. For example, this study only used the total number of extreme days based on the local 95^{th} percentile of MSWEP rainfall for the analysis and not other measures of extreme rainfall. The direct relationship between ENSO and extreme precipitation in coastal Bangladesh was also not investigated. Instead, the study sought to fulfill the objectives of the NSF funded project on how seasonal and local

precipitation affect riverbank erosion in coastal Bangladesh. This study defined a water routing distance spatial scale, but due to time limitations this unit of analysis was not related to riverbank erosion. This will be a priority for future work. Finally, integrating gauge-based local precipitation data with larger areas of riverbank change (e.g. both banks) would be helpful for the riverbank erosion study. Other factors could also be considered besides precipitation such as haphazard human settlement, agriculture practices, and land use land cover change.

REFERENCES

Abidin, R. Z., Sulaiman, M. S., & Yusoff, N. (2017). Erosion risk assessment: A case study of the Langat River bank in Malaysia. *International Soil and Water Conservation Research*, *5*(1), 26–35. https://doi.org/10.1016/j.iswcr.2017.01.002

ADB. (2013). *Technical Assistance Consultant ' s Report Bangladesh : Main River Flood and Bank Erosion Risk Management Program Government of the People ' s Republic of Bangladesh Aricha Main River Flood and Bank Erosion Risk Management Program Final Report , Annex E R* (Issue December).

Ahmad, I., Tang, D., Wang, T., Wang, M., & Wagan, B. (2015). Precipitation trends over time using Mann-Kendall and spearman's Rho tests in swat river basin, Pakistan. *Advances in Meteorology*, *2015*. https://doi.org/10.1155/2015/431860

Ahmed, M. K., Alam, M. S., Yousuf, A. H. M., & Islam, M. M. (2017). A long-term trend in precipitation of different spatial regions of Bangladesh and its teleconnections with El Niño/Southern Oscillation and Indian Ocean Dipole. *Theoretical and Applied Climatology*, *129*(1–2), 473–486. https://doi.org/10.1007/s00704-016-1765-2

Ajjur, S. B., & Riffi, M. I. (2020). Analysis of the observed trends in daily extreme precipitation indices in Gaza Strip during 1974–2016. *International Journal of Climatology*, *40*(14), 6189–6200. https://doi.org/10.1002/joc.6576

Akhtar, M. P., Sharma, N. A. Y. A. N., & Ojha, C. S. P. (2011). Braiding process and bank erosion in the Brahmaputra River. *International Journal of Sediment Research*, *26*(4), 431–444. https://doi.org/10.1016/S1001-6279(12)60003-1

Alamgir, S. (2009). Characterization and Estimation of Rainfall in Bangladesh Based on Ground Radar and Satellite Observations [Université du Québec]. In *Recherche* (Issue May 2009). http://scholar.google.com/scholar?hl=en&btnG=Search&q=intitle:CHARACTERIZATION+AND+ESTIMATION+OF+RAINFALL+IN+BANGLADESH+BASED+ON+GROUND+RADAR+AND#0

Alsdorf, D. E. (2003). Water storage of the central amazon floodplain measured with GIS and remote sensing imagery. *Annals of the Association of American Geographers*, *93*(1), 55–66. https://doi.org/10.1111/1467-8306.93105

Aravamuthan, V., Kothyari, U. C., & Singh, V. P. (1997). An Investigation of Changes in Rainfall and Temperature Regimes of the Ganga Basin in India. *Water Resources Management*, *17*, 17–34.

Arvor, D., Funatsu, B. M., Michot, V., & Dubreui, V. (2017). Monitoring rainfall patterns in the southern amazon with PERSIANN-CDR data: Long-term characteristics and trends. *Remote Sensing*, *9*(9). https://doi.org/10.3390/rs9090889

Ashok, K., Guan, Z., Saji, N. H., & Yamagata, T. (2004). Individual and combined influences of ENSO and the Indian Ocean Dipole on the Indian summer monsoon. *Journal of Climate*, *17*(16), 3141–3155. https://doi.org/10.1175/1520-0442(2004)017<3141:IACIOE>2.0.CO;2

Ashok, K., & Saji, N. H. (2007). On the impacts of ENSO and Indian Ocean dipole events on sub-regional Indian summer monsoon rainfall. *Natural Hazards*, *42*(2), 273–285. https://doi.org/10.1007/s11069-006-9091-0

Ashouri, H., Hsu, K. L., Sorooshian, S., Braithwaite, D. K., Knapp, K. R., Cecil, L. D., Nelson, B. R., & Prat, O. P. (2015). PERSIANN-CDR: Daily precipitation climate data record from

multisatellite observations for hydrological and climate studies. *Bulletin of the American Meteorological Society*, *96*(1), 69–83. https://doi.org/10.1175/BAMS-D-13-00068.1

Ashouri, H., Nguyen, P., Thorstensen, A., Hsu, K. L., Sorooshian, S., & Braithwaite, D. (2016). Assessing the efficacy of high-resolution satellite-based PERSIANN-CDR precipitation product in simulating streamflow. *Journal of Hydrometeorology*, *17*(7), 2061–2076. https://doi.org/10.1175/JHM-D-15-0192.1

Atiah, W. A., Amekudzi, L. K., Aryee, J. N. A., Preko, K., & Danuor, S. K. (2020). Validation of satellite and merged rainfall data over Ghana, West Africa. *Atmosphere*, *11*(8). https://doi.org/10.3390/ATMOS11080859

Awange, J. L., Hu, K. X., & Khaki, M. (2019). The newly merged satellite remotely sensed, gauge and reanalysis-based Multi-Source Weighted-Ensemble Precipitation: Evaluation over Australia and Africa (1981–2016). *Science of the Total Environment*, *670*, 448–465. https://doi.org/10.1016/j.scitotenv.2019.03.148

Ayehu, G. T., Tadesse, T., Gessesse, B., & Dinku, T. (2018). Validation of new satellite rainfall products over the Upper Blue Nile Basin, Ethiopia. *Atmospheric Measurement Techniques*, *11*(4), 1921–1936. https://doi.org/10.5194/amt-11-1921-2018

Bai, P., & Liu, X. (2018). Evaluation of five satellite-based precipitation products in two gauge-scarce basins on the Tibetan Plateau. *Remote Sensing*, *10*(8). https://doi.org/10.3390/RS10081316

Baidya, S. K., Shrestha, M. L., & Sheikh, M. M. (2008). Trends in daily climatic extremes of Temperature and Precipitation in Nepal. *Journal of Hydrology and Meteorology*, *5*(1), 38–51. http://soham.org.np/wp-content/uploads/2008/03/v5-38-51.pdf

Bajracharya, S. R., Palash, W., Shrestha, M. S., Khadgi, V. R., Duo, C., Das, P. J., & Dorji, C. (2015). Systematic evaluation of satellite-based rainfall products over the brahmaputra basin for hydrological applications. *Advances in Meteorology*, *2015*. https://doi.org/10.1155/2015/398687

Beck, H. E., Van Dijk, A. I. J. M., Levizzani, V., Schellekens, J., Miralles, D. G., Martens, B., & De Roo, A. (2017). MSWEP: 3-hourly 0.25° global gridded precipitation (1979-2015) by merging gauge, satellite, and reanalysis data. *Hydrology and Earth System Sciences*, *21*(1), 589–615. https://doi.org/10.5194/hess-21-589-2017

Beck, H. E., Wood, E. F., Pan, M., Fisher, C. K., Miralles, D. G., Van Dijk, A. I. J. M., McVicar, T. R., & Adler, R. F. (2019). MSWep v2 Global 3-hourly 0.1° precipitation: Methodology and quantitative assessment. *Bulletin of the American Meteorological Society*, *100*(3), 473–500. https://doi.org/10.1175/BAMS-D-17-0138.1

Bhatla, R., Singh, M., Mall, R. K., Tripathi, A., & Raju, P. V. S. (2015). Variability of summer monsoon rainfall over Indo-Gangetic plains in relation to El-Nino/La-Nina. *Natural Hazards*, *78*(2), 837–853. https://doi.org/10.1007/s11069-015-1746-2

Bisht, D. S., Chatterjee, C., Raghuwanshi, N. S., & Sridhar, V. (2018). Spatio-temporal trends of rainfall across Indian river basins. *Theoretical and Applied Climatology*, *132*(1–2), 419–436. https://doi.org/10.1007/s00704-017-2095-8

Bitew, M. M., & Gebremichael, M. (2011). Assessment of satellite rainfall products for streamflow simulation in medium watersheds of the Ethiopian highlands. *Hydrology and Earth System Sciences*, *15*(4), 1147–1155. https://doi.org/10.5194/hess-15-1147-2011

Blöschl, G., Hall, J., Viglione, A., Perdigão, R. A. P., Parajka, J., Merz, B., Lun, D., Arheimer, B.,

Aronica, G. T., Bilibashi, A., Boháč, M., Bonacci, O., Borga, M., Čanjevac, I., Castellarin, A., Chirico, G. B., Claps, P., Frolova, N., Ganora, D., … Živković, N. (2019). Changing climate both increases and decreases European river floods. *Nature*, *573*(7772), 108–111. https://doi.org/10.1038/s41586-019-1495-6

Brammer, H. (2014). Bangladesh's dynamic coastal regions and sea-level rise. *Climate Risk Management*, *1*, 51–62. https://doi.org/10.1016/j.crm.2013.10.001

Chowdhury, M. R. (2003). The El Niño-Southern Oscillation (ENSO) and seasonal flooding - Bangladesh. *Theoretical and Applied Climatology*, *76*(1–2), 105–124. https://doi.org/10.1007/s00704-003-0001-z

Chowdhury, R., & Ward, N. (2004). Hydro-meteorological variability in the greater Ganges-Brahmaputra-Meghna basins. *International Journal of Climatology*, *24*(12), 1495–1508. https://doi.org/10.1002/joc.1076

Crawford, T. W., Rahman, M. K., Miah, M. G., Islam, M. R., Paul, B. K., Curtis, S., & Islam, M. S. (2020). Coupled Adaptive Cycles of Shoreline Change and Households in Deltaic Bangladesh: Analysis of a 30-Year Shoreline Change Record and Recent Population Impacts. *Annals of the American Association of Geographers*, *0*(0), 1–23. https://doi.org/10.1080/24694452.2020.1799746

Curtis, S., Crawford, T., Munshi, K., & Paul, B. (2017). *Monsoon Dynamics in the Ganges-Brahmaputra-Meghna Basin*. *1*(November), 4865. https://doi.org/10.3390/chycle-2017-04865

Curtis, S., Crawford, T., Rahman, M., Paul, B., Miah, M. G., Islam, M. R., & Patel, M. (2018). A hydroclimatological analysis of precipitation in the Ganges-Brahmaputra-Meghna river

basin. *Water (Switzerland)*, *10*(10), 1–11. https://doi.org/10.3390/w10101359

DAHAL, R. K. (2012). Rainfall-induced Landslides in Nepal. *International Journal of Erosion Control Engineering*, *5*(1), 1–8. https://doi.org/10.13101/ijece.5.1

Das, T. K., Haldar, S. K., Gupta, I. Das, & Sen, S. (2014). River bank erosion induced human displacement and its consequences. *Living Reviews in Landscape Research*, *8*(1), 1–35. https://doi.org/10.12942/lrlr-2014-3

De Luca, D. L., Petroselli, A., & Galasso, L. (2020). A transient stochastic rainfall generator for climate changes analysis at hydrological scales in central Italy. *Atmosphere*, *11*(12), 1–21. https://doi.org/10.3390/atmos11121292

Dikshit, A., Sarkar, R., Pradhan, B., Acharya, S., & Dorji, K. (2019). Estimating rainfall thresholds for landslide occurrence in the Bhutan Himalayas. *Water (Switzerland)*, *11*(8), 1–12. https://doi.org/10.3390/w11081616

dos Reis, J. B. C., Rennó, C. D., & Lopes, E. S. S. (2017). Validation of satellite rainfall products over a mountainouswatershed in a humid subtropical climate region of Brazil. *Remote Sensing*, *9*(12). https://doi.org/10.3390/rs9121240

Duncan, J. M. A., & Biggs, E. M. (2012). Assessing the accuracy and applied use of satellite-derived precipitation estimates over Nepal. *Applied Geography*, *34*, 626–638. https://doi.org/10.1016/j.apgeog.2012.04.001

FAO. (2011). AQUASTAT Transboundary River Basins-Ganges-Brahmaputra-Meghna River Basin. In *FAO Aquastat*. www.fao.org/

Gadgil, S., Vinayachandran, P. N., Francis, P. A., & Gadgil, S. (2004). Extremes of the Indian

summer monsoon rainfall, ENSO and equatorial Indian Ocean oscillation. *Geophysical Research Letters*, *31*(12), 2–5. https://doi.org/10.1029/2004GL019733

Gajbhiye, S., Meshram, C., Singh, S. K., Srivastava, P. K., & Islam, T. (2016). Precipitation trend analysis of Sindh River basin, India, from 102-year record (1901-2002). *Atmospheric Science Letters*, *17*(1), 71–77. https://doi.org/10.1002/asl.602

Gao, X., Zhu, Q., Yang, Z., & Wang, H. (2018). Evaluation and hydrological application of CMADS against TRMM 3B42V7, PERSIANN-CDR, NCEP-CFSR, and gauge-based datasets in Xiang River basin of China. *Water (Switzerland)*, *10*(9), 1–24. https://doi.org/10.3390/w10091225

GC, R. K., Ranganathan, S., Hammett, A. L. (Tom), & Hall, R. P. (2021). What factors determine the technical performance of community-managed rural water systems in the middle hills of Nepal? *Journal of Water, Sanitation and Hygiene for Development*, *11*(2), 222–230. https://doi.org/10.2166/washdev.2020.189

Gerrard, J., & Gardner, R. A. M. (2000). Relationships between rainfall and landsliding in the Middle Hills, Nepal. *Norsk Geografisk Tidsskrift*, *54*(2), 74–81. https://doi.org/10.1080/002919500423807

Ghalhari, G. F., Roudbari, A. D., & Asadi, M. (2016). Identifying the spatial and temporal distribution characteristics of precipitation in Iran. *Arabian Journal of Geosciences*, *9*(12). https://doi.org/10.1007/s12517-016-2606-4

GOB-Bangladesh Planning Commission. (2018). Bangladesh Delta Plan 2100. *Ministry of Planning Government of the People's Republic of Bangladesh*, *55*, 1–42.

Goswami, B. N., & Xavier, P. K. (2005). ENSO control on the south Asian monsoon through the length of the rainy season. *Geophysical Research Letters*, *32*(18), 1–4. https://doi.org/10.1029/2005GL023216

Guo, H., Chen, S., Bao, A., Hu, J., Gebregiorgis, A. S., Xue, X., & Zhang, X. (2015). Inter-comparison of high-resolution satellite precipitation products over Central Asia. *Remote Sensing*, *7*(6), 7181–7211. https://doi.org/10.3390/rs70607181

Hamal, K., Sharma, S., Khadka, N., Baniya, B., Ali, M., Shrestha, M. S., Xu, T., Shrestha, D., & Dawadi, B. (2020). Evaluation of MERRA-2 precipitation products using gauge observation in Nepal. *Hydrology*, *7*(3), 1–21. https://doi.org/10.3390/hydrology7030040

Hamed, K. H., & Rao, A. R. (1998). A modified Mann-Kendall trend test for autocorrelated data. *Journal of Hydrology*, *204*(1–4), 182–196. https://doi.org/10.1016/S0022-1694(97)00125-X

Hassan, M. A., Ratna, S. J., Hassan, M., & Tamanna, S. (2017). Remote Sensing and GIS for the Spatio-Temporal Change Analysis of the East and the West River Bank Erosion and Accretion of Jamuna River (1995-2015), Bangladesh. *Journal of Geoscience and Environment Protection*, *05*(09), 79–92. https://doi.org/10.4236/gep.2017.59006

Hirpa, F. A., Gebremichael, M., & Hopson, T. (2010). Evaluation of high-resolution satellite precipitation products over very complex terrain in Ethiopia. *Journal of Applied Meteorology and Climatology*, *49*(5), 1044–1051. https://doi.org/10.1175/2009JAMC2298.1

Hou, A. Y., Kakar, R. K., Neeck, S., Azarbarzin, A. A., Kummerow, C. D., Kojima, M., Oki, R., Nakamura, K., & Iguchi, T. (2014). The global precipitation measurement mission. *Bulletin of the American Meteorological Society*, *95*(5), 701–722. https://doi.org/10.1175/BAMS-D-13-00164.1

Hu, Q., He, X., Lu, X. A., & Zhang, X. (2019). Trend analysis of seasonal precipitation (1960–2013) in subregions of hunan province, central south china using discrete wavelet transforms. *Journal of Applied Meteorology and Climatology*, *58*(10), 2159–2175. https://doi.org/10.1175/jamc-d-19-0023.1

Huffman, G. J., Adler, R. F., Bolvin, D. T., Gu, G., Nelkin, E. J., Bowman, K. P., Hong, Y., Stocker, E. F., & Wolff, D. B. (2007). The TRMM Multisatellite Precipitation Analysis (TMPA): Quasi-global, multiyear, combined-sensor precipitation estimates at fine scales. *Journal of Hydrometeorology*, *8*(1), 38–55. https://doi.org/10.1175/JHM560.1

Huffman, G. J., Bolvin, D. T., Nelkin, E. J., & Tan, J. (2019). September 2019. *Journal of Ubiquitous Computing and Communication Technologies*, *01*(01). https://doi.org/10.36548/jucct.2019.1

Hussain, Y., Satgé, F., Hussain, M. B., Martinez-Carvajal, H., Bonnet, M. P., Cárdenas-Soto, M., Roig, H. L., & Akhter, G. (2018). Performance of CMORPH, TMPA, and PERSIANN rainfall datasets over plain, mountainous, and glacial regions of Pakistan. *Theoretical and Applied Climatology*, *131*(3–4), 1119–1132. https://doi.org/10.1007/s00704-016-2027-z

Ibáñez, C., Alcaraz, C., Caiola, N., Prado, P., Trobajo, R., Benito, X., Day, J. W., Reyes, E., & Syvitski, J. P. M. (2019). Basin-scale land use impacts on world deltas: Human vs natural forcings. *Global and Planetary Change*, *173*(June 2018), 24–32. https://doi.org/10.1016/j.gloplacha.2018.12.003

Ihara, C., Kushnir, Y., Cane, M. A., & Kaplan, A. (2008). Timing of El Niño-related warming and Indian summer monsoon rainfall. *Journal of Climate*, *21*(11), 2711–2719. https://doi.org/10.1175/2007JCLI1979.1

Immerzeel, W. (2008). Historical trends and future predictions of climate variability in the Brahmaputra basin. *INTERNATIONAL JOURNAL OF CLIMATOLOGY*, *28*(243–254 (2008)). https://doi.org/10.1002/joc.1528

Islam, A. S., Haque, A., & Bala, S. K. (2010). Hydrologic characteristics of floods in Ganges-Brahmaputra-Meghna (GBM) delta. *Natural Hazards*, *54*(3), 797–811. https://doi.org/10.1007/s11069-010-9504-y

Islam, M. D. F., & Rashid, A. N. M. B. (2011). Riverbank erosion displacees in Bangladesh: need for institutional response and policy intervention. *Bangladesh Journal of Bioethics*, *2*(2), 4–19.

Janes, T., McGrath, F., Macadam, I., & Jones, R. (2019). High-resolution climate projections for South Asia to inform climate impacts and adaptation studies in the Ganges-Brahmaputra-Meghna and Mahanadi deltas. *Science of the Total Environment*, *650*, 1499–1520. https://doi.org/10.1016/j.scitotenv.2018.08.376

Jiménez-Esteve, B., & Domeisen, D. I. V. (2018). The tropospheric pathway of the ENSO-North Atlantic teleconnection. *Journal of Climate*, *31*(11), 4563–4584. https://doi.org/10.1175/JCLI-D-17-0716.1

Joyce, R. J., Janowiak, J. E., Arkin, P. A., & Xie, P. (2004). CMORPH: A method that produces global precipitation estimates from passive microwave and infrared data at high spatial and temporal resolution. *Journal of Hydrometeorology*, *5*(3), 487–503. https://doi.org/10.1175/1525-7541(2004)005<0487:CAMTPG>2.0.CO;2

Júnior, S., Xavier, A., Jale, S., Stosic, T., Antonio, C., & Singh, V. P. (2020). *Precipitation Trends Analysis by Mann-Kendall Test : A Case Study of Análise de Tendência da Precipitação*

Usando o Teste de Mann-Kendall : Um Estudo de Caso na Paraíba , Brasil. *2012*, 187–196.

Karki, Rahul, & Gurung, A. (2012). An Overview of Climate Change And Its Impact on Agriculture: a Review From Least Developing Country, Nepal. *International Journal of Ecosystem*, *2*(2), 19–24. https://doi.org/10.5923/j.ije.20120202.03

Karki, Ramchandra, ul Hasson, S., Schickhoff, U., Scholten, T., & Böhner, J. (2017). Rising precipitation extremes across Nepal. *Climate*, *5*(1), 1–25. https://doi.org/10.3390/cli5010004

Karpouzos, D., Kavalieratou, S., & Babajimopoulos, C. (2010). Trend analysis of precipitation data in Pieria Region (Greece). *European Water*, *30*, 31–40.

Katiraie-Boroujerdy, P. S., Akbari Asanjan, A., Hsu, K. lin, & Sorooshian, S. (2017). Intercomparison of PERSIANN-CDR and TRMM-3B42V7 precipitation estimates at monthly and daily time scales. *Atmospheric Research*, *193*(March), 36–49. https://doi.org/10.1016/j.atmosres.2017.04.005

Kendall, M. G. (1975). *Rank Correlation Methods* (4th ed.). London, Griffin.

Khandu, Awange, J. L., Anyah, R., Kuhn, M., & Fukuda, Y. (2017). Assessing regional climate simulations of the last 30 years (1982–2012) over Ganges–Brahmaputra–Meghna River Basin. *Climate Dynamics*, *49*(7–8), 2329–2350. https://doi.org/10.1007/s00382-016-3457-0

Khandu, Awange, J. L., Kuhn, M., Anyah, R., & Forootan, E. (2017). Changes and variability of precipitation and temperature in the Ganges–Brahmaputra–Meghna River Basin based on global high-resolution reanalyses. *International Journal of Climatology*, *37*(4), 2141–2159. https://doi.org/10.1002/joc.4842

Khandu, Awange, L., J., Anyah, Richard, Kuhn, Michael, Fukuda, & Yoichi. (2017). Assessing

regional climate simulations of the last 30 years (1982–2012) over Ganges–Brahmaputra–Meghna River Basin. *Climate Dynamics*, *49*(7–8), 2329–2350. https://doi.org/10.1007/s00382-016-3457-0

Kiguchi, M., Matsumoto, J., Kanae, S., & Oki, T. (2016). Pre-monsoon rain and its relationship with monsoon onset over the indochina peninsula. *Frontiers in Earth Science*, *4*(May), 1–13. https://doi.org/10.3389/feart.2016.00042

Kirtman, B. P., & Shukla, J. (2000). Influence of the Indian summer monsoon on ENSO. *Quarterly Journal of the Royal Meteorological Society*, *126*(562), 213–239. https://doi.org/10.1002/qj.49712656211

Kothyari, U. C., SINGH, V. P., & ARAVAMUTHAN, V. (1997). An Investigation ofChanges in Rainfall and Temperature Regimes of the Ganga Basin in India. *Water Resources Management 11:*, *11*(17).

Kumar, V. P., & Naidu, V. C. (2020). Is Pre-monsoon Rainfall Activity Over India Increasing in the Recent Era of Global Warming? *Pure and Applied Geophysics*. https://doi.org/10.1007/s00024-020-02471-7

Kummerow, C., Simpson, J., Thiele, O., Barnes, W., Chang, A. T. C., Stocker, E., Adler, R. F., Hou, A., Kakar, R., Wentz, F., Ashcroft, P., Kozu, T., Hong, Y., Okamoto, K., Iguchi, T., Kuroiwa, H., Im, E., Haddad, Z., Huffman, G., … Nakamura, K. (2000). The status of the tropical rainfall measuring mission (TRMM) after two years in orbit. *Journal of Applied Meteorology*, *39*(12 PART 1), 1965–1982. https://doi.org/10.1175/1520-0450(2001)040<1965:tsottr>2.0.co;2

Lakew, H. B. (2020). Investigating the effectiveness of bias correction and merging MSWEP with

gauged rainfall for the hydrological simulation of the upper Blue Nile basin. *Journal of Hydrology: Regional Studies*, *32*(February), 100741. https://doi.org/10.1016/j.ejrh.2020.100741

Lehner, B., & Grill, G. (2013). Global river hydrography and network routing: Baseline data and new approaches to study the world's large river systems. *Hydrological Processes*, *27*(15), 2171–2186. https://doi.org/10.1002/hyp.9740

Leopold, L. B., & Wolman, M. G. (1970). River Channel Patterns. *Rivers and River Terraces*, 197–237. https://doi.org/10.1007/978-1-349-15382-4_8

Liebmann, B., Jones, C., & de Carvalho, L. M. V. (2001). Interannual variability of daily extreme precipitation events in the state of Saõ Paulo, Brazil. *Journal of Climate*, *14*(2), 208–218. https://doi.org/10.1175/1520-0442(2001)014<0208:IVODEP>2.0.CO;2

Madej, M. A., Weaver, W. E., & Hagans, D. K. (1994). Analysis of bank erosion on the Merced River, Yosemite Valley, Yosemite National Park, California, USA. *Environmental Management*, *18*(2), 235–250. https://doi.org/10.1007/BF02393764

Malik, N., Marwan, N., & Kurths, J. (2010). Spatial structures and directionalities in Monsoonal precipitation over South Asia. *Nonlinear Processes in Geophysics*, *17*(5), 371–381. https://doi.org/10.5194/npg-17-371-2010

Mann, H. B. (1945). Nonparametric Tests Against Trend Author (s): Henry B . Mann Published by : The Econometric Society Stable URL : https://www.jstor.org/stable/1907187 REFERENCES Linked references are available on JSTOR for this article : You may need to log in to JSTOR. *Econometrica*, *13*(3), 245–259. http://www.jstor.com/stable/1907187

Marelle, L., Myhre, G., Hodnebrog, Ø., Sillmann, J., & Samset, B. H. (2018). The Changing Seasonality of Extreme Daily Precipitation. *Geophysical Research Letters*, *45*(20), 11,352-11,360. https://doi.org/10.1029/2018GL079567

Mazzoleni, M., Bhattacharya, B., Laverde Barajas, M. A., & Solomatine, D. (2018). *Exploring the Use of the Three Rainfall Remote Sensing Products for Flood Prediction in the Brahmaputra Basin*. *3*, 1366–1358. https://doi.org/10.29007/h6z1

Miao, C., Ashouri, H., Hsu, K. L., Sorooshian, S., & Duan, Q. (2015). Evaluation of the PERSIANN-CDR daily rainfall estimates in capturing the behavior of extreme precipitation events over China. *Journal of Hydrometeorology*, *16*(3), 1387–1396. https://doi.org/10.1175/JHM-D-14-0174.1

Mirza, M. Q. M. (2011). Climate change, flooding in South Asia and implications. *Regional Environmental Change*, *11*(SUPPL. 1), 95–107. https://doi.org/10.1007/s10113-010-0184-7

Mirza, M. Q., Warrick, R. A., Ericksen, N. J., & Kenny, G. J. (1998). Tendances et persistance des précipitations des bassins des fleuves Gange, Brahmapoutre et Meghna. *Hydrological Sciences Journal*, *43*(6), 845–858. https://doi.org/10.1080/02626669809492182

Mondal, A., Kundu, S., & Mukhopadhyay, A. (2012). *Case Study RAINFALL TREND ANALYSIS BY MANN-KENDALL TEST : A CASE STUDY OF NORTH-EASTERN PART OF CUTTACK DISTRICT , ORISSA School of Oceanographic Studies , Jadavpur University , Kolkata-700032 * Author for Correspondence Case Study Trend Analysis*. *2*(1), 70–78.

Mondal, A., Lakshmi, V., & Hashemi, H. (2018). Intercomparison of trend analysis of Multisatellite Monthly Precipitation Products and Gauge Measurements for River Basins of India. *Journal of Hydrology*, *565*(April), 779–790.

https://doi.org/10.1016/j.jhydrol.2018.08.083

Mosaffa, H., Sadeghi, M., Hayatbini, N., Gorooh, V. A., Asanjan, A. A., Nguyen, P., & Sorooshian, S. (2020). Spatiotemporal variations of precipitation over Iran using the high-resolution and nearly four decades satellite-based PERSIANN-CDR dataset. *Remote Sensing*, *12*(10), 1–14. https://doi.org/10.3390/rs12101584

Nair, A. S., & Indu, J. (2017). Performance assessment of Multi-Source Weighted-Ensemble Precipitation (MSWEP) product over India. *Climate*, *5*(1). https://doi.org/10.3390/cli5010002

Narayanan, P., Basistha, A., Sarkar, S., & Kamna, S. (2013). Trend analysis and ARIMA modelling of pre-monsoon rainfall data for western India. *Comptes Rendus - Geoscience*, *345*(1), 22–27. https://doi.org/10.1016/j.crte.2012.12.001

Nath, B., Naznin, S. N., & Alak, P. (2013). Trends analysis of river bank erosion at Chandpur, Bangladesh: A remote sensing and GIS approach. *International Journal of Geomatics and Geosciences*, *3*(3), 454–463.

Nguyen, P., Ombadi, M., Sorooshian, S., Hsu, K., AghaKouchak, A., Braithwaite, D., Ashouri, H., & Rose Thorstensen, A. (2018). The PERSIANN family of global satellite precipitation data: A review and evaluation of products. *Hydrology and Earth System Sciences*, *22*(11), 5801–5816. https://doi.org/10.5194/hess-22-5801-2018

Nyenzi, B., & Lefale, P. F. (2006). Advances in Geosciences ˜ Southern Oscillation (ENSO) and global warming El Ni no. *Change*, 95–101.

Petley, D. N., Hearn, G. J., Hart, A., Rosser, N. J., Dunning, S. A., Oven, K., & Mitchell, W. A.

(2007). Trends in landslide occurrence in Nepal. *Natural Hazards*, *43*(1), 23–44. https://doi.org/10.1007/s11069-006-9100-3

Pfafstetter, O. (1989). *Classification of hydrographic basins: coding methodology*. *18*(1989), 1–2.

Rahman, M. (2013). Impact of Riverbank Erosion Hazard in the Jamuna Floodplain Areas in Bangladesh. *Journal of Science Foundation*, *8*(1–2), 55–65. https://doi.org/10.3329/jsf.v8i1-2.14627

Rahman, M. R., & Lateh, H. (2017). Climate change in Bangladesh: a spatio-temporal analysis and simulation of recent temperature and rainfall data using GIS and time series analysis model. *Theoretical and Applied Climatology*, *128*(1–2), 27–41. https://doi.org/10.1007/s00704-015-1688-3

Ramage, C. S. (1971). *Monsoon meteorology*. New York ; London : Academic Press.

Richardson, W. R., & Thorne, C. R. (2001). Multiple thread flow and channel bifurcation in a braided river: Brahmaputra-Jamuna River, Bangladesh. *Geomorphology*, *38*(3–4), 185–196. https://doi.org/10.1016/S0169-555X(00)00080-5

Romatschke, U., & Houze, R. A. (2011). Characteristics of precipitating convective systems in the South Asian monsoon. *Journal of Hydrometeorology*, *12*(1), 3–26. https://doi.org/10.1175/2010JHM1289.1

Ropelewski, C. F., & Halpert, M. S. (1987). No Title. *Monthly Weather Review*, *115*, 1606–1626. https://doi.org/10.1175/1520-0493(1987)115<1606:GARSPP>2.0.CO;2

Roy, S. Sen, & Balling, R. C. (2004). Trends in extreme daily precipitation indices in India. *International Journal of Climatology*, *24*(4), 457–466. https://doi.org/10.1002/joc.995

Ruiz-Alvarez, O., Singh, V. P., Enciso-Medina, J., Ontiveros-Capurata, R. E., & dos Santos, C. A. C. (2020). Observed trends in daily extreme precipitation indices in Aguascalientes, Mexico. *Meteorological Applications*, *27*(1), 1–20. https://doi.org/10.1002/met.1838

Sarma, J. N., & Acharjee, S. (2018). A study on variation in channel width and braiding intensity of the Brahmaputra River in Assam, India. *Geosciences (Switzerland)*, *8*(9), 1–19. https://doi.org/10.3390/geosciences8090343

Sayemuzzaman, M., & Jha, M. K. (2014). Seasonal and annual precipitation time series trend analysis in North Carolina, United States. *Atmospheric Research*, *137*, 183–194. https://doi.org/10.1016/j.atmosres.2013.10.012

Shah, H. L., & Mishra, V. (2016). Uncertainty and bias in satellite-based precipitation estimates over Indian subcontinental basins: Implications for real-time streamflow simulation and flood prediction. *Journal of Hydrometeorology*, *17*(2), 615–636. https://doi.org/10.1175/JHM-D-15-0115.1

Shahid, S. (2011). Trends in extreme rainfall events of Bangladesh. *Theoretical and Applied Climatology*, *104*(3–4), 489–499. https://doi.org/10.1007/s00704-010-0363-y

Sharma, C., Shukla, A. K., & Zhang, Y. (2021). Climate change detection and attribution in the Ganga-Brahmaputra-Meghna river basins. *Geoscience Frontiers*, *12*(5), 101186. https://doi.org/10.1016/j.gsf.2021.101186

Shiu, C. J., Liu, S. C., Fu, C., Dai, A., & Sun, Y. (2012). How much do precipitation extremes change in a warming climate? *Geophysical Research Letters*, *39*(17), 1–5. https://doi.org/10.1029/2012GL052762

Shrestha, M. L. (2000). Interannual variation of summer monsoon rainfall over Nepal and its relation to Southern Oscillation Index. *Meteorology and Atmospheric Physics*, *75*(1–2), 21–28. https://doi.org/10.1007/s007030070012

Sorooshian, S., Hsu, K. L., Gao, X., Gupta, H. V., Imam, B., & Braithwaite, D. (2000). Evaluation of PERSIANN system satellite-based estimates of tropical rainfall. *Bulletin of the American Meteorological Society*, *81*(9), 2035–2046. https://doi.org/10.1175/1520-0477(2000)081<2035:EOPSSE>2.3.CO;2

Stefanidis, S., & Stathis, D. (2018). Spatial and temporal rainfall variability over the mountainous central Pindus (Greece). *Climate*, *6*(3). https://doi.org/10.3390/cli6030075

Tan, M. L., Gassman, P. W., & Cracknell, A. P. (2017). Assessment of three long-term gridded climate products for hydro-climatic simulations in tropical river basins. *Water (Switzerland)*, *9*(3). https://doi.org/10.3390/w9030229

Tan, M. L., Ibrahim, A. L., Duan, Z., Cracknell, A. P., & Chaplot, V. (2015). Evaluation of six high-resolution satellite and ground-based precipitation products over Malaysia. *Remote Sensing*, *7*(2), 1504–1528. https://doi.org/10.3390/rs70201504

Tang, X., Zhang, J., Wang, G., Ruben, G. B., Bao, Z., Liu, Y., Liu, C., & Jin, J. (2021). Error correction of multi-source weighted-ensemble precipitation (MSWEP) over the Lancang–Mekong river basin. *Remote Sensing*, *13*(2), 1–27. https://doi.org/10.3390/rs13020312

Tanvir Rahman, M. A. T. M., Islam, S., & Rahman, S. H. (2015). Coping with flood and riverbank erosion caused by climate change using livelihood resources: a case study of Bangladesh. *Climate and Development*, *7*(2), 185–191. https://doi.org/10.1080/17565529.2014.910163

Thakur, P. K., Laha, C., & Aggarwal, S. P. (2012). River bank erosion hazard study of river Ganga, upstream of Farakka barrage using remote sensing and GIS. *Natural Hazards*, *61*(3), 967–987. https://doi.org/10.1007/s11069-011-9944-z

Thiemig, V., Rojas, R., Zambrano-Bigiarini, M., Levizzani, V., & De Roo, A. (2012). Validation of satellite-based precipitation products over sparsely Gauged African River basins. *Journal of Hydrometeorology*, *13*(6), 1760–1783. https://doi.org/10.1175/JHM-D-12-032.1

Turner, A. G., & Annamalai, H. (2012). Climate change and the South Asian summer monsoon. *Nature Climate Change*, *2*(8), 587–595. https://doi.org/10.1038/nclimate1495

Vinay Kumar, P., & Venkateswara Naidu, C. (2020). Is Pre-monsoon Rainfall Activity Over India Increasing in the Recent Era of Global Warming? *Pure and Applied Geophysics*, *177*(9), 4423–4442. https://doi.org/10.1007/s00024-020-02471-7

Vu, T. T., Li, L., & Jun, K. S. (2018). Evaluation of multi-satellite precipitation products for streamflow simulations: A case study for the Han River Basin in the Korean Peninsula, East Asia. *Water (Switzerland)*, *10*(5). https://doi.org/10.3390/w10050642

Walker, G. T. (1924). Correlation in seasonal variations of weather. IV: A further study of world weather. *Memoirs of India Met Dept*.

Wentz, F. J., Ricciardulli, L., Hilburn, K., & Mears, C. (2007). How much more rain will global warming bring? *Science*, *317*(5835), 233–235. https://doi.org/10.1126/science.1140746

Whitaker, D. W., Wasimi, S. A., & Islam, S. (2001). *0 O – Southern Oscillation and Long-Range the El Nin* (Vol. 87).

Wu, R., & Kirtman, B. P. (2004). Impacts of the Indian Ocean on the Indian Summer Monsoon-

ENSO relationship. *Journal of Climate*, *17*(15), 3037–3054. https://doi.org/10.1175/1520-0442(2004)017<3037:IOTIOO>2.0.CO;2

Xavier, K. P., Marzin, C., & Goswamib, B. N. (2007). An objective definition of the Indian summer monsoon season and a new perspective on the ENSO–monsoon relationship. *QUARTERLY JOURNAL OF THE ROYAL METEOROLOGICAL SOCIETY*, *133*, 749–764. https://doi.org/10.1002/qj.45

Zaveri, E., Grogan, D. S., Fisher-Vanden, K., Frolking, S., Lammers, R. B., Wrenn, D. H., Prusevich, A., & Nicholas, R. E. (2016). Invisible water, visible impact: Groundwater use and Indian agriculture under climate change. *Environmental Research Letters*, *11*(8). https://doi.org/10.1088/1748-9326/11/8/084005